Analysis of the mechanistic link between micro-climate and macro-biogeographic patterns of intertidal rocky shore organisms

Rui Seabra Alves Martinho

Supervisors:
David S. Wethey
António M. Santos
Fernando P. Lima

Porto, 2015

Dissertação apresentada à Faculdade de Ciências da Universidade do Porto para obtenção do grau de Doutor em Biodiversidade, Genética e Evolução. Porto, 2015.

Em todas as publicações decorrentes deste trabalho é devidamente referido que as instituições de origem do doutorando Rui Seabra Alves Martinho são:

- Departamento de Biologia, Faculdade de Ciências da Universidade do Porto, R. Campo Alegre, s/n, 4169-007 Porto, Portugal.
- CIBIO-InBIO, Centro de Investigação em Biodiversidade e Recursos Genéticos, Campus Agrário de Vairão, Universidade do Porto, 4485-661, Vairão, Portugal.

Este trabalho foi apoiado financeiramente pela Fundação para a Ciência e a Tecnologia (FCT) através de uma bolsa de doutoramento (ref. SFRH/BD/68521/2010) e dois projectos científicos (HINT, ref. PTDC/MAR/099391/2008, e COASTAL4CAST, ref. PTDC/MAR/117568/2010), e pelo FEDER (FCOMP-01-0124-FEDER-010564, FCOMP-01-0124-FEDER-020817).

Na elaboração desta tese, e nos termos do número 2 do Artigo 4° do Regulamento Geral dos Terceiros Ciclos de Estudos da Universidade do Porto e do Artigo 31° do D.L. 74/2006, de 24 de Março, com a nova redação introduzida pelo D.L. 230/2009, de 14 de Setembro, foi efetuado o aproveitamento total de um conjunto coerente de trabalhos de investigação já publicados ou submetidos para publicação em revistas internacionais indexadas e com arbitragem científica, os quais integram alguns dos capítulos da presente tese. Tendo em conta que os referidos trabalhos foram realizados com a colaboração de outros autores, o candidato esclarece que, em todos eles, participou ativamente na sua concepção, na obtenção, análise e discussão de resultados, bem como na elaboração da sua forma publicada.

To my parents and my wife

"Because it's there"
- George Mallory

"Once I get on a puzzle, I can't get off"
- Richard Feynman

"Somewhere, something incredible is waiting to be known"
- Carl Sagan

"Hofstadter's Law: It always takes longer than you expect,
even when you take into account Hofstadter's Law"
- Douglas Hofstadter

Acknowledgements

This work was mainly supported by Fundação para a Ciência e a Tecnologia (FCT), under contract number SFRH/BD/68521/2010. I was also beneficiary of financial and logistic support from the Centro de Investigação em Biodiversidade e Recursos Genéticos (CIBIO-InBIO), and from the Departamento de Biologia da Faculdade de Ciências da Universidade do Porto (DB-FCUP). In addition, two research project grants from FCT/FEDER (HINT, ref. PTDC/MAR/099391/2008, FCOMP-01-0124-FEDER-010564, and COASTAL4CAST, ref. PTDC/MAR/117568/2010, FCOMP-01-0124-FEDER-020817) covered most costs related to field work and the set-up of the aquaria facilities.

I feel very fortunate for all the good friends and colleagues who collectively carried me during this demanding period of my life. A special thank goes to my surf buddies Pedro Costa, Pedro Monterroso and Pedro Pinho, and my high-school mates Susana Pedro, Julio Cabral and Miguel Polónia, with whom I shared some of the most memorable moments of my life, filling me with energy for the tasks ahead.

Arriving at CIBIO was truly a *random walk* process, and numerous people were determinant in saving me from going astray. As an undergraduate, my friends Ana Goios, André Maia, Daniela Ferreira, Fabian Sá and Pedro Moreira made biology classes much easier and entertaining. In particular, André Maia provided me with all the lecture notes I was too lazy to take, but then badly needed (recurrently). Paula Tamagnini, my supervisor during an undergraduate project and the MSc thesis, was instrumental in getting me to publish, and wisely steered me away from lab work and into the field, where she knew I belonged even before I realized it. During my stay in CIIMAR, Vitor Vasconcelos was incredibly welcoming, and still is a great source of inspiration. Lastly, during a seemingly unimportant dinner, Diana Castro and Pedro Monterroso *revealed* the existence of a research centre named CIBIO, which until then I had been oblivious about.

After eventually arriving at CIBIO, the work leading to this thesis was filled with hurdles that I was only able to overcome with the help of many. Much of this work would not have been possible without free access to numerous software tools, databases and instructions (R Project, Arduino, Google Maps, StackExchange, among many others). The level of spontaneous collaboration that arises within these communities of contributors (agencies and individuals) never ceases to amaze me, and is a source of inspiration. For their invaluable help during lab/field work, great discussions and friendship, I thank my research colleagues Cristián Monaco,

Filipa Gomes, Lara Sousa, Nick Burnett, Pedro Ribeiro, Raquel Xavier and Stephen Sabatino, and my "co-co-supervisors" Jerry Hilbish and Sarah Woodin. I also extend my gratitude to the unparalleled Nuno Queiroz, for the constructive scientific discussions, hilariously awkward moments, multiplayer tank games and fantastic friendship. Notwithstanding the relevance all the other support I received, the guidance, friendship and incentive provided by my *dream team* of supervisors was the single most important factor leading to the completion of this thesis. Thus, I would like to thank David Wethey for all the amazing insights on environmental analysis, biogeography, programming and electronics, as well as for hosting me in his peculiar lab in the University of South Carolina, Columbia. I would also like to thank António Múrias, the *go-to* person for issues on biodiversity, statistics and programming (countless issues...), and a great joke teller. Finally, I would like to express my deepest gratitude to Fernando Lima. Fernando is, hands down, the best supervisor I could have ever had, instilling in me the right amount of drive, curiosity and responsibility necessary to get things done, all while mastering the balance between never lowering the bar on research quality and fostering a great friendship. I am extremely happy to have shared epic field work trips, countless stories and bad jokes, and nervous multiplayer tank games with such a friend (I hope to one day supervise like you...).

Lastly, my family, which makes up a large part of me. I thank all my cousins, aunts and uncles for the memories and support. To Ana Paula and José Queiroga, I thank the love and support, expressed during so many weekend dinners spent together. I thank my grandparents, which have always inspired me to work harder - especially my grandmother Glória Neves. A special thank is also due to my uncle Zeferino Martinho "*Fino*", one of the wittiest and good spirited persons I have ever known, showing constant interest for my advancements in this project. In equal amounts, I thank my unconditionally loving and supportive parents, who have always been there for me, who have taught me to put problems into perspective (*"o que é isso comparado com o raio da Terra?"*), and who, from the very beginning, have fueled my passion for science and nature.

... and Catarina, my wife, my life companion, my friend, my *lover*. Together we faced turbulent seas, but you were always loving and caring. These past years have been incredible, and sharing field work with you was absolutely amazing. For all the travel and good memories that were, and for all that will be... *I would have been lost without you*.

Abstract

Temperature is considered one of the most important drivers of biological processes affecting the physiology and ecology of both endotherms and ectotherms. Intertidal species, despite their marine ancestry, are periodically exposed to extremely stressful and variable terrestrial conditions, and thus have long been regarded as ideal models for understanding how the physical environment drives physiology, biotic interactions, and ecological patterns in nature. The rocky intertidal environment is remarkably variable at a centimeter scale, and the complexity of its small-scale topography ensures that most locations encapsulate a myriad of contrasting microhabitats for species to explore, with vastly different thermal characteristics. Yet, the importance of this variability in determining large-scale macro-ecological processes remains virtually unknown. This thesis takes advantage of this singular system to gain insights on the basic ecological process driving the distribution of species, setting their range limits, and dictating change.

The first chapter sets the context of this thesis by introducing the main theoretical concepts, environmental setting and studied species, and briefly identifying the current gaps in knowledge. The general introduction ends with an outline of the rationale and with a list of the manuscripts that compose the thesis.

The second chapter aims at unravelling the intricate patterns of environmental variability. Firstly, the complexity of the thermal environment of rocky shores along the European Atlantic coast is detailed, showing that thermal differences between sun-exposed and shaded microhabitats are higher than those related to seasons, latitude or shore level. Secondly, a global look into the role of shading provided by coastal topography reveals that in some regions topographical shading may be a major source of habitat complexity. Although likely, the biological significance of this new pattern is yet to be ascertained, opening exciting new opportunities for future research.

Focusing on the microhabitat level, the third chapter sets out to evaluate the implications of the striking levels of environmental variability identified. Through the quantification of the heat-shock proteins present in individuals of *Patella vulgata* Linnaeus, 1758 from different microsites along the European Atlantic coast, it is shown that different thermal histories are consistently associated with differences in physiological performance. The link found confirms that the limiting effects of temperature, rather than being related to latitude, seem to be tightly associated with microsite variability, which therefore is likely to have profound effects on the way local populations (and species) respond to climatic changes. In order to evaluate the relative contribution of water and air temperature during emersion for the build-up of thermal stress, a modern and simplified infrared heartbeat rate sensing system was designed.

This technique overcomes obstacles encountered with previous methods of heartbeat rate measurement, and due to the sensor's small size, versatility, and noninvasive nature, creates new possibilities for studies across a wide range of organismal types. Making use of this new apparatus, a set of laboratorial experiments shows that thermal stress is directly linked to elevated water temperature, while warm air temperature during emersion plays a secondary role. In conjunction with population density data, these results suggest that high water temperature represents a threshold that the intertidal limpet *P. vulgata* is unable to tolerate.

The fourth chapter builds on the previous findings, exploring how complex biogeographic responses to climatic changes may arise from the thermal complexity of the intertidal environment. Importantly, it emphasizes that unless the appropriate temperature metrics (e.g., daily range, min, max) are analyzed, the impacts of climate change may be misinterpreted.

Finally, a general discussion integrates and synthesizes the work in this thesis.

Resumo

A temperatura desempenha um papel crucial no controlo de inúmeros processos biológicos, afetando a fisiologia e ecologia de animais endotérmicos e ectotérmicos. No que se refere aos animais ectotérmicos que ocorrem em zonas intertidais, a sua ascendência marinha significa que a exposição periódica a condições terrestres resulta em elevados níveis de stress, podendo por isso ser considerados modelos ideais para o estudo do modo como o ambiente físico controla a fisiologia, interacções bióticas e padrões ecológicos na natureza. As condições ambientais na zona entre marés de praias rochosas são extremamente variáveis, e a complexidade da sua micro-topografia significa que a maioria dos locais encapsula uma grande quantidade de micro-habitats que as espécies que aí habitam podem potencialmente explorar. Contudo, a importância desta variabilidade para o desenrolar de processos macro-ecológicos ainda permanece praticamente desconhecida. Fazendo uso deste sistema singular, esta tese tem por objetivo a investigação dos processos ecológicos básicos que determinam a distribuição das espécies e que modelam a resposta destas a alterações ambientais.

O primeiro capítulo define o contexto desta tese, introduzindo os principais conceitos teóricos, descrevendo as características mais relevantes do ambiente e das espécies estudadas, identificando também as principais lacunas no conhecimento atual. A introdução geral termina com uma breve descrição do encadeamento das várias tarefas desenvolvidas, bem como com uma lista dos artigos científicos que compõem a tese.

O segundo capítulo tem como objetivo a caracterização da variabilidade ambiental. No primeiro trabalho é feita uma descrição da complexidade do ambiente térmico em praias rochosas ao longo da costa Atlântica da Europa. Os resultados mostram que as diferenças térmicas entre micro-habitats sombreados e expostos ao sol excedem as diferenças associadas às estações do ano, latitude ou posição na zona intertidal. No segundo trabalho é apresentada uma perspetiva global do papel desempenhado pela topografia costeira como fonte de complexidade ambiental. Ainda que provável, a relevância deste novo padrão ambiental permanece especulativa, o que por seu turno abre novas e interessantes vias de trabalho futuro.

Centrando a atenção na escala do micro-habitat, o terceiro capítulo tem como objetivo avaliar as implicações dos elevados níveis de variabilidade ambiental identificados. Através da quantificação dos níveis de proteínas de choque térmico (*heat-shock proteins*) presentes em indivíduos de *Patella vulgata* Linnaeus, 1758 recolhidos de micro-habitats diferentes ao longo da costa Atlântica Europeia, demonstrou-se a associação entre o historial térmico e diferenças no desempenho fisiológico destes animais. A identificação desta conexão confirma que o efeito limitador da temperatura está fortemente associado à variabilidade entre micro-habitats - e não à latitude, o que por sua vez tem diversas implicações na forma como

populações locais (ou mesmo espécies) respondem a alterações ambientais. Seguidamente, de forma a avaliar o contributo relativo da temperatura da água e do ar para os níveis de stress térmico, foi desenvolvido um sistema moderno e simplificado de medição de atividade cardíaca usando radiação infravermelha. A utilização desta técnica permite ultrapassar vários obstáculos frequentemente encontrados noutras técnicas de medição de atividade cardíaca. O tamanho reduzido do sensor, aliado à versatilidade e carácter não invasivo do sistema, permite a realização de inúmeros tipos de estudos em invertebrados com diversas formas corporais. Utilizando este novo equipamento, foram realizadas experiências laboratoriais que demonstraram que o stress térmico está directamente relacionado com temperaturas de água elevadas, tendo a temperatura do ar um papel secundário. Estes resultados, em conjunto com dados de densidade populacional, sugerem que valores elevados de temperatura de água representam um limite que a lapa *P. vulgata* não é capaz de tolerar.

O quarto capítulo recupera os resultados anteriores e explora a forma como alterações climáticas podem levar a respostas biogeográficas não-intuitivas devido à complexidade do ambiente térmico das zonas intertidais, salientando a importância da utilização das métricas da temperatura (e.g., amplitude diária, mínimo, máximo) mais ajustadas à questão e ao organismo em estudo.

Por último, as conclusões extraídas em todos os trabalhos que compõem esta tese são discutidos e sintetizados numa discussão geral.

Contents

List of Tables

List of Figures

1. General Introduction

The final goal of biogeography is to understand why organisms exist where they do today, and where will they exist in the future, especially in face of change. Thus, unsurprisingly, distribution patterns, and the factors that control them, comprise a vast portion of the research effort of biogeographers. However, despite considerable attention and effort, numerous gaps persist in our comprehension of species' distributions. In particular, understanding how environmental factors acting at the scale of organisms are translated into distribution patterns remains a remarkably complex task. Still, those difficulties have not deterred researchers from addressing the issue, especially as society grows conscious of the impending biological impacts brought about by climate change. In this thesis, I analyze environmental complexity and attempt to shed light on the mechanisms by which the influence of microclimate on organisms is scaled up, eventually determining species' distributions. Results are interpreted not only in the context of climatic changes, but also in terms of their contribution to fundamental ecology. Due to their remarkable environmental complexity, and building on centuries of research, attention was focused on the thermal regimes of intertidal rocky shores of the European Atlantic coast.

1.1 Temperature, a major driver of species' distribution patterns

Temperature controls the pace of biochemical reactions, and beyond certain levels it can damage an organism's biochemical machinery. The pervasive influence of temperature has long been recognized, and it is considered to be one of the most important drivers of biological processes on rocky shore ecosystems, affecting the physiology (Dahlhoff et al., 2001; Somero, 2002; Fuller et al., 2010; Hofmann and Todgham, 2010) and ecology (Porter and Gates, 1969; Wethey, 2002; Helmuth et al., 2006a; Yamane and Gilman, 2009) of intertidal species. Owing to its spatial heterogeneity, temperature is also a key factor in determining the distribution patterns and range limits of species (Southward, 1958; Southward et al., 1995; Helmuth, 1998; Sagarin et al., 1999; Helmuth et al., 2006a; Lima et al., 2007a; Wethey and Woodin, 2008; Berke et al., 2010).

1.2 The rocky intertidal

The rocky intertidal zone, which lies between the high and low tide marks on the shores of the world's oceans, has long served as a natural laboratory for examining relationships between abiotic stresses, biotic interactions, and ecological patterns in nature (Orton, 1929;

Southward, 1958; Connell, 1972; Wethey, 1984; Bertness et al., 1999; Somero, 2002). The intertidal environment is remarkably dynamic, and despite their marine ancestry, organisms inhabiting there are periodically exposed to extremely stressful and variable terrestrial conditions (Southward, 1958; Southward et al., 1995; Raffaelli and Hawkins, 1996; Denny and Wethey, 2000; Harley, 2008).

1.2.1 Environmental mosaic

The thermal regimes of intertidal ecosystems are inherently complex. During high tide they are dominated by the stability of water temperature, while during low tide air temperature, humidity, solar radiation and wind generate highly variable temperature profiles. More importantly, given that most intertidal organisms are small in size, the micro-topographical complexity of rocky outcrops ensures that most shores encapsulate a myriad of microhabitats for species to explore, with vastly different thermal profiles (Helmuth, 1998, 2002; Wethey, 2002; Helmuth et al., 2005; Harley, 2008; Lima and Wethey, 2009). In fact, the availability of such microhabitats has been recognized as a major factor determining the distribution of intertidal species, particularly towards the limits of their distribution ranges (Helmuth et al., 2006a; Bennie et al., 2008). In addition, micro-scale variability of desiccation and wave impact forces (Foster, 1971; Denny et al., 1985; McMahon, 1990; Burrows et al., 2008) further enhances intertidal habitat complexity.

1.2.2 The European Atlantic coast

There are various reasons why the European Atlantic coast is the ideal location for the study of the interplay between environmental factors and species' distributions. First and foremost, this region of the world has long been the subject of a vast research effort in numerous fields, resulting in a continuous record of the environment and organisms inhabiting its intertidal ecosystem which dates back many decades (Orton, 1929; Fischer-Piette, 1935; Smith, 1935; Evans, 1948; Southward and Crisp, 1952; Fischer-Piette, 1953; Southward and Crisp, 1954). This provides researchers with an important historical context and facilitates the interpretation of biogeographic patterns. Second, the polar and equatorial range limits of numerous intertidal species occur along its coast (Fischer-Piette and Gaillard, 1959; Fischer-Piette, 1959, 1963; Ardré, 1970), providing a richness of biological models for the testing of important biogeographic questions. Third, the convoluted nature and peculiar coastal geomorphology of the European Atlantic coast generates complex regional atmospheric and oceanographic features that accentuate environmental gradients (Lemos and Pires, 2004; Lemos and Sansó, 2006). This in turn leads to complex distribution patterns, such as the distribution gap shared by many species along the shores of the Bay of Biscay (Fischer-Piette, 1955; Crisp and Fischer-Piette, 1959; Fischer-Piette and Gaillard, 1959; Christiaens, 1973).

1.3 Climate change

Since the establishment of the Intergovernmental Panel on Climate Change (IPCC) in 1988, climatic patterns continue to change at a steady pace (Karl et al., 2015), and so has our knowledge about this phenomenon. In particular, the scientific community is now aware that climate change does not simply mean homogenous global warming, but instead a global warming trend accompanied by increasing climatic instability (Easterling et al., 2000; Helmuth et al., 2011; Lima and Wethey, 2012; IPCC, 2013; Vasseur et al., 2014). Furthermore, such changes are now known to have a spatially heterogeneous impact, with regions warming at different rates – or even cooling (Lima and Wethey, 2012; Baumann and Doherty, 2013), and precipitation, wind and wave patterns being redistributed at a global scale (Bakun, 1990; Easterling et al., 2000; Hemer et al., 2013; Varela et al., 2015).

1.4 Complex biological responses

The challenges imposed by such climatic changes in biological systems are enormous. Response via adaptation, the main mechanism that has allowed species to negate – or even profit – from environmental change, is severely precluded by the extreme pace of recent climatic changes (Burrows et al., 2011; Mahlstein et al., 2013). Thus, it is no surprise that the effects of climate change are being detected in numerous species, mainly in the form of alterations to phenological timings and retreat or expansion of range limits (Walther et al., 2002; Parmesan and Yohe, 2003; Root et al., 2003; Hickling et al., 2006; Lima et al., 2007a; Poloczanska et al., 2013). And future scenarios offer no comfort, as climate change is forecasted to strain environmental conditions further, even under the most optimistic projections (IPCC, 2013). Intertidal ecosystems, where organisms already exist close to their physiological limits (Somero, 2002; Stillman, 2003; Sunday et al., 2012), are expected to take the brunt of the impact (Harley et al., 2006), with hard-to-predict consequences for ecosystem structure and function (Paine and Trimble, 2004; Girard et al., 2012; Jurgens et al., 2015).

1.5 General objectives

The present compilation of studies can be conceptually divided into three main sections. The first section entails the description of the thermal environment of rocky shores, and how it shapes thermal stress experienced by intertidal organisms. It exposes the heterogeneity of microhabitat temperatures along European Atlantic rocky shores (section 2.1) and explores the effect of regional coastal morphology in modifying local environmental conditions (section 2.2). The second comprises the analysis of how environmental variability shapes thermal stress experienced by intertidal organisms. It confirms that microhabitat heterogeneity has direct consequences in the thermal stress levels of the intertidal limpet *Patella vulgata* (section

3.1), describes the development of a tool for measuring the cardiac activity of invertebrates, vital for non-invasively assessing the physiological state of intertidal animals responding to environmental conditions (section 3.2), and identifies water temperature as the main driver for the establishment of *P. vulgata*'s range limits (section 3.3). Finally, the third and last part of the work explores how complex biogeographic responses to climatic changes may arise from the thermal complexity of the intertidal environment (section 4.1).

1.6 Submitted and published manuscripts

The present thesis encompasses results from a project that was developed during the last six years. The thesis is presented as a series of linked chapters, each including one or more sections. Each section is a paper or a manuscript (accepted, or submitted). A general discussion integrates and synthesizes the work in the thesis.

List of papers and manuscripts:

- Seabra R, Wethey DS, Santos AM & Lima FP (2011). Side matters: microhabitat influence on intertidal heat stress over a large geographical scale. Journal of Experimental Marine Biology and Ecology. 400(1-2):200-208. (DOI: 10.1016/j.jembe.2011.02.010)
- Seabra R, Wethey DS, Santos AM & Lima FP (Submitted). Topographical shading shapes coastal habitat complexity.
- Lima FP, Gomes F, Seabra R, Wethey DS, Seabra I, Cruz T, Santos AM & Hilbish TJ (2015). Loss of thermal refugia near equatorial range limits. Global Change Biology. (in press, DOI: 10.1111/gcb.13115)
- Burnett NP, Seabra R, de Pirro M, Wethey DS, Woodin SA, Helmuth B, Zippay ML, Sarà G, Monaco C & Lima FP (2013). An improved noninvasive method for measuring heartbeat of intertidal animals. Limnology and Oceanography: Methods. 11(2):91-100. (DOI: 10.4319/lom.2013.11.91)
- Seabra R, Wethey DS, Santos AM, Gomes F & Lima FP (Submitted). Equatorial range limits of an intertidal ectotherm are more linked to water than air temperature.
- Seabra R, Wethey DS, Santos AM & Lima FP (2015). Understanding complex biogeographic responses to climate change. Scientific Reports. 5, 12930. (DOI: 10.1038/srep12930)

2. The environment at multiple scales

2.1 Side matters: Microhabitat influence on intertidal heat stress over a large geographical scale

2.1.1 Abstract

The present study examined the relative magnitudes of local-scale versus large-scale latitudinal patterns of intertidal body temperatures, using data loggers mimicking limpets from the genus *Patella*. Over approximately 18 months, loggers collected continuous 30-minute resolution data on body temperatures at a variety of microhabitats on 13 rocky shores along the Atlantic coast of the Iberian Peninsula. Data showed that during low tide, body temperatures of sun-exposed animals routinely reached much higher temperatures than their counterparts attached to north-facing, shaded surfaces. Sunny versus shaded differences were consistently larger than the variability associated with the seasons and with shore level. Moreover, daily variation far exceeded that observed when considering only averaged sea surface temperature. Therefore, analyzing temperature at the scales of the organisms may provide a wealth of information more suited to understand and model the distribution of intertidal species under present and future climatic scenarios.

2.1.2 Introduction

The intertidal environment is inhabited by organisms that, despite their marine ancestry, are periodically exposed to extremely stressful and variable terrestrial conditions (Southward, 1958; Southward et al., 1995; Raffaelli and Hawkins, 1996; Denny and Wethey, 2000; Harley, 2008; Firth et al., 2011). Among all terrestrial stressors (e.g., temperature, desiccation, solar radiation), temperature has been identified as one of the most effective, affecting the physiology (Dahlhoff et al., 2001; Somero, 2002; Fuller et al., 2010; Hofmann and Todgham, 2010; Lockwood and Somero, 2011), ecology (Porter and Gates, 1969; Wethey, 2002; Helmuth et al., 2006b; Yamane and Gilman, 2009; Helmuth et al., 2011; Sorte et al., 2011) and biogeography (Southward, 1958; Southward et al., 1995; Helmuth, 1998; Sagarin et al., 1999; Helmuth et al., 2006b; Lima et al., 2007a; Wethey and Woodin, 2008; Berke et al., 2010) of intertidal animals and algae.

Even though it has long been shown that body temperatures of intertidal organisms can depart significantly from air and surface temperatures (Evans, 1948; Southward, 1958; Wethey, 2002) the lack of appropriate technology forced most studies to indirectly estimate thermal stress from low-resolution sea surface temperature (SST) data (e.g., see the aforementioned

articles). Crucial long-term body temperature data have only recently been routinely recorded, following the development of miniaturized sensors and loggers, now available to intertidal ecologists (Helmuth and Hofmann, 2001; Fitzhenry et al., 2004; Lima and Wethey, 2009; Lima et al., 2010). These data have shown that many invertebrate species can experience daily fluctuations in body temperatures exceeding 20 °C while exposed to the air (Helmuth and Hofmann, 2001; Helmuth, 2002; Helmuth et al., 2010), a range that is far greater than the yearly variation of coastal sea temperature at most locations.

Daily variations in temperature may also be radically different between individuals just a few meters apart but in surfaces facing different directions (Helmuth, 1998, 2002; Wethey, 2002; Helmuth et al., 2005; Harley, 2008; Lima and Wethey, 2009) because during aerial exposure other factors such as the micro-topography, air temperature, wind speed, solar radiation and relative humidity come into play, interacting with the physical characteristics of the organisms such as their thermal inertia (Spotila et al., 1973), shape and color (Helmuth, 1999; Denny et al., 2006; Gilman et al., 2006) to determine the organism's body temperature. Thus, temperatures during aerial exposure are likely to be one of the major sources of acute stress for intertidal organisms (Pincebourde et al., 2008; Mislan et al., 2009; Helmuth et al., 2010; Schneider et al., 2010).

The present study aimed primarily at examining the relative magnitudes of local-scale versus large-scale latitudinal patterns of intertidal body temperatures, using data loggers mimicking limpets from the genus *Patella* (Lima and Wethey, 2009). In addition, since the work focused on intertidal organisms, we investigated how much the observed patterns differed between high and low tide periods. In the North-eastern Atlantic, limpets are keystone players in the complex network of ecological relations among intertidal organisms, determining algal abundance and modifying ecosystem stability (Southward, 1964; Hawkins and Hartnoll, 1983; Southward et al., 1995; Boaventura et al., 2003; Coleman et al., 2006; Jenkins et al., 2008). Thus, any change on their physiological performance or distribution will likely have cascading effects on the community. Other factors were important in choosing *Patella* spp. as models to build biomimetic temperature loggers. These included the large geographical distribution of the genus (with different species displaying different latitudinal limits and distributional gaps), the association of each species with a characteristic microhabitat or shore level (each one is exposed to a different thermal regime) and, in particular, the fact that recent data suggest a strong association between distributional changes in one of the species (*Patella rustica* Linnaeus, 1758) and changes in SST (Lima et al., 2006).

2.1.3 Material and Methods

Biomimetic temperature data loggers

Robolimpets (autonomous temperature sensor/loggers mimicking the visual aspect and temperature trajectories of real limpets) were built following Lima and Wethey (2009). Briefly,

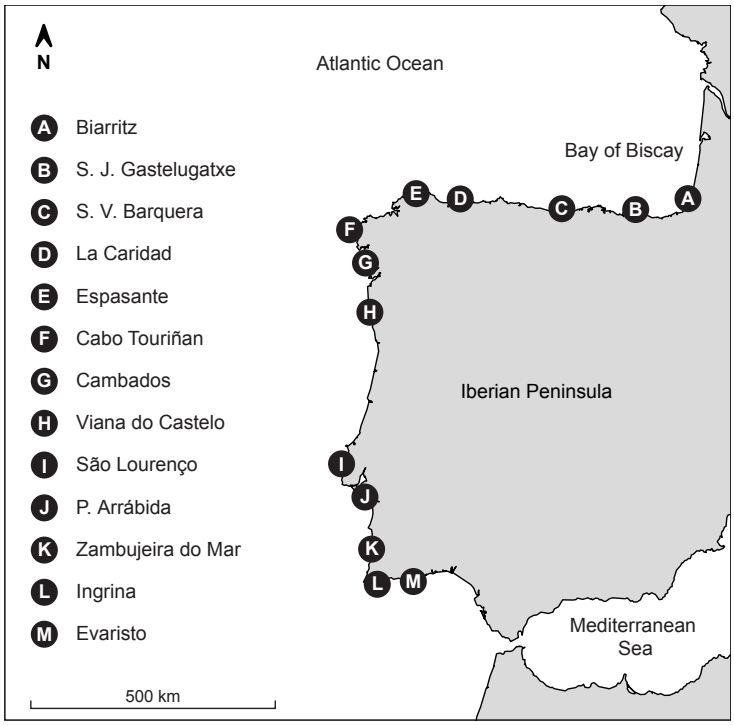

Figure 2.1: Study area. Deployment locations along the Atlantic coast of the Iberian Peninsula are depicted by the black circles.

these devices consist of a lithium battery powering the circuit board extracted from a DS1922L iButton (Dallas Semiconductor), embedded in a waterproof resin (3M Scotchcast 2130 Flame Retardant Compound), and placed inside an empty limpet shell (in the present work, from *Patella* spp.). Two exposed wires penetrating the shell serve as contacts for logger programming and subsequent data retrieval. This design has previously been shown to accurately track the temperature profiles of live animals in the field, with errors smaller than the variability obtained by measuring the temperature of live animals a couple of meters apart (Lima and Wethey, 2009). Finally, because factory calibrations were lost when a Panasonic BR1255-1VC 3 V cell was used to replace the iButton battery (Lima and Wethey, 2009), assembled loggers were calibrated in the lab prior to field deployments (see Lima et al., 2010, for more details), restoring the original 0.5 °C logger accuracy.

Study area and deployment scheme

Intertidal temperatures were measured at 13 exposed or moderately exposed rocky shores along 1500 km of the Atlantic coast of the Iberian Peninsula (Fig. 2.1). This coast encompasses a wide range of climatic and oceanographic conditions, such as a north to south cline in SST during the winter, and an alternation between warm and cold SST regions in summer. In this season, the strong upwelling off NW Iberia disrupts the latitudinal SST cline, making this region much cooler than either the NE or the SW Iberia (Lima et al., 2006; Wethey and Woodin, 2008; Berke et al., 2010).

At each location, biomimetic loggers were attached to steep rocky surfaces (i.e., with slopes between 60° and 90°) with Z-Spar Splash Zone Compound (Kop-Coat Inc., Pittsburgh, Pennsylvania, USA) at three tidal heights, thus covering the entire vertical range inhabited

by limpets. 'Low-shore' loggers were attached to the rock at the upper limit of the red algae belt, horizontally aligned with the lower distributional limit of *P. ulyssiponensis* Gmelin, 1791. 'Mid-shore' loggers were deployed centred in the zone dominated by mussels (*Mytilus* sp.) and barnacles (*Chthamalus* spp.), amongst *P. depressa* Pennant, 1777 and *P. vulgata* Linnaeus, 1758. 'High-shore' loggers were placed close to the lower limit of the black lichen *Lichina pygmaea* (Lightfoot) Agarth, 1821, at the upper limit of the distribution of *P. vulgata* and *P. rustica*. At each level, robolimpets were deployed in both north-facing (typically shaded) and south-facing (sun-exposed) rock surfaces. The combination of three heights and two orientations defined six microhabitats with potentially distinct thermal characteristics. Loggers were deployed in triplicate, for a total of 18 per shore. Robolimpets were programmed in the field with a laptop computer using a custom made communication cable (see Lima and Wethey, 2009) in association with the OneWireViewer software (www.maxim-ic.com). Loggers were programmed to record data at every 30 min, using a resolution of 0.5 °C in order to achieve long deployments (i.e., periods of 170 days). Thus, servicing occurred with a periodicity of approximately five months. At each visit to the shore, data was downloaded from working loggers, which were then reprogrammed, while malfunctioning loggers were replaced. Deployments were made between January 2008 and September 2009.

Data analysis

Data files were individually checked for any evidence of logger malfunction (e.g., in a few devices the internal clock stopped during the deployment), and discarded if necessary. Additionally, any interference due to logger handling in the field was eliminated by removing the first and the last 24 h of data from each logger. At each location, and for each deployment period x microhabitat combination, logged temperatures were averaged whenever data from multiple sensors was available. Thus, depending on the deployment period, the long-term thermal profiles could have been derived from 1–3 loggers (see Supp. Fig. 2.8 for the data coverage map). Finally, because tide cycles are not in phase across large geographical scales, an additional computation step was performed so that temperature values could be compared among locations. For example, in a one-to-one data point comparison, two identical thermal trajectories from distinct locations would be apparently different simply because they were 1h out-of-synchrony (which is, for instance, the average time difference in tide timing between SW France and SW Portugal). Thus, three different statistics were calculated (daily maximum, daily minimum and daily accumulated degrees-hour) to obtain single daily values which could then be compared across locations. In addition, to separately quantify thermal stress during aerial and submerged periods, statistics were also calculated for two data subsets (one consisting exclusively of temperature measurements two hours around local high tide, and a second one encompassing only those measurements taken two hours around local low tide). Both day-time and night-time tides were considered. Tidal elevation was obtained using the WTides software package (www.wtides.com).

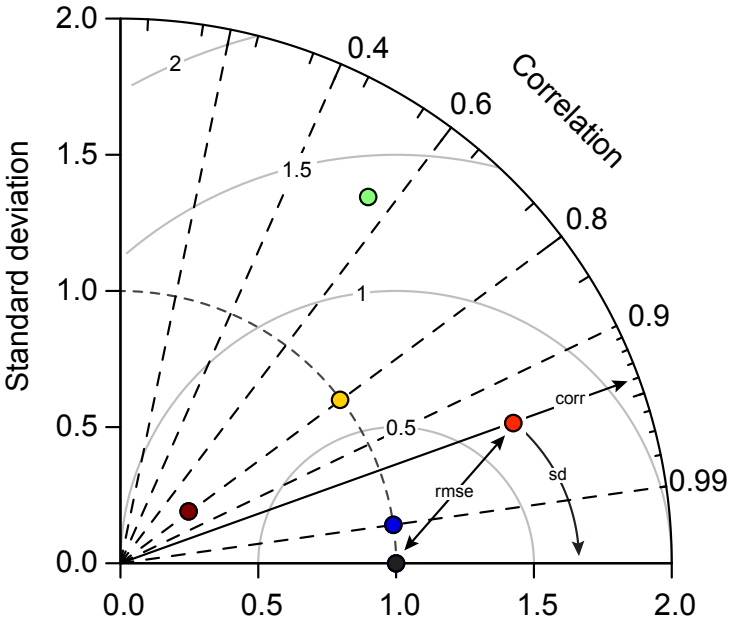

Figure 2.2: Example of a Taylor diagram. The colored circles represent different temperature profiles being compared with a reference (depicted in black). The angular coordinate of a given point indicates the correlation between that dataset and the reference (corr). Its radial distance from the reference shows its centred root mean square error (rmse), and the distance from the origin of the graph equals to the standard deviation (sd), normalized by the reference value.

Taylor diagrams were used to analyze similarity between thermal profiles. These diagrams have originally been devised for concisely summarizing the degree of correspondence between a suite of climatological model outputs and a known reference (Taylor, 2001). Taylor diagrams are particularly useful in evaluating multiple aspects of complex data series, since each graph shows a statistical summary of how well patterns match each other in terms of their correlation, their centred root mean square error (RMSE), and the ratio of their variances. When used separately, these three metrics provide quite incomplete estimates of the similarity between two datasets. For example, the RMSE is widely used to express the mean difference between two data series, but from a given RMSE alone it is impossible to understand if the two series are in phase or out-of-phase. This can be easily solved by providing a correlation coefficient along with the RMSE. Thus, two datasets are more similar if they have a small RMSE and a high correlation. Still, from those two metrics alone it is still not possible to determine whether two patterns have the same amplitude of variation, and so there is the need to consider the ratio of their variances (two patterns are more alike as the ratio of their variance approaches 1). Taylor diagrams show a visual representation of the three values at once and thus provide a quick but comprehensive summary of the degree of pattern correspondence. This method can also be used to summarize the relative skill of several datasets, identifying which one better resembles the reference.

A sample Taylor diagram can be found in Fig. 2.2. Each dataset is represented by a point and its position in the plot quantifies how closely it matches the reference. The radial distance from the origin represents the amplitude of the temperature variation (standard deviation), normalized by the reference value. Thus, the closer a given point is to the radial line that crosses through the normalized reference value (sd $= 1$), the most similar that data is to the reference. The azimuthal angle of a particular point indicates its correlation to the reference. Thus, points closer to the bottom of the graph are generally more correlated with the reference.

Finally, the distance between a point and the reference shows the mean absolute difference between those datasets. Also here, points closer to the reference are more similar. For example, in Fig. 2.2, the hypothetical temperature trajectory represented by the red point has: (i) a correlation slightly higher than 0.9 in relation to the reference — as seen on the projection of the point in the curved right margin of the graph, (ii) an internal variability equivalent to approximately 1.5 times the standard deviation of the reference — as seen on the projection of the point on the horizontal axis, and finally, (iii) a mean absolute difference (RMSE) of 0.6 °C — as determined by its radial distance from the reference (black) point. In this example, it is also possible to see that even though the yellow and brown datasets have similar correlation coefficients (0.8) in relation to the reference, the variability of the data represented by the yellow point perfectly resembles the variability of the reference, while the brown dataset is much less variable. On average, data represented by the brown circle is also more different from the reference (~0.77 °C), when compared with the yellow dataset (~0.6 °C). Thus, the yellow point represents a data series more similar to the reference than the data series shown by the brown point. The green point has the worst correlation (approximately 0.5) and the worst RMSE (1.4 °C), but its variability in relation to the reference is similar to that of the red point. Still, and overall, the green point represents the dataset less similar to the reference. On the other hand, the blue circle shows the temperature profile with the highest similarity. It is the point that is closest to the reference, with a correlation of 0.99, a RMSE of less than 0.1 °C and a variability equivalent to the reference data.

A key analysis in the present work was to determine if the magnitude of the differences in body temperature was larger between opposing (sun versus shade) microhabitats at the same shore or, on the other hand, if it was greater across the latitudinal gradient for the same microhabitat. Thus, using a single Taylor diagram, each microhabitat (e.g., Biarritz mid-shore, sun-exposed) was directly compared with the opposing microhabitat from the same shore (Biarritz mid-shore, shade) and with the same microhabitat from the remaining shores (mid-shore, sun-exposed in all other locations). All data manipulation and subsequent analyses were done in R 2.11 (R Development Core Team, 2010), and Taylor plots were produced using the plotrix package (Lemon, 2006) for R.

2.1.4 Results

The data coverage map is shown in Supp. Fig. 2.8. Despite some sporadic logger failures, temperature data was available for most microhabitats throughout the deployment period. Simultaneous data gaps (as happened in the beginning of 2009 across most locations) were caused by loggers' memory limitations. Apart from that, the few cases of complete data loss across an entire microhabitat were almost invariably caused by deliberated logger destruction by beach combers or by fishermen harvesting intertidal gastropods. Generally, individual profiles were dominated by two main sources of variability. On one hand, all robolimpets displayed the

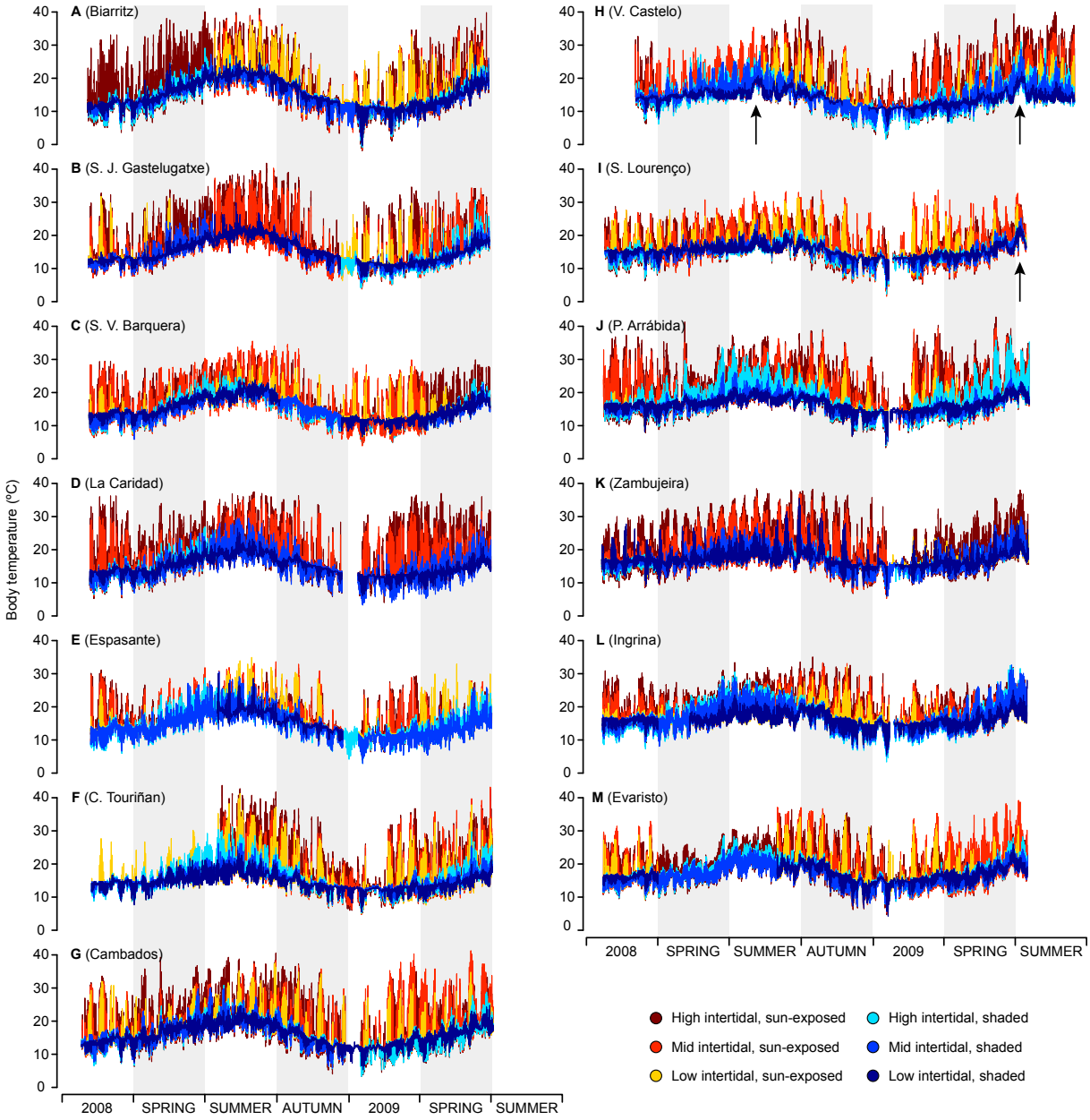

Figure 2.3: Body temperature profiles obtained by robolimpets deployed at different microhabitats (depicted by the different line colors), within the 13 sampled locations, ordered from NE to SW Iberia (letters A–M, see also Fig. 2.1). Arrows indicate periods of upwelling relaxation off W Iberia.

typical seasonal pattern of sea water temperature variation, with the warmest temperatures during summer and the coldest temperatures during the winter (Fig. 2.3). Seasonality was also more evident along the northern coast of the Iberian Peninsula (Fig. 2.3A–E) in comparison with the upwelling-dominated western Iberia (Fig. 2.3F–M). On the other hand, high-frequency temperature oscillations, routinely exceeding 20 °C in less than 12 h (and even 30 °C on high shore loggers in summer) were clearly associated with tidal effects. High-frequency variability was especially remarkable in data from sun-exposed microhabitats, irrespectively of their height on the shore (see Fig. 2.4A for an example and Supp. Fig. 2.9 for all locations).

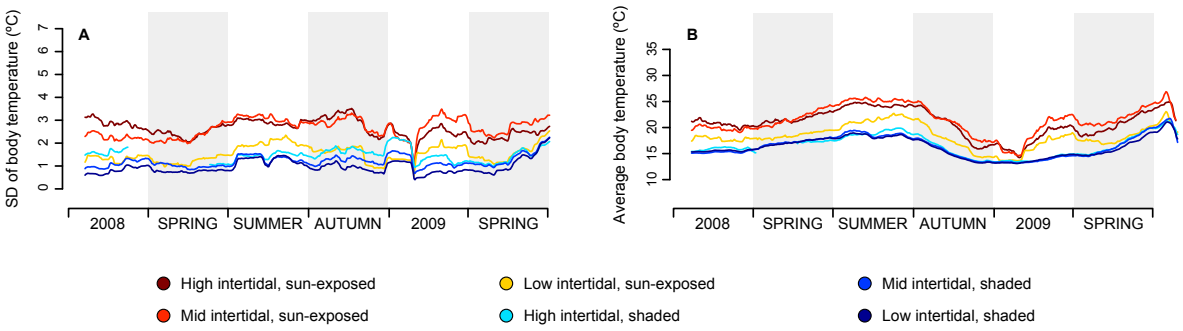

Figure 2.4: 30-day rolling average of standard variation (SD) of temperature profiles (A), and 30-day rolling average of daily temperature maxima (B) for São Lourenço, in W Iberia.

During low tide, sun-exposed robolimpets reached much higher maximum temperatures than their counterparts attached to north-facing surfaces (see Fig. 2.4B for an example and Supp. Fig. 2.10 for all locations), despite the fact that they were at the same tidal height and horizontally separated by less than a couple of meters. This difference was visible year-round, although its magnitude varied between seasons and locations. Temperature trajectories also showed the alternation between spring and neap tides, with daily maxima regularly oscillating in periods of approximately two weeks. This was particularly visible at locations with weaker seasonal influence (e.g., Fig. 2.3I,K). Taylor plots displayed analogous patterns across locations (the complete set of plots can be found at Supp. Fig. 2.11; a small subset is shown for the mid-intertidal at Biarritz in Figs. 2.5, 2.6 and 2.7). In general, results showed that either (i) the reference microhabitat was more closely related to the opposing microhabitat in the same shore, or (ii) that differences between the sun-exposed and shaded microhabitats were large enough so that the same habitat in other geographical locations was more similar to the reference. The first outcome was observed in 93% of the analyses comparing body temperatures measured during high tide (e.g., Fig. 2.5) or in 80% of the analyses where only minimum temperatures were considered, regardless of the tidal cycle (e.g., Figs. 2.5A,D, 2.6A,D and 2.7A,D). The latter minimum temperatures are a proxy for emersion during the night. Hence, both cases reflect conditions where temperature experienced by organisms is homogeneous throughout the habitat, being independent of the shore level or surface orientation. Additionally, in any of the aforementioned cases, a clear latitudinal pattern in likeliness was also observed, with locations geographically near showing higher similarity values (clustering) in the Taylor diagrams. The second outcome was observed in 91% of the analyses focusing on maximum body temperatures or on the sum of all degree-hours measured either during low tide (Fig. 2.6B,E,C,F) or in 70% of the analyses involving the whole tidal cycle (Fig. 2.7B,E, and C,F). Thus, whenever the analyses encompassed periods of air exposure during the day, shaded microhabitats were consistently more similar to shaded microhabitats on any other location than to any sun-exposed microhabitat on the same shore.

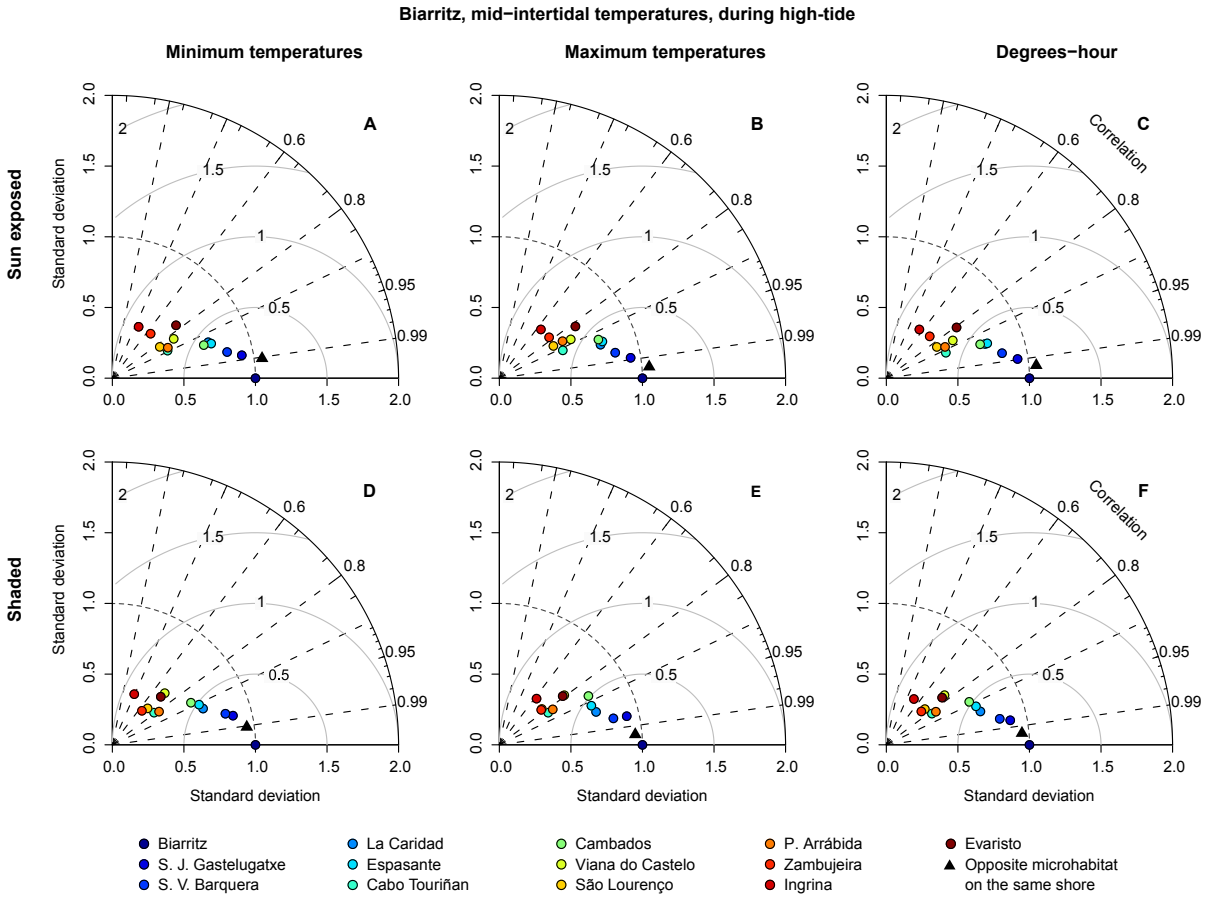

Figure 2.5: Taylor diagrams for robolimpet temperatures at Biarritz during a two-hour interval around high tide. The radial distance from the origin represents the amplitude of temperature variation (standard deviation). The azimuthal angle depicts the correlation coefficient between the reference and the remaining microhabitats, while their RMSE is shown by the concentric lines centred on the reference.

2.1.5 Discussion

This work provided the first long-term series of intertidal animals' body temperatures in a range of microhabitats, obtained by means of standardized methods, across a large geographical area. Overall, at each sampled location, maximum daily body temperatures were frequently associated with day-time emersions, while low peaks were linked to radiative and evaporative cooling during nocturnal low tides (see Denny and Harley, 2006; Gilman et al., 2006). Moreover, stable, overlapping temperature trajectories among different microhabitats corresponded to periods of logger immersion at high tide (hence reaching thermal equilibrium with sea water). Even though daily body temperature peaks during low tide have already been described for several intertidal animals (e.g., Denny and Harley, 2006; Szathmary et al., 2009; Jones et al., 2010) and algae (Pearson et al., 2009), data from the present work showed that even low-shore organisms are periodically exposed to temperatures exceeding 30 °C. Unexpectedly, these values were routinely experienced even at the northernmost locations (e.g., Fig. 2.3A). The most relevant finding of the present study is that the pervasive difference in temperature trajectories between sun-

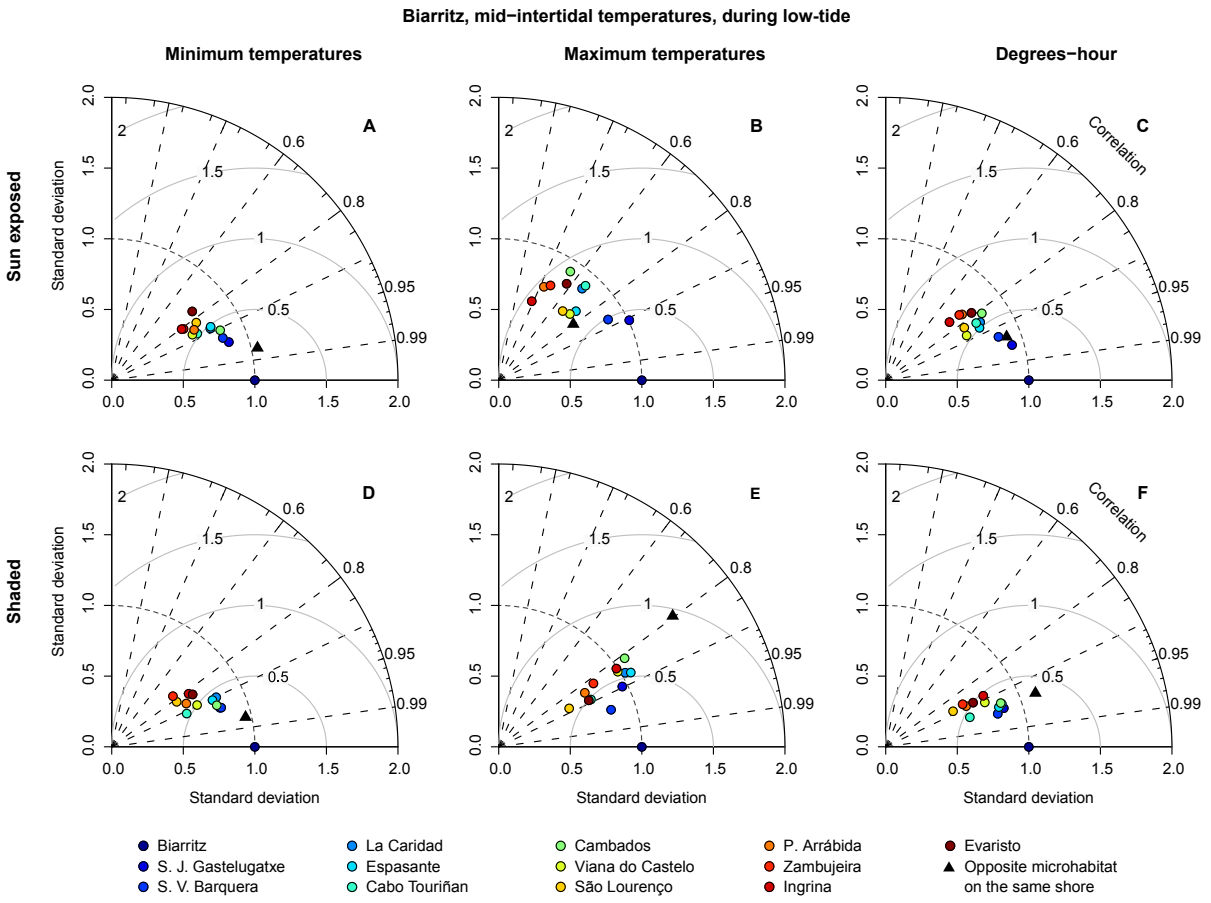

Figure 2.6: Taylor diagrams for robolimpet temperatures at Biarritz during a two-hour interval around low tide. The radial distance from the origin represents the amplitude of temperature variation (standard deviation). The azimuthal angle depicts the correlation coefficient between the reference and the remaining microhabitats, while their RMSE is shown by the concentric lines centred on the reference.

exposed and shaded microhabitats may be a common feature of intertidal habitats, even across large geographical areas subjected to heterogeneous climatic and oceanographic conditions. Sunny versus shaded differences were consistently larger than the variability associated with the seasons, with shore-specific characteristics (topography, orientation, wave exposure, etc.) and with shore level (Fig. 2.3). Regarding the similarity patterns found during high tide, robolimpets' thermal trajectories were clearly driven by sea temperature, which suppressed any differences attained during emersions. In this scenario, similarities were typically higher between areas that were spatially closer (the opposite surfaces of the same rocky outcrop), decreasing consistently as geographical distance increased. Temperature profiles exhibited a more pronounced seasonality in the N and NE Iberia, when compared with the western coast. While the oceanographic conditions in the Bay of Biscay are in general characterized by a weak upwelling and low turbulence, particularly during the warm season (Borja et al., 1996, 2008; Bode et al., 2009), in the western Iberia coastal temperatures are strongly influenced by the development of an upwelling system during summer and early autumn months (Peliz et al., 2002; Lemos and Pires, 2004; Lemos and Sansó, 2006; Relvas et al., 2007). Interestingly,

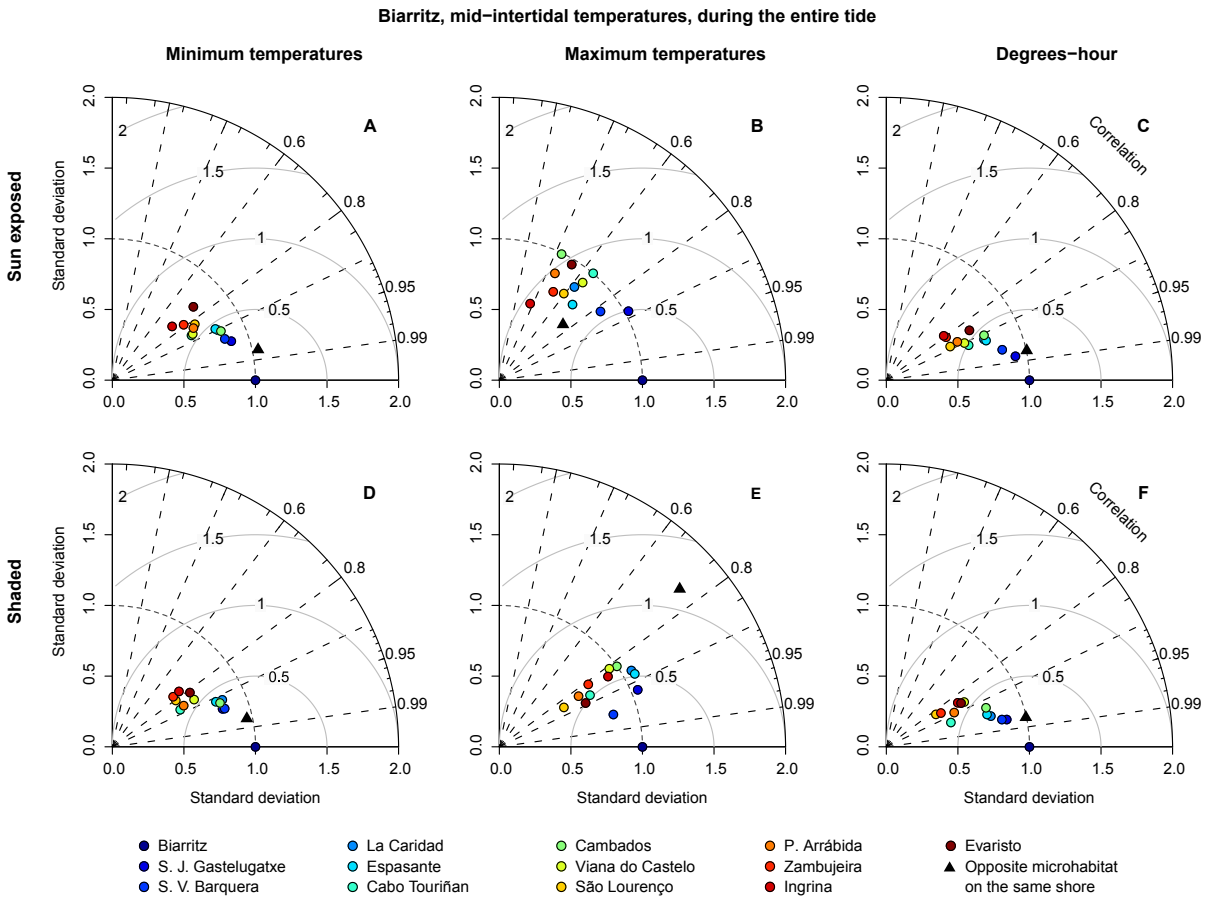

Figure 2.7: Taylor diagrams for robolimpet temperatures at Biarritz during the entire tide. The radial distance from the origin represents the amplitude of temperature variation (standard deviation). The azimuthal angle depicts the correlation coefficient between the reference and the remaining microhabitats, while their RMSE is shown by the concentric lines centred on the reference.

present results suggest that the cooling influence of the upwelling system propagates into the innermost coastal waters, driving, to a great extent, body temperatures of intertidal animals (see for instance how temperature profiles south of Viana do Castelo in Fig. 2.3H–L are more leveled than in the northernmost locations). Even higher-frequency and smaller-scale events such as the intermittent upwelling relaxation which is characteristic of this region (Moncoiffe et al., 2000; Relvas et al., 2007) influenced logged temperatures (e.g., rapid increases in sea temperature registered at Viana do Castelo and S. Lourenço in the summers of 2008 and 2009 — please see arrows in Fig. 2.3H,I). The present findings emphasize the importance of analyzing temperature variability at scales relevant to the organisms, since the usage of SST derived from remote sensed data to model the distribution of intertidal species (e.g., Poloczanska et al., 2008) may be missing key environmental features (Helmuth et al., 2010). Results clearly show that other factors than SST play a much stronger role in determining the body temperatures of these organisms, even at lower levels on the shore. Hence, even the organisms that are only exposed during extreme low tides can be routinely subjected to potentially stressful conditions. Overall, the observed temperature variability may explain the weak correlations

found in many studies modeling the distribution of intertidal species using SST data (e.g., Lima et al., 2007b), which negatively impacts attempts of forecasting distributional changes in response to predicted climate warming. Conversely, habitat heterogeneity as determined by surface orientation and, to a lesser extent, height on the shore may provide thermal refugia allowing species to occupy habitats apparently inhospitable when considering only average temperatures. This may be important for understanding range shifts contrary to global warming predictions (e.g., Lima et al., 2007a, 2009; Hilbish et al., 2010). In the specific case of intertidal limpets, the present results may be used for establishing theoretical frameworks upon which hypotheses can be formulated and tested. For example, future studies could try to find whether different body temperatures observed in association with sunny/shaded microhabitats translate into different levels of physiological stress. It would also be interesting to understand if limpets take advantage of the small-scale thermal differences in their habitat to regulate their body temperature according to their physiological requirements (e.g., by seeking shade in response to intense solar radiation). There is evidence that the more northern limpet species (e.g., *Patella vulgata*) seek shade under fucoid clumps, whilst other species (e.g., *Patella depressa*, a southern species) do not (Moore et al., 2007). On the other hand, biomimetic loggers (robolimpets) could be used in association with experimental manipulations in the field to find if (and to which extent) limpet grazing is determined by the thermal environment. That information is important not only for the study of the ecology, physiology and behavior of these gastropods but also for understanding the network of ecological relations among intertidal organisms, given the broad importance of limpet grazing in intertidal systems (e.g., Hawkins and Hartnoll, 1983; Coleman et al., 2006; Jenkins et al., 2008). These results are remarkable in that they show that thermal differences between microhabitats separated by only a few meters on a shore (sunny versus shaded microhabitats) are more different than sites hundreds of km apart. It has long been appreciated that there are strong physical gradients between the high and low tide-marks on shores, but differences between sunny and shaded microhabitats have been less well understood, and the data presented here indicated that they overwhelm differences between shore levels. These results suggest that thermal heterogeneity within habitats must be fully understood in order to interpret patterns of biogeographic response to climate change.

2.1.6 Acknowledgements

The authors thank Nuno Queiroz, Lara Sousa, Raquel Xavier, Sérgia Velho, Pedro Ribeiro and Jerry Hilbish for their help during fieldwork and for their insightful suggestions. Funding was provided by grants from NOAA (NA04NOS4780264), NASA (NNG04GE43G and NNX07AF20G), National Science Foundation (OCE1039513) and Fundação para a Ciência e a Tecnologia (PTDC/MAR/099391/2008 and SFRH/BPD/34932/2007).

2.1.7 Supplementary data

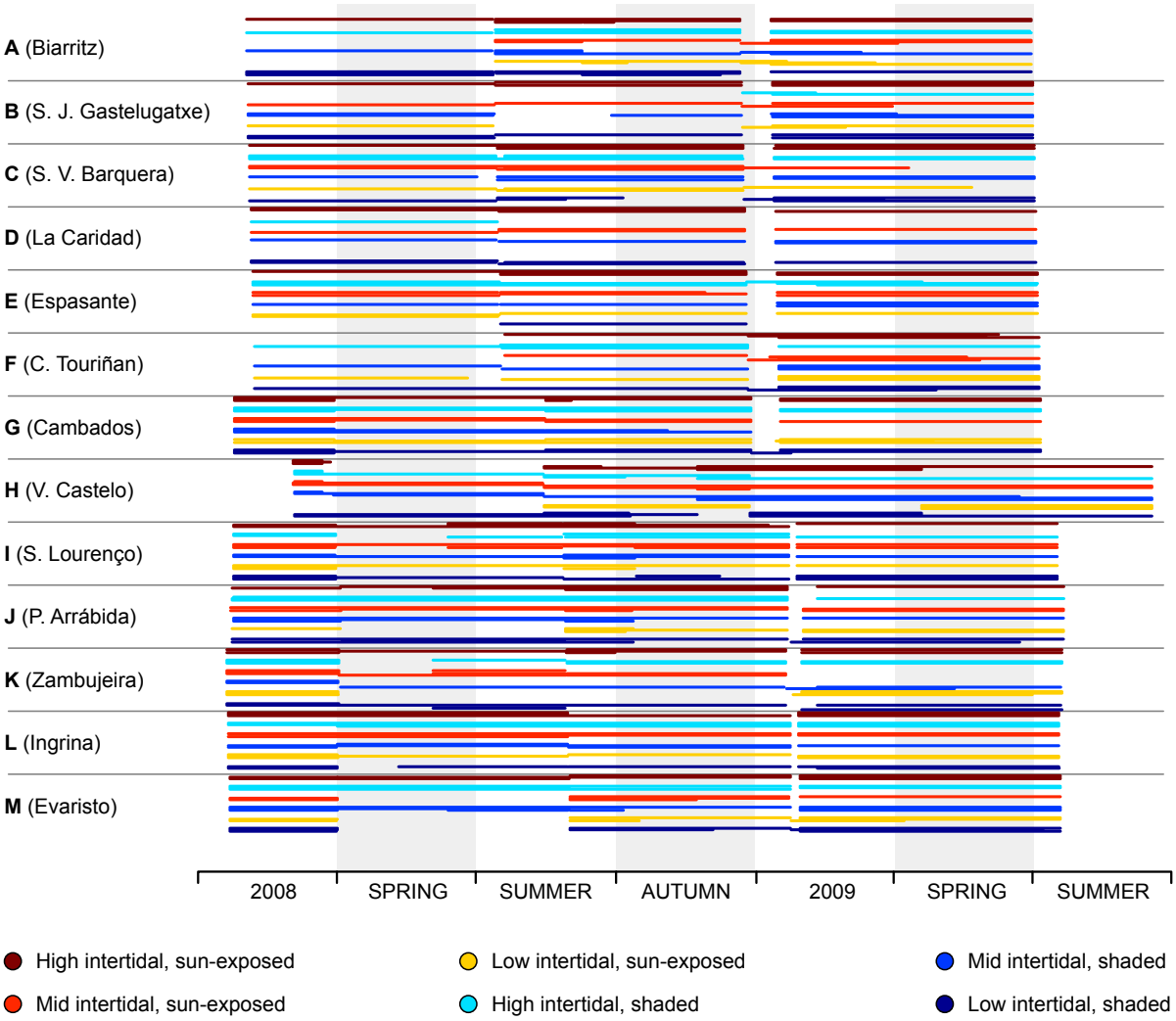

Figure 2.8: Data coverage map showing the number of operational robolimpets at a given time (thickness of line) on the 6 intertidal microhabitats of the 13 sampled shores. Shores are arranged from ordered from NE (top) to SW Iberia (bottom). Each line color represents a different intertidal microhabitat.

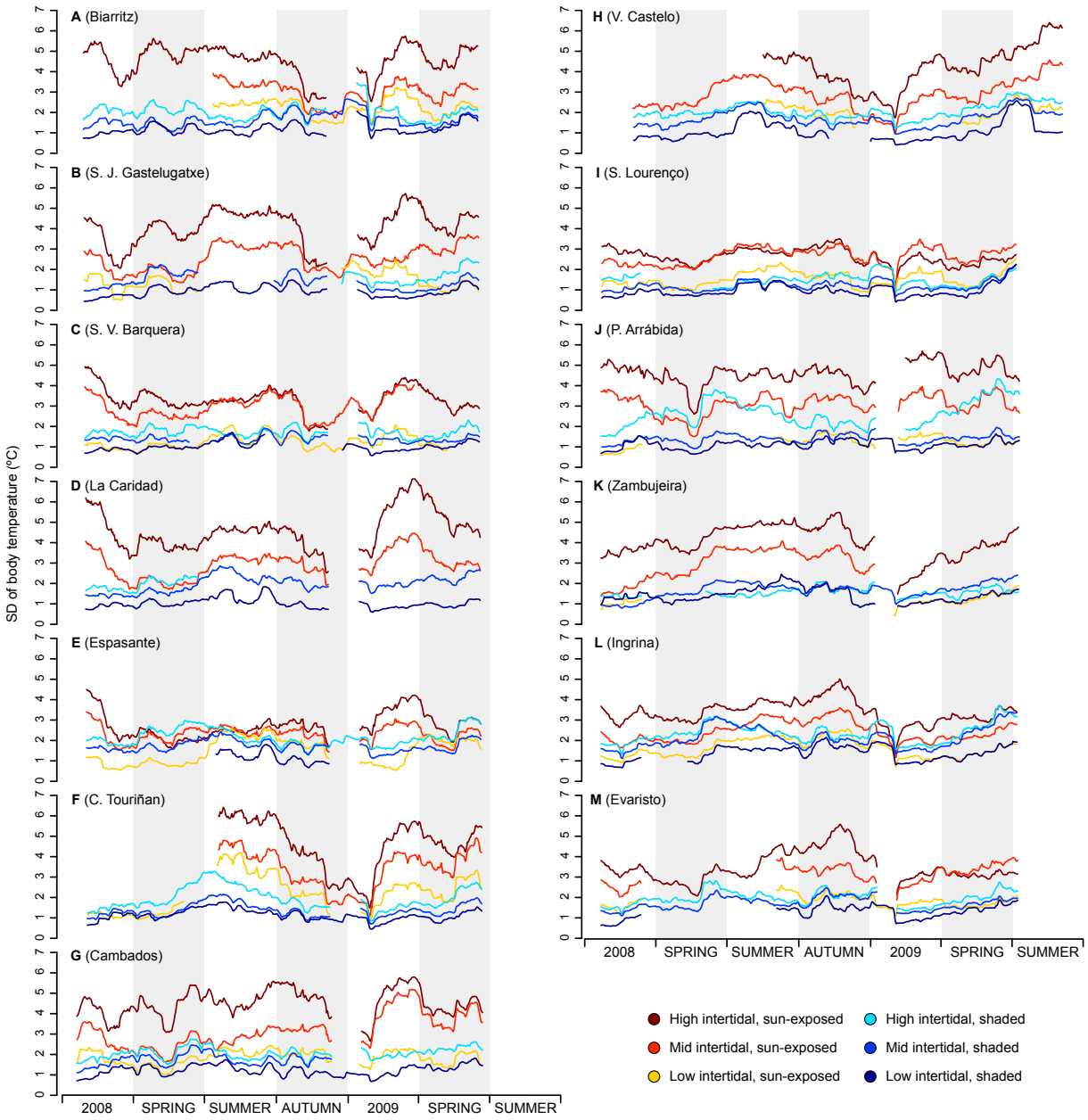

Figure 2.9: 30-day rolling average of standard variation (SD) of temperature profiles within the 13 sampled locations, ordered from NE to SW Iberia (letters A-M, see also Fig. 2.1).

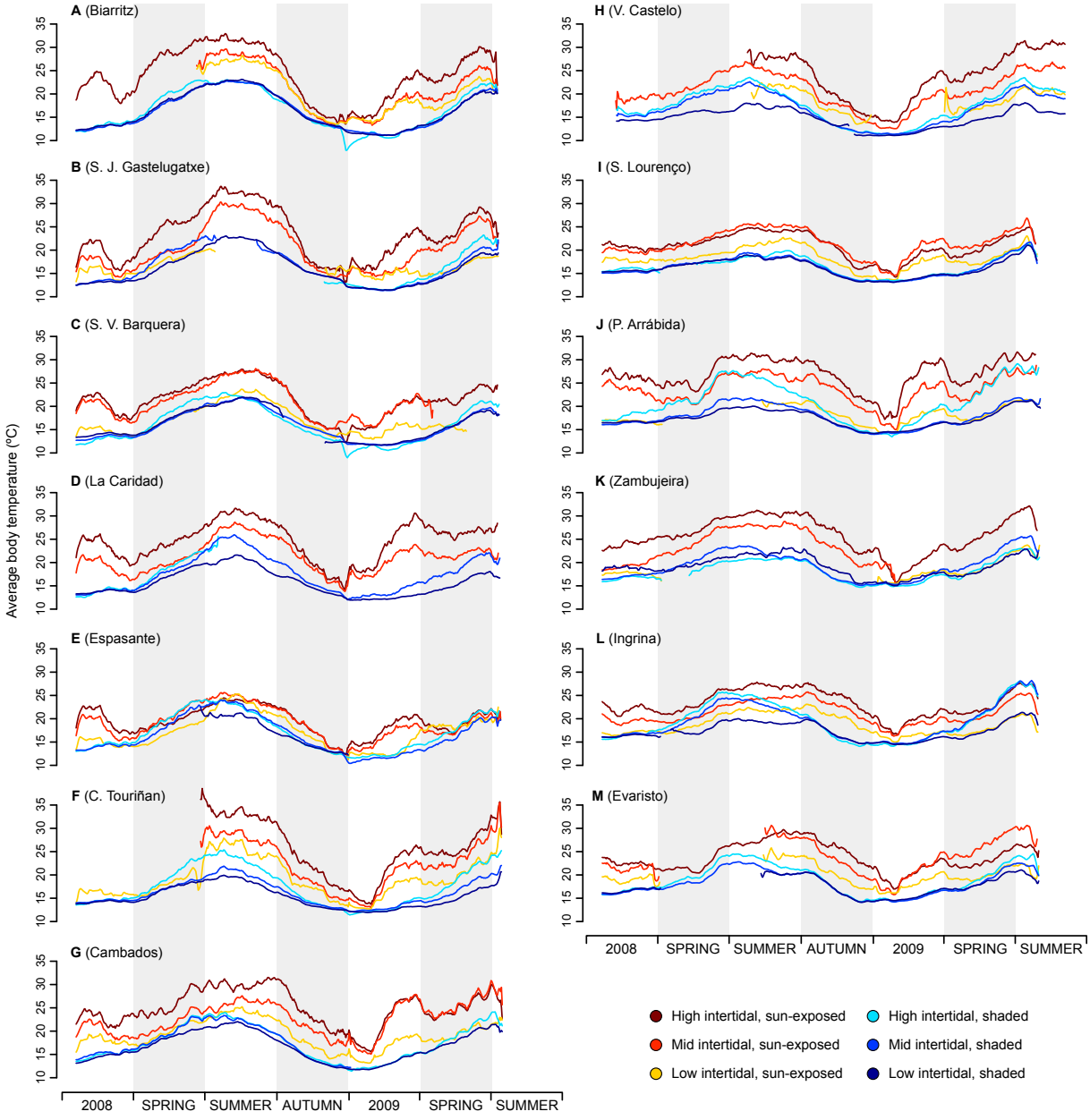

Figure 2.10: 30-day rolling average of daily temperature maxima of temperature profiles within the 13 sampled locations, ordered from NE to SW Iberia (letters A-M, see also Fig. 2.1).

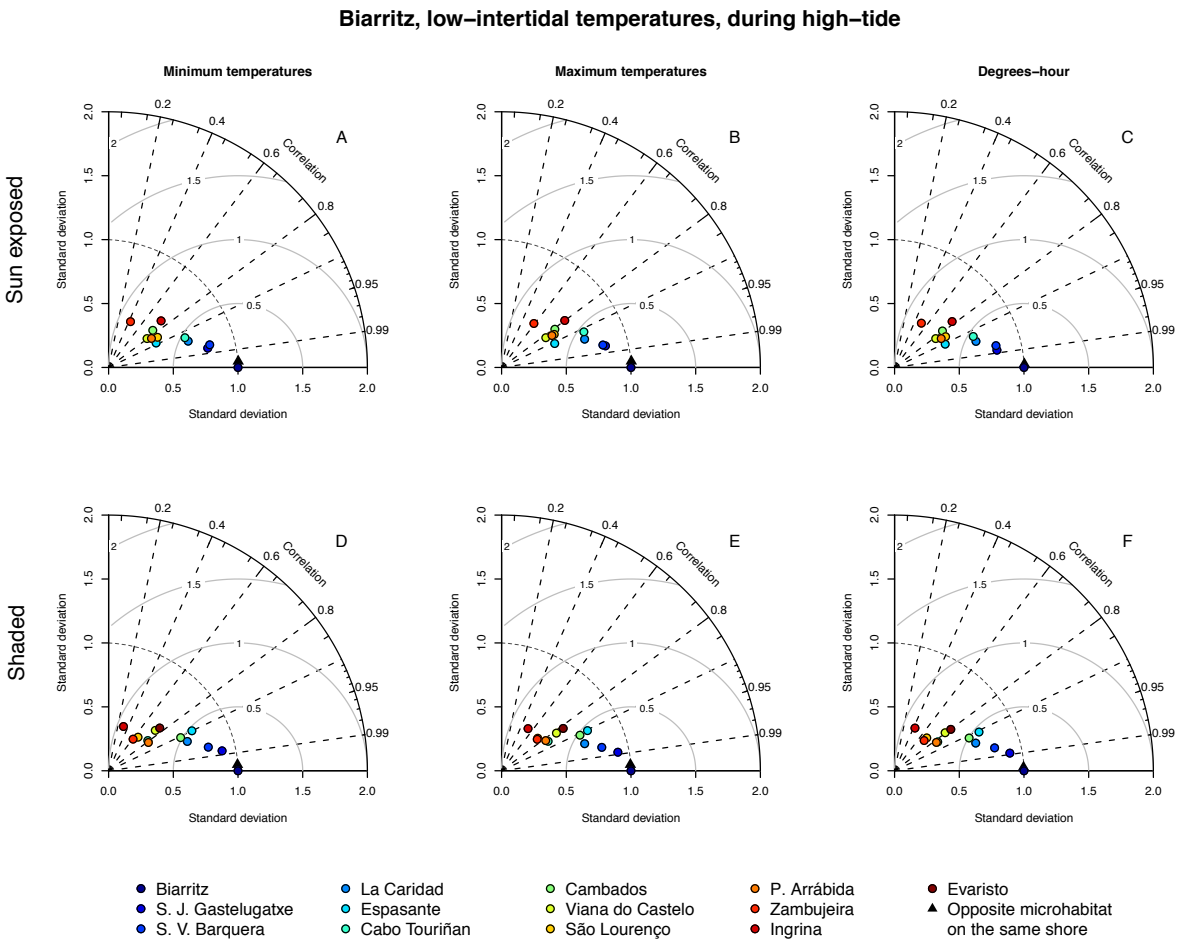

Figure 2.11: Taylor diagrams for robolimpet temperatures measured within the 13 sampled locations, during (i) a two-hour interval around high tide, (ii) a two-hour interval around low tide and (iii) the entire tide, at three intertidal levels (low-, mid- and high-intertidal). On each diagram, the radial distance from the origin represents the amplitude of temperature variation (standard deviation). The azimuthal angle depicts the correlation coefficient between the reference and the remaining microhabitats, while their RMSE is shown by the concentric lines centred on the reference. The full set of 114 panels can be found online at doi:10.1016/j.jembe.2011.02.010.

2.2 Topographical shading shapes coastal habitat complexity

2.2.1 Abstract

The blocking of incoming solar radiation by topography along the world's coastlines creates a complex mosaic of radiation environments, in which some locations closer to the equator can receive solar radiation levels comparable to unshaded sites located thousands of kilometers towards the poles. As this effect is immutable over long spans of time, topographical shading creates a stable and heterogeneous environmental pattern over which climate change-induced alterations take place. The geographical distribution of thermal and radiative stress or long-lasting refugia is most likely influenced by the imbalanced distribution of topographically shaded environments.

2.2.2 Main text

A central goal in ecology is to understand how current biodiversity patterns came to be, and how climate change will affect them in the future. Global patterns of biodiversity are intrinsically linked to environmental conditions (Darwin, 1859; Tittensor et al., 2010; Belanger et al., 2012), and habitat complexity has been associated with species richness (Allouche et al., 2012; Fjeldså et al., 2012; Meager and Schlacher, 2013). Therefore, a full understanding of biodiversity patterns requires in-depth knowledge on the environmental conditions experienced by individuals. This is especially true for coastal ecosystems, where organisms are regularly pushed close to their physiological limits (Vincent and Neale, 2000; Stillman, 2003; Somero, 2005). Solar radiation, one of the most important environmental factors influencing coastal ecosystems (Bristow and Campbell, 1984; Lubin et al., 1998) and the main driver of body temperature and thermal stress of intertidal organisms (Helmuth et al., 2010; Seabra et al., 2011), sets distribution limits and influences biodiversity patterns (Hutchins, 1947; Wethey, 2002; Bischof et al., 2006; Mota et al., 2015; Seabra et al., 2015b; Lima et al., 2015). The amount of available radiant energy determines the pace of photosynthesis, controlling primary productivity along the world's coastlines (King and Schramm, 1976; Pinckney and Zingmark, 1991). In unshaded locations and under clear-sky conditions, average yearly insolation is highest at the equator, gradually decreasing towards the poles. Not all radiation reaches the earth's surface, however, with a significant portion being filtered out by cloud cover (Frederick and Snell, 1990; Bordewijk et al., 1995) and topographical shading. Despite several studies highlighting the role played by shade in determining coastal microenvironment complexity and providing microrefugia (Wethey, 1984; Farnsworth and Ellison, 1996; Helmuth and Hofmann, 2001; Harley, 2002; Allen et al., 2003; Tomanek and Sanford, 2003; Blockley, 2007; Wing et al., 2007; Seabra

et al., 2011), a global assessment of the importance of topographical shading for the radiation budget of the world's coastlines has been impractical thus far. The small size and reduced mobility of most coastal organisms (i.e., invertebrates, plants, and macro- and microalgae), coupled with the static nature of topographical shading (which unlike cloud cover only changes over geological timespans), means that even small patches of forgiving habitat may provide sufficient long-term amelioration to sustain populations that would otherwise be excluded from vast regions. Moreover, as climate change has no effect on topographical shading, the value of the refugia it provides can be expected to increase substantially in the near future (Hannah et al., 2014; Scheffers et al., 2014; Maclean et al., 2015).

We used a digital elevation model (Farr et al., 2007) to map topographical shading along the world's coastlines between 60°N and 56°S, at a resolution of 1 arc-second (~30 m)[1]. Yearly average clear-sky solar radiation was determined both for a hypothetical flat earth (*potential insolation*), and for the topographically complex earth (*realized insolation*)[2]. Topographical shading was characterized in terms of its relative importance, determined as the distance between each location and the nearest latitude with equivalent *potential insolation* levels. Thus, the computed Topographical Shading Index (TSI) indicates how far towards the poles does a similar amount of solar radiation occur on unshaded surfaces. The $>$ 33 million data points originated were summarized at different scales to emphasize global or regional patterns (Fig. 2.12). Results revealed a complex mosaic of vast regions where topographical shading is minimal, interspersed with regions offering extensive shading opportunities (Fig. 2.12A). Most of the locations analyzed had very low TSI (58%, distance $\leq$ 32 km), while almost a quarter exhibited moderate to high TSI (23%, distance $\geq$ 128 km). A breakdown of TSI by latitude revealed that locations around the tropics tend to have lower TSI values, in contrast with locations around the equator and towards the poles, where high TSI values can be found (Fig. 2.13A). This pattern results from the compound effect of two aspects of solar geometry. First, the curve of potential radiation is shallower both at the equator and towards the poles (Fig. 2.13B), meaning that at these locations even moderate shading results in radiation levels that can only be found thousands of km away. Conversely, the steeper slope polewards from

[1]Global elevation and water body data were taken from the Shuttle Radar Topography Mission 1 Arc-Second digital elevation model dataset, produced by NASA and NGA (Farr et al., 2007). These data were acquired by the Space Shuttle Endeavour in February, 2000, and can be accessed from the Earthexplorer portal, hosted by the U.S. Geological Survey (http://earthexplorer.usgs.gov).

[2]Coastal pixels at 1 arc-second resolution (~30m) were selected as all pixels along the edges of water body polygons, with elevation of 0 m and bordering a pixel with elevation greater than 0 m. Remaining inland waters were removed manually. A minimum of 15 km of surrounding topography was used to cast shadows on each coastal pixel every 30 minutes during one day per month (Corripio, 2003). Monthly data was then used to produce yearly averages. Estimation of clear-sky direct radiation on a horizontal surface (Meinel and Meinel, 1976) included the effect of the earth's orbit eccentricity, the angle of beam incidence (Brock, 1981), and the thickness of the atmosphere along the beam's trajectory (Kasten and Young, 1989). Computations didn't account for slope and aspect of each coastal pixel, in order to ensure that values can be directly compared across latitudes, and provide a general view of radiation patterns irrespective of local micro-topography. The Indirect radiation was considered 10% of the direct radiation (Tuller, 1976). Whenever shaded, a coastal pixel only received indirect radiation. All computations were performed using R (R Development Core Team, 2015).

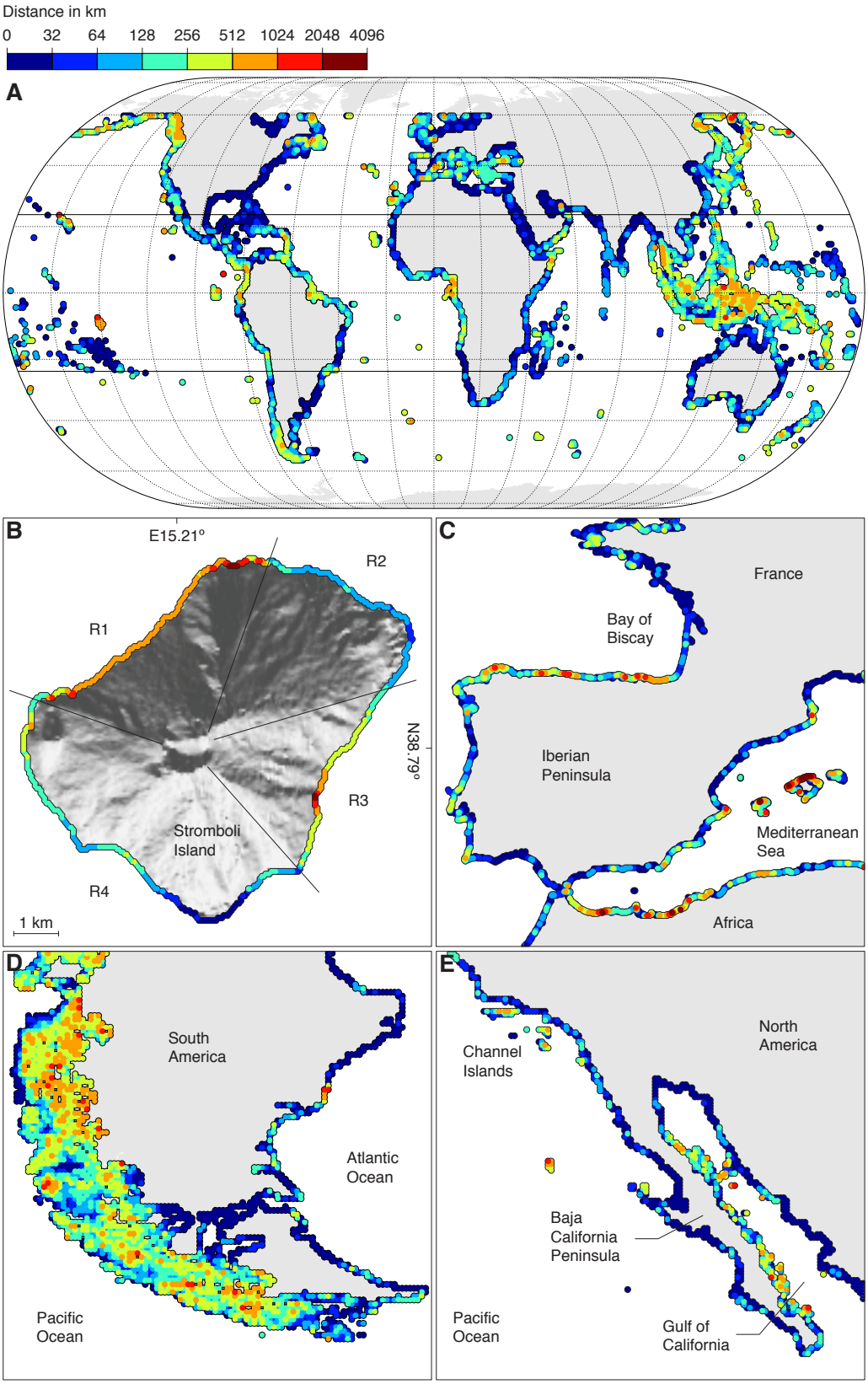

Figure 2.12: Topographical shading along the world's coastlines. Distance to the nearest latitude with matching unshaded solar radiation profiles was averaged globally over a 1°grid (A), and for details of Europe, South America and North America over a 1/10°grid (C, D, E). (B) Full resolution elevation and topographical shading data (1 arc-second, ~30 m) for the volcanic island of Stromboli (Italy). The lines diverging from the caldera delimit the four main slopes faces of the pyramidal cone.

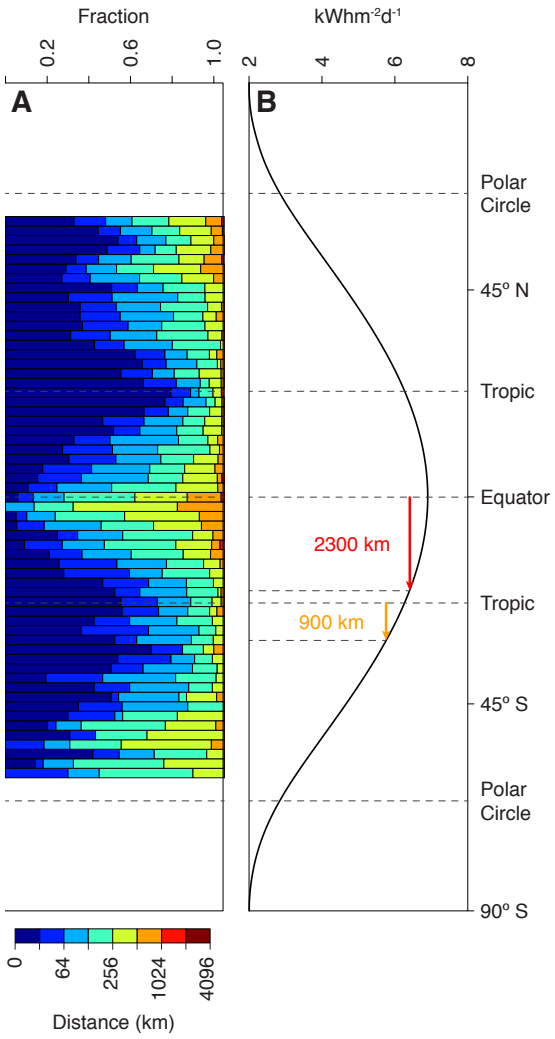

Figure 2.13: (A) Latitudinal breakdown of the TPI in 1-degree latitude bins. (B) Curve of yearly average potential radiation. Arrows indicate the distance to the nearest latitude with radiation levels equivalent to a reduction of 0.5 kWh.m^{-2}.d^{-1} at the equator and southern tropic.

the tropics reduces the relative value of shading in these regions because similar radiation levels can be found at shorter distances. Secondly, in the tropics no shadows are cast by hills or cliffs during the summer solstice when the sun reaches its highest point in the sky. Thus, in these regions, no attenuation of radiation occurs via topographical shading exactly during the periods when the major portion of radiation is reaching the earth's surface. While the summary maps emphasize the presence of high TSI values, unshaded habitats are ubiquitous, with 97.5% of all tiles on a 1/4°grid (~25 km at the equator) containing at least one unshaded location (distance $\leq$ 32 km, Fig. 2.12A). Thus, stretches of coast with moderate to high TSI often provide a larger variety of environmental conditions, from unshaded to shaded, generating habitat complexity rather than being homogeneously deprived of solar radiation.

Data shows that neither near (150 m) nor far range (15 km) maximum elevation can be used alone to accurately estimate the effect of topographical shading (correlation coefficients of 0.61 and 0.26, respectively)[3]. This highlights the fact that for substantial topographical shading to occur a coastline needs to not only feature a steep topography, but also be facing away

[3]Maximum elevation at near and far range was computed in square areas centered around each individual coastal pixel (sides of 300 m and 30000 m, respectively).

from the equator. The patterns of topographical shading here reported clearly reflect these constraints. For example, topographical shading is impossible along flat coastal regions, as is the case in most of the east coast of the US, northern Canada's Hudson Bay, parts of Argentina, the shores of northern mainland Europe, the northern shores of the Black Sea, the southeast portion of the Mediterranean Sea, northeast India and Bangladesh, northeast China, parts of northern Australia, and all atoll-like islands. In these locations, where coastlines typically consist of sandy beaches or river deltas, the contribution of topographical shading to habitat complexity is minimal, and radiation attenuation can only occur via atmospheric effects such as cloud cover. Shading is also minimal at shores bordered by gently sloped coastal hills or desert sand dunes. These types of coasts occur on the shores of Namibia and western South Africa, many regions along northwest and southeast Africa, southern Madagascar, and the coasts bordering the Red Sea and the Persian Gulf. On the other end of the spectrum, fjords and other convoluted coasts at high latitudes, such as those in Chilean Patagonia, the northwest coast of North America and New Zealand's South Island, generate intricate topographical shading patterns which result in ample habitat complexity. The combination of convoluted coastlines and steep coastal topography is also responsible for the strong topographical shading found throughout Japan, northeast Russia, most of mainland Southeast Asia and the Indo-Australian Archipelago, as well as in many islands in the Mediterranean Sea. Volcanic archipelagos such as the Hawaii, French Polynesia, Galápagos, Azores, Madeira, Canaries, Cape Verde and the islands in the Gulf of Guinea also provide important shading opportunities due to their highly sloped profiles. Although generally steepness and direction must be simultaneously present for meaningful topographical shading to occur, there are exceptions such as the southeastern shores of Yemen and Oman, where an extreme elevation profile (mountains with 700 m within 2 km of the coast) appears to override the equatorward exposure to some extent. The fractal nature of coastlines means that the conditions determining topographical shading replicate at a variety of spatial scales. This is especially evident when examining a location with simple features, such as the cone-shaped Stromboli Island, at full resolution (~30 m, Fig. 2.12B). This island has four distinct slopes with contrasting levels of topographic shading arising for different reasons. Despite both facing poleward, slope R1 has more shading that R2 because the coast there lays at the bottom of cliffs (Fig. 2.12B). This is comparable to the pattern observed along the southwestern coast of the Mediterranean Sea (Fig. 2.12C), where the abrupt cliffs on the Moroccan coast provide more shading than the gently sloped coastal hills of Algiers. The very strong shading in slope R3 results from the extreme steepness of that slope in spite of its slightly equatorward exposure, a pattern very similar to the one described above for the shores of Yemen and Oman. The entire slope R4 is facing towards the equator, and therefore it is unsurprising that shading is minimal at most locations, as happens at the bottom of cliffs in the south coast of Iberia (Fig. 2.12C). The macro-ecological significance of the topographical shading patterns here described is difficult to ascertain due to the scarcity of global biodiversity databases focusing on the littoral fringe. One notable exception is the

Atlantic coast of Europe, whose intertidal ecosystems have been extensively studied for decades. In southwest Europe, right-angled coastlines generate abrupt discontinuities in topographical shading patterns (Fig. 2.12C). While the equatorward-facing cliffs in the south coast of the Iberian Peninsula barely shade the intertidal, the shading provided by the poleward-facing cliffs in northern Iberian Peninsula results in radiation levels found at latitudes northwards of France. The equatorial distribution limits of many species of invertebrates and macroalgae occur at the northeast and southwest corners of the Iberian Peninsula (Fischer-Piette, 1955; Crisp and Fischer-Piette, 1959; Fischer-Piette and Gaillard, 1959; Pereira et al., 2006; Nicastro et al., 2013), and although other factors have been shown to contribute to that pattern, recent studies suggest that the availability of thermal refugia provided by shaded microhabitats plays a pivotal role there (Lima et al., 2015). Topographical shading may also offer new perspectives on ongoing change. For photosynthetic organisms in the Chilean fjords (Fig. 2.12D), the availability of a wide range of shading levels may have reduced the negative impact of photoinhibition of photosynthesis and cellular damage from high levels of ultraviolet radiation (Franklin and Forster, 1997) due to the Antarctic Ozone Hole (Farman et al., 1985). Present and future assessments of thermal stress and rate of photosynthesis could reveal if the recent pause and reversal of the Antarctic global ozone depletion trend (Varai et al., 2015) will reduce the relative importance of topographical shading in this region. Finally, the identification of a new pattern of environmental variability can be used to guide upcoming research efforts. For example, while most studies on the biodiversity patterns of the Gulf of California focus on north-south contrasts, topographical data suggests that the poleward-facing coastal cliffs along the west coast of the Gulf of California (Fig. 2.12E) offer far more shaded habitats than the opposite east coast, and Pacific Baja California. This arrangement of three parallel coastlines with strikingly different environmental conditions, including the asymmetrical presence of shading, suggests that this region could be an ideal testing ground for numerous ecological questions. Overall, the high-resolution atlas of topographical shading here presented is an important tool for the accurate identification of locations with persistent refugia, which in turn are crucial for the study of evolutionary processes in coastal organisms, evaluating of ecosystem productivity and the refinement of conservation efforts.

2.2.3 Acknowledgements

Supported by FEDER (FCOMP-01-0124-FEDER-010564, FCOMP-01-0124-FEDER-020817), FCT (PTDC/MAR/099391/2008, PTDC/MAR/117568/2010, PTDC/MAR/118205/2010, SFRH/BD/68521/2010 and IF/00043/2012), NASA (NNX11AP77G) and NSF (OCE1129401). The authors declare no conflict of interest.

3. Patterns of thermal stress

3.1 Loss of thermal refugia near equatorial range limits

3.1.1 Abstract

This study examines the importance of thermal refugia along the majority of the geographic range of a key intertidal species (*Patella vulgata* Linnaeus, 1758) on the Atlantic coast of Europe. We asked whether differences between sun-exposed and shaded microhabitats were responsible for differences in physiological stress and ecological performance, and examined the availability of refugia near equatorial range limits. Thermal differences between sun-exposed and shaded microhabitats are consistently associated with differences in physiological performance, and the frequency of occurrence of high temperatures is most likely limiting the maximum population densities supported at any given place. Topographic complexity provides thermal refugia throughout most of the distribution range, although towards the equatorial edges the magnitude of the amelioration provided by shaded microhabitats is largely reduced. Importantly, the limiting effects of temperature, rather than being related to latitude, seem to be tightly associated with microsite variability, which therefore is likely to have profound effects on the way local populations (and consequently species) respond to climatic changes.

3.1.2 Introduction

Climate change is a major threat to global biodiversity, and one of the greatest challenges today is to predict how it will impact natural systems (Pereira et al., 2010). Mechanistic models hold great promise as predictive tools (Kearney and Porter, 2009), but are hard to implement because they require the ability to downscale global climatic patterns into microclimates, and to understand how these, in turn, drive the physiology of the organisms (Huey, 1991; Helmuth et al., 2010). In fact, while body temperatures are neither necessarily correlated with latitude or easily obtained from large-scale climatic data (Helmuth and Hofmann, 2001; Potter et al., 2013; Lathlean et al., 2014a; Seabra et al., 2015b), the recent development of autonomous biomimetic devices has given researchers long-needed tools to tackle this problem (Helmuth and Hofmann, 2001; Fitzhenry et al., 2004; Lima and Wethey, 2009), allowing them to obtain long-term records of body temperatures over continental scales (e.g., Seabra et al., 2011, 2015b). Rocky intertidal systems are inhabited by species that can be exposed to extreme thermal stress during tide-out emersion (see Helmuth et al., 2006b, for a review). Solar radiation is usually the dominant component of the surface energy balance during low tide, causing body temperature variations of up to 30 °C in just a few hours (e.g., Southward, 1958;

Helmuth and Hofmann, 2001). Yet, solar radiation does not reach all intertidal organisms in a uniform way. Poleward-facing surfaces receive less direct radiation and thus are cooler than equatorward-facing surfaces (Wethey, 2002; Kearney and Porter, 2009; Miller et al., 2009), and it has been recently shown that temperature differences between sun-exposed and shaded microhabitats are higher than those associated with seasons, latitude or shore level (Seabra et al., 2011). Thus, local geomorphology has the potential to either amplify the deleterious effects of regional climatic conditions or to provide thermal refugia, which may be extremely important for some species, particularly towards their distributional limits (Bennie et al., 2008). It must be acknowledged, however, that different temperatures do not necessarily imply different thermal stress levels. Other factors, such as species-specific variability in physiological tolerance (e.g., Dong et al., 2008), mobility (which may allow for behavioral thermoregulation, see Huey et al., 1989; Chapperon and Seuront, 2011; Marshall et al., 2013), or the ability to acclimate (e.g., Meng et al., 2009) are also important as well. In that sense, elevated temperatures are only relevant if they lead to physiological stress (Helmuth et al., 2010). Therefore, the main aims of this study were: (i) to find whether the pervasive temperature differences associated with sun-exposed and shaded microhabitats (Seabra et al., 2011) translated into different levels of physiological stress, and (ii) to evaluate if differences in physiological stress between sun-exposed and shaded microhabitats within each shore vary along the geographical distribution of a key intertidal species, in particular towards its equatorial range limit. To that end, we quantified the endogenous levels of heat shock proteins (Hsp) on the intertidal limpet *Patella vulgata* Linnaeus, 1758, collected from both sun-exposed and shaded microhabitats over most of its distribution along the European Atlantic coast. Ecological physiologists have been using Hsps as indicators of thermal stress because their synthesis closely tracks the thermal history of organisms (Hofmann, 2005). These proteins are molecular chaperones that confer thermal tolerance by stabilizing other proteins that would otherwise denature, thus allowing normal cellular functions to continue even at elevated temperatures (Feder and Hofmann, 1999; Hofmann et al., 2002). Hsp can be divided in several families based on their molecular weight (Feder and Hofmann, 1999). Endogenous levels of the Hsp70 family, which includes constitutive and inducible isoforms, have been shown to vary between congeneric species (Tomanek and Sanford, 2003; Dong et al., 2008) and in relation to experimental acclimation in lab and seasonal acclimatization in the field (Buckley et al., 2001). Importantly, Hsp70 expression reflects both the thermal variability associated with different microhabitats and with large-scale environmental gradients across whole distributional ranges (Halpin et al., 2002; Snyder and Rossi, 2004; Sorte and Hofmann, 2004; Sagarin and Somero, 2006). *Patella vulgata* is appropriate for this study due to several reasons. It can be abundantly found over the majority of the Atlantic European continental coast south of Norway but reaches its equatorward distribution limit in SW Iberia and is absent from the Bay of Biscay (Fischer-Piette and Gaillard, 1959; Christiaens, 1973). This geographic pattern is repeated in a variety of algae and invertebrates (Fischer-Piette, 1955; Crisp and Fischer-Piette,

Table 3.1: Geographical locations and respective sampling dates.

Ref	Location name	Latitude	Longitude	Sampling date
1	South Cairn, UK	54°58'19.85"N	5°10'46.75"W	August 2, 2012
2	Emlagh, Ireland	53°45'03.02"N	9°54'11.52"W	August 5, 2012
3	Holyhead, UK	53°19'09.85"N	4°39'41.92"W	August 3, 2012
4	Annascaul, Ireland	52°07'32.88"N	10°6'36.03"W	August 4, 2012
5	Wembury, UK	50°18'48.29"N	4°06'25.57"W	June 5, 2012
6	Landunvez, France	48°32'45.94"N	4°44'45.84"W	June 6, 2012
7	Batz-sur-Mer, France	47°16'18.18"N	2°28'36.68"W	June 4, 2012
8	Royan, France	45°37'41.85"N	1°03'45.31"W	June 3, 2012
9	Biarritz, France	43°29'03.84"N	1°33'47.74"W	June 22, 2012
10	Prellezo, Spain	43°23'37.63"N	4°26'25.25"W	June 21, 2012
11	La Caridad, Spain	43°33'55.24"N	6°49'41.41"W	July 7, 2012
12	Cabo Touriñan, Spain	43°02'34.65"N	9°17'24.30"W	July 8, 2012
13	Moledo do Minho, Portugal	41°50'23.83"N	8°52'26.37"W	July 5, 2012
14	Mindelo, Portugal	41°18'37.48"N	8°44'32.83"W	August 8, 2012
15	São Lourenço, Portugal	39°00'48.48"N	9°25'20.91"W	June 7, 2012
16	Alteirinhos, Portugal	37°31'09.33"N	8°47'20.91"W	June 5, 2012
17	Evaristo, Portugal	37°04'27.39"N	8°18'13.66"W	June 3, 2012

1959; Southward et al., 1995), meaning that *P. vulgata* is a good model for a wider range of organisms. In addition, *P. vulgata* is a keystone species whose grazing activities control, to a large extent, local biodiversity and community structure throughout much of its range in Europe (Southward, 1964; Hawkins and Hartnoll, 1983; Raffaelli and Hawkins, 1996; Jenkins and Hartnoll, 2001; Jenkins et al., 2005; Coleman et al., 2006). Experimental work has confirmed that changes in the abundance of *P. vulgata* influence the entire community (Hawkins et al., 2008, 2009). Thus, a better understanding of the factors that control the distribution of this species can improve our ability to forecast responses of intertidal ecosystems to climate change.

3.1.3 Material and methods

Microhabitat body temperature

Intertidal temperatures were recorded at 17 wave-exposed shores along the European Atlantic coast, spanning nearly 20° of latitude, from southwest Scotland to south Portugal (Fig. 3.1c). Data was acquired using robolimpets, autonomous temperature logging devices mimicking the visual aspect and temperature trajectories of real limpets (Lima and Wethey, 2009). Loggers were deployed following (Seabra et al., 2011). We sampled temperatures from four distinct combinations of height above the low water mark (mid and high shore) and exposure to sun (shaded and sun-exposed), thus covering the majority of the range of microhabitats occupied by *P. vulgata*. Data were collected continuously between the summers of 2010 and 2014 at a sampling interval of 60 minutes and a resolution of 0.5 °C. For each location, we averaged data from loggers sharing the same orientation in relation to the sun (i.e., sun-exposed and shaded).

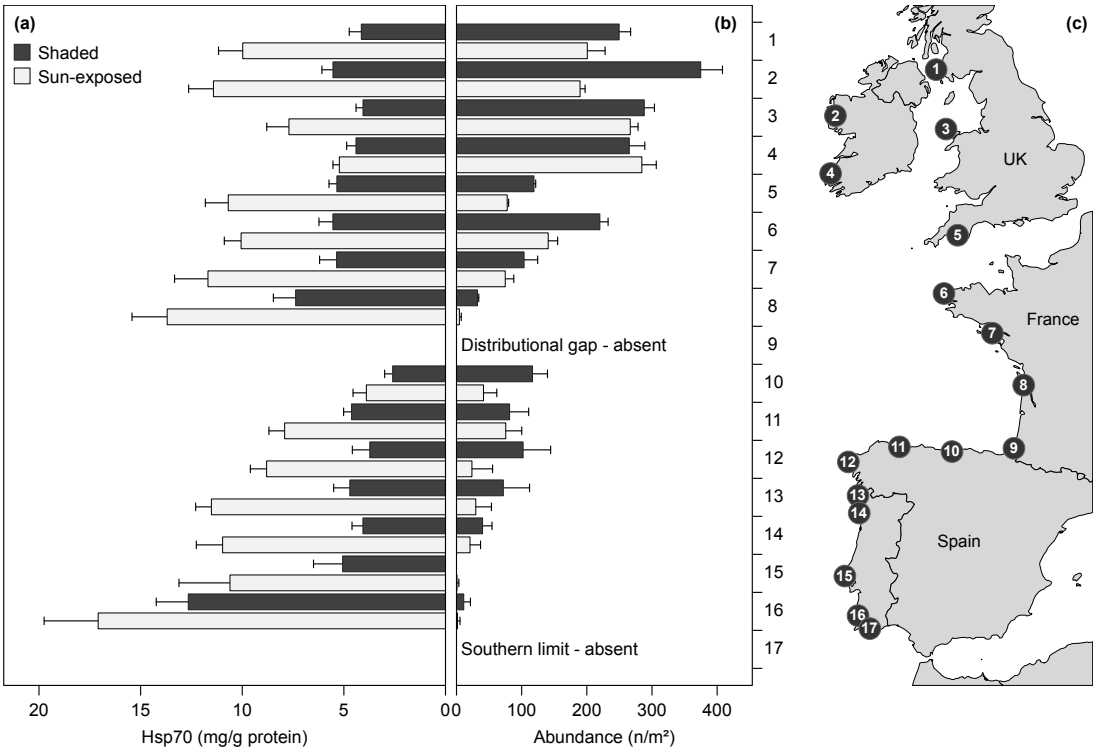

Figure 3.1: Hsp70 levels and abundances of *Patella vulgata* along the European Atlantic coast. (a) Mean Hsp70 levels ± 1 SEM (standard error of the mean) from animals collected in shaded (light grey) and sun-exposed (dark grey) microhabitats (n = 8 for all bars). Hsp70 levels were significantly higher in sun-exposed than in shaded microhabitats ($p < 0.01$ after ANOVA). (b) Mean abundances ± 1 SEM in shaded (light grey) and sun-exposed (dark grey) microhabitats (n = 15 for all bars with the exception of location 8 where n = 10). (c) Map of the sampled locations (for further details, see Table 3.1).

Distribution of *Patella vulgata*

Population densities of *Patella vulgata* were measured during spring low tides in July and August 2012 (see Table 3.1). At each location, individuals were counted using a total of thirty 30x30 cm quadrats haphazardly placed at locations equivalent to the microhabitats where temperature loggers were deployed (half in shaded microhabitats, and the other half in sun-exposed microhabitats, throughout the vertical distribution of the species in the mid and high intertidal).

Tissue sampling and western blotting

Patella vulgata were collected at each location, in close proximity to the loggers (< 5 m), during the summer of 2012 in all studied shores (see Table 3.1). We collected eight individuals from shaded microhabitats (north-facing walls and/or crevices) and eight individuals from sun-exposed microhabitats (south-facing rocky outcrops), throughout the range of shore heights in which *P. vulgata* occurs in each location. To minimize potential physiological variation related to endogenous tidal rhythms, collections were made within 30 min of low tide (Tomanek and Sanford, 2003). Animals were immediately frozen on dry ice upon collection and kept

at -80 °C until further processing. *Patella vulgata* displays a range of homing habits, mostly depending on the geographical region and inclination of rock surfaces. In the middle of its range (UK), it may forage during the day at high tide (Hartnoll and Wright, 1977), at low tide when it is damp (but not raining, Santini et al., 2004), or during night-time low tides (Hawkins and Hartnoll, 1982). At lower latitudes, unless the environment is extremely humid, it moves only during the night, and returns to its home scar during the day, firmly clamping to the rock to reduce desiccation (Branch, 1981; Gray and Naylor, 1996). Thus, throughout the entire species range, individuals stay immobilized during the most thermally stressful part of the day. As part of a separate monitoring program, 800 individuals of *P. vulgata* were color-tagged in four locations along the Portuguese coast (400 in shaded and 400 in sun-exposed microhabitats), and their movement patterns registered at a monthly basis for one year (2010-2011). All tagged individuals remained faithful to their home scars during the entire duration of the study (F. P. Lima, *unpub. data*). Consequently, there is high confidence that, prior to collection, individuals used for Hsp70 quantification had been in the same microhabitat where they were collected from (at least at the temporal scales relevant for this study). Likewise, temperatures logged by (static) robolimpets are representative of the diurnal body temperatures experienced by *Patella* spp. found in their vicinity during low tide. In the laboratory, approximately 20 mg of tissue were dissected from the foot of each animal and placed in lysis buffer [0.4% Tris-HCl, 2% sodium dodecyl sulphate (SDS), 1% ethylenediaminetetraacetic acid (EDTA), 1% Protease inhibitor cocktail (Thermo Scientific #78444, IL, USA), pH 6.8]. Samples were incubated for 5 min at 100 °C and mechanically homogenized at 30 Hz for 5 min using a Retsch MM400 homogenizer. After repeating this procedure two times, homogenates were spun for 15 min at 15,800 g and stored the supernatant at -80 °C until further processing. 10 µl of each sample were used for total protein concentration determination, using a BCA protein assay kit (Pierce #23225, IL, USA). These protein concentrations were later used for loading similar amounts (mass-wise) of sample into the gels. Samples were taken from the -80 °C freezer, boiled at 100 °C for 5 min and then diluted 1:1 in Laemmli sample buffer (Sigma-Aldrich #S3401, MO, USA). Protein separation was done by electrophoresis on small format SDS-polyacrylamide gels using Mini-PROTEAN Tetra Cell cast systems, BioRad, CA, USA (4% for stacking gels and 7.5% for the resolving gels for optimal protein resolution). To allow quantitative comparison between samples from different gels, we prepared a "common sample" by mixing aliquots of several homogenates (totaling 1 ml). In each gel, two lanes were loaded with 15 µg of "common sample", two "standard" lanes were loaded with 80 ng of purified recombinant human HSP70B' protein (#ADI-SPP-762, Enzo Life Sciences, NY, USA), one lane was loaded with 5 µl of pre-stained markers (#161-0374, BioRad, CA, USA), and the remaining eight lanes were loaded with the samples to be quantified (15 µg each). Gels were run at 100 V for 20 min followed by 120 V for 65 min in running buffer (1.4% glycine, 0.3% Tris-base, 0.1% SDS, pH 8.3). Proteins were transferred to 0.45 µm polyvinylidene difluoride (PVDF) membranes (Millipore Immobilon #IPVH00010, Fisher Scientific, MA, USA) in transfer buffer (0.06% Tris-base,

0.03% glycine, 20% methanol), at 100 V for 35 min in a Mini Trans-Blot Electrophoretic Transfer Cell (#170-3930, BioRad, CA, USA). After transfer, membranes were treated with blocking buffer [0.1% non-fat dried milk in PBST solution (0.2% Tween, 8.5% NaCl, 0.2% monosodium phosphate, 1.1% disodium phosphate)] and then incubated for 10 min in a solution of both 1:1000 monoclonal anti-Hsp70 rat antibody (Thermo Scientific #MA3-006, IL, USA) and monoclonal 1:8000 anti-α-tubulin mouse antibody (Sigma-Aldrich #T5168, MO, USA) diluted in blocking buffer. Membranes were then washed three times with 15 ml of PBST solution, incubated with a 1:1000 solution of sheep-anti-mouse secondary antibody (#NA931, Sigma-Aldrich MO, USA) diluted in blocking buffer, and then washed three more times with PBST. Finally, membranes were exposed to an enhanced chemiluminescence solution (ECL, #RPN2106, GE Healthcare, NJ, USA) for 1 min and then exposed under dark-room conditions to ECL Hyperfilm (#28-9068-37, GE Healthcare, NJ, USA) for 2-7 min to obtain various exposures that were in the linear range of detection. We processed digitized films with ImageJ v1.4 (Abramoff et al., 2004). All samples were run at least three times.

Data processing and analysis

Quantitative western blotting across gels is sensitive to (i) variations in the efficiency of protein transfer and binding to the blotting membrane, and to (ii) irregularities in the preparation and pipetting of samples, which can lead to inconsistent densitometry data (Taylor et al., 2013). To control for variations in optical density and background noise typically found between gels, we quantified the optical density of the two "common sample" bands relative to the average optical density of the bands in the two "standard" lanes (those with a known amount of purified HSP70B'), per gel. To account for loading uncertainties, we normalized the optical density of the Hsp70 by the optical density of a housekeeping protein band (α-tubulin), per sample. Then, normalized values were quantified relative to the optical density of the "common sample" bands previously assessed for each gel. We compared variation in Hsp70 levels with sampling location (random effect factor) and with exposure to solar radiation (fixed effect factor, sun vs. shade) using a two-factor analysis of variance (ANOVA). Because variances were not homogeneous (Cochran's test, $P < 0.05$), data were transformed by $\sqrt{log(x+1)}$ prior to analysis. Hsp70 levels were regressed against the maximum temperature measured by robolimpets in the period that preceded tissue collection. Because the temporal dynamics of Hsp70 anabolism and catabolism in *P. vulgata* are still unknown, a conservative period of two weeks (which is roughly equal to the period of the neap-spring tidal cycle) was chosen. The plot of Hsp70 as a function of temperature maxima prior to sample collection was used to find a temperature threshold above which Hsp70 levels increased significantly (i.e., was used to find the minimum temperature with potential to trigger a stress response). Then, we used long-term robolimpet data (hourly temperatures collected between the summers of 2010 and 2014) to compute the average number of potentially stressful days per year (i.e., yearly mean number of days in which there were temperature registers higher than the temperature

threshold) at sun-exposed and shaded microhabitats in the studied locations, and regressed against populations densities in a potential limiting factor analysis (95^{th} regression quantile estimation, (Cade et al., 1999; Cade and Noon, 2013)). All data processing and analyses were done in R 3.1.2 (R Development Core Team, 2014).

3.1.4 Results

Population densities of *Patella vulgata* were highest along the coasts of Great Britain and Ireland, decreasing southwards (see Fig. 3.1b). With the exception of a single location in Ireland (#4, Fig. 3.1b), average densities in shaded microhabitats were higher than average densities in sun-exposed rocky surfaces. We confirmed the absence of the species in the locations of Biarritz, in SW France, and Evaristo, in SW Portugal (shores 9 and 17, respectively, Fig. 3.1b). Northward from these locations, population densities were extremely low (just a few individuals per square meter, shores 8, 15 and 16, Fig. 3.1b). The Hsp70 antibody detected a single band in foot tissue of *P. vulgata*. Although we did not quantify its molecular mass, the migration pattern was similar to that of the recombinant human Hsp70 isoform. In this assay, and despite extensive modifications to the protocol, we were never able to reliably distinguish the constitutive from inducible forms of Hsp70. This has been reported in other studies, where, depending upon species, the two isoforms cannot always be distinguished (e.g., Schill et al., 2002; Dong and Dong, 2008; Dong et al., 2008; Dalvi et al., 2011; Dong and Williams, 2011). However, because both forms play a role in organismal thermal tolerance, the quantification of total Hsp70 levels summarizes the organism ability to cope with thermal stress, and thus has been considered more informative from an ecological point of view (Sorte and Hofmann, 2004; Sagarin and Somero, 2006). Consequently, we report here the combined quantity of both the constitutive and inducible forms of Hsp70. The two-factor analysis of variance showed both a significant effect of location ($F_{14,\ 210} = 9.89$, $p < 0.01$) and exposure to the sun ($F_{1,\ 14} = 96.93$, $p < 0.01$) in the endogenous levels of Hsp70, but no significant interaction between location and solar exposure (see Table 3.2 for details). In fact, within each location, the average level of Hsp70 among individuals collected from sun-exposed microhabitats was consistently higher than the average level of those collected in the shade (Fig. 3.1a). Hsp70 levels from animals collected in sun-exposed microhabitats were, on average, 1.9 times higher than the levels found in animals collected in shaded microhabitats. Hsp70 showed no apparent correlation with latitude (Pearson's correlations: r = -0.33, t = -1.25, df = 13, *n.s.* for sun-exposed individuals and r = -0.34, t = -1.31, df = 13, *n.s.* for shade-exposed individuals, see also Fig. 3.1a). Hsp70 levels were particularly high at the locations immediately north of the distributional gap in the Bay of Biscay (#8, Fig. 3.1a), and north of the distributional limit in southern Portugal (#16, Fig. 3.1a). In effect, at these locations, individuals from sun-exposed microhabitats had, on average, the highest levels of Hsp70 in the whole range, and even animals from shaded microhabitats at their distribution limit in Portugal displayed Hsp70 levels comparable to

Table 3.2: Two-factor ANOVA to measure the effect of exposure to solar radiation (sun vs. shade) and sampling location on the endogenous levels of Hsp on *Patella vulgata*.

Source of variation	SS	DF	MS	F	P	Against
Location	1.041	14	0.074	9.888	<0.01	Error
Sun Exposure	1.08	1	1.08	96.927	<0.01	Location x Sun Exposure
Location x Sun Exposure	0.156	14	0.011	1.481	0.12	Error
Error	1.58	210	0.008			
Total	3.857	239				

sun-exposed habitats elsewhere. Hsp70 levels were significantly correlated with maximum body temperatures measured by robolimpets during the two weeks that preceded tissue collection (Pearson's correlation $r = 0.70$, t = 5.15, df = 28, $p < 0.05$). The scatterplot in Fig. 3.2 shows two main groups. In general, limpets from shaded microhabitats (light grey dots) experienced relatively low temperatures and had low levels of Hsp70, irrespective of their geographical origin. Conversely, animals from sun-exposed microhabitats (dark grey dots) experienced high temperatures prior to collection and had elevated levels of Hsp70. Interestingly, the only two cases of sun-exposed individuals with low levels of Hsp70 (dark grey dots #4 and #10) match the overall pattern because they also experienced relatively cold temperatures prior to collection. It is also remarkable that even locations thousands of km apart (such as #1 and #13) group together in both extremes of the graph, reinforcing the idea that geographical location had little contribution for the overall pattern shown in Fig. 3.2. Locations close to the geographical limits (#8 and #16), matched the overall pattern, but had Hsp70 levels approximately 1.5x to 2x higher than what would be predicted given the temperatures experienced in the two weeks before collection. Finally, the Hsp70 vs. temperature plot suggests that ~27.5 °C can be used as an estimate for the minimum stressful temperature, above which a marked increase in Hsp70 levels may be expected. The "wedge-shaped" distribution of *P. vulgata*'s densities plotted against number of potentially stressful days (i.e., the average yearly number of days with maximum temperature above 27.5 °C, see Fig. 3.3) is consistent with the hypothesis that high temperatures act as a limiting factor for *P. vulgata* (Southward et al., 1995; Cade et al., 1999). The potential limiting factor analysis suggested that the 95th quantile of the densities in the field are significantly and inversely correlated with the average yearly number of days with maximum temperature above 27.5 °C, and that each additional hot day per year reduces the maximum potential density of *P. vulgata* by -2.14 $\pm$ 0.34 s.e. individuals m^{-2} ($p < 0.05$ after 1000 bootstraps).

3.1.5 Discussion

Our study was designed to examine the importance of thermal refugia in the geographic distribution of an intertidal species. We asked whether differences between sun-exposed and shaded microhabitats were responsible for differences in physiological stress and ecological performance, and examined the availability of refugia near equatorial range limits. Using the

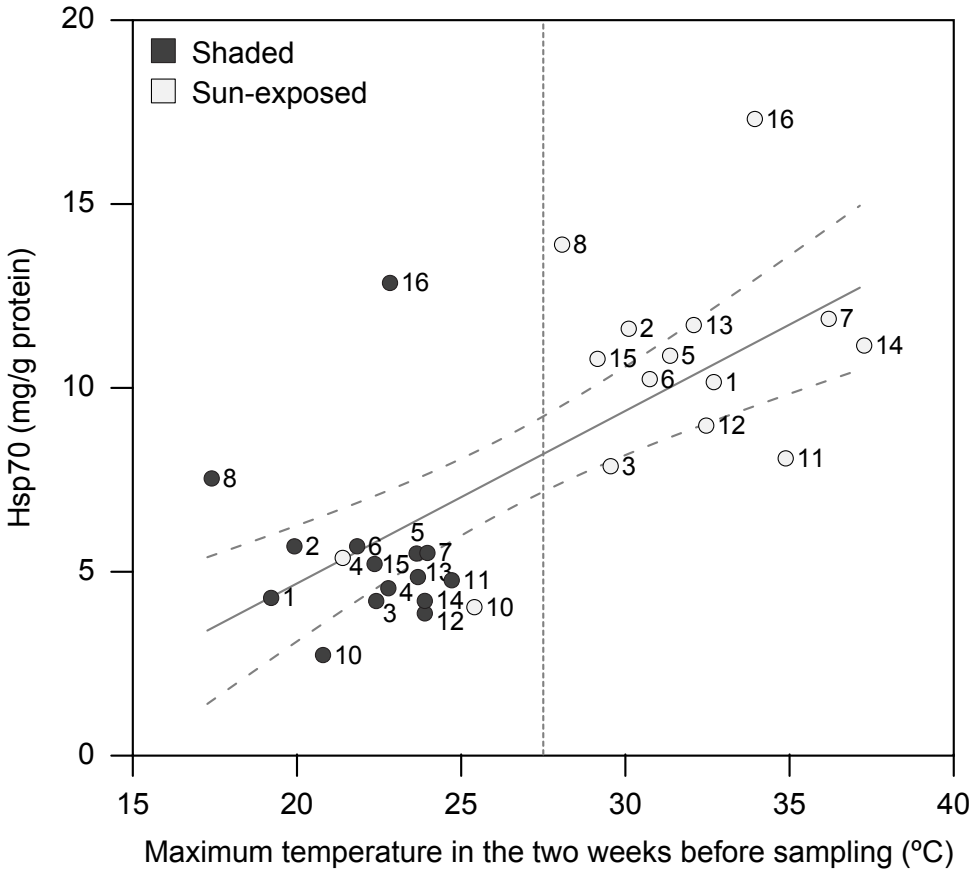

Figure 3.2: Correlation between Hsp70 and temperatures experienced prior to sample collection. Each dot represents either a shaded microhabitat (light grey) or sun-exposed microhabitat (dark grey). Reported Hsp70 is the average level among the 8 individuals collected at each microhabitat type within each location. Curved dashed lines enclose the 95% confidence interval. Reported temperature is the maximum temperature measured by robolimpets in the two weeks that preceded tissue collection for Hsp70 quantification. Vertical dotted line shows the temperature threshold of 27.5 °C used in Fig. 3.3. See Fig. 3.1c for a map with sampled locations.

HSP response and population densities as proxies, we show that limiting effects of temperature, rather than being related to latitude, seem to be tightly associated with micro-topography.

Microhabitat-associated variability in thermal stress

Our study encompassed the majority of the geographic range of *Patella vulgata*. Despite the wide latitudinal breadth, there was not a single location where animals inhabiting sun-exposed rock surfaces did not have, on average, higher Hsp70 levels than animals collected from the corresponding shaded microhabitats (Fig. 3.1a). This is remarkable, especially considering the site to site variability introduced by the geographical extent of the study (with locations featuring different geomorphology, exposure to wave action, food availability, or community composition, among others). Taking into account the combined metabolic cost of replacing heat damaged proteins (Hofmann and Somero, 1995) and the heat-shock response itself (including the expenditure of ATP in heat-shock gene transcription, synthesis of Hsp, and maintenance of

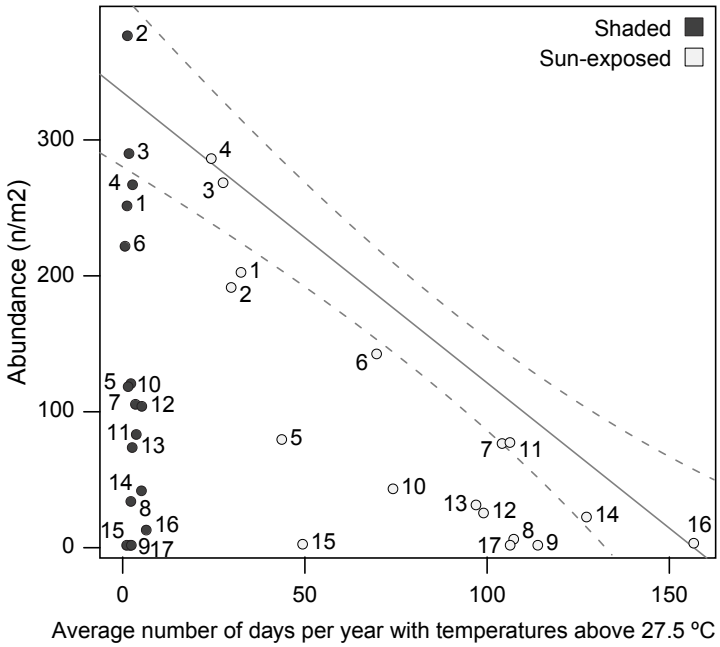

Figure 3.3: Temperature as a potential limiting factor for *Patella vulgata*. The solid line shows the 95th regression quantile estimate for the abundance of *P. vulgata* as a function of the yearly number of days exceeding 27.5 °C. Dashed lines enclose the 95% confidence interval. The temperature threshold of 27.5 °C was obtained from Fig. 3.2 (see Material and Methods). Number of days based on 1 h-resolution robolimpet data collected between the summers of 2010 and 2014. Each dot represents either a shaded microhabitat (light grey) or sun-exposed microhabitat (dark grey). Reported abundance is the mean density of *P. vulgata* quantified in 15 quadrats of 30x30 cm at each microhabitat type within each location. See Fig. 3.1c for a map with sampled locations.

their chaperoning functions, Somero, 2002), the present data suggests that thermal differences between sun-exposed and shaded microhabitats (Figs. 3.2, 3.3) are indeed associated with differences in physiological performance, and thus, have the potential to significantly affect processes such as survival, growth or reproduction.

Biogeographic consequences of recurrent thermal stress

Our data show that the contrasting temperatures between sun-exposed and shaded microhabitats previously reported by Seabra et al. (2011) for the Iberian Peninsula are common over much wider spatial scales (at least over the majority of the European Atlantic coast), and over larger temporal scales (at least four years). Temperatures at sun-exposed microsites routinely exceed 27.5 °C even at high latitudes; for example, sun-exposed microsites in the British Isles had, on average, approximately 30 such days per year. In contrast in shaded microhabitats temperatures hardly ever exceeded 27.5 °C, even at the southernmost locations, in southern Portugal (Fig. 3.3). Our study suggests that the frequency of occurrence of high temperatures imposes a limit on the maximum population densities supported at any given place. We hypothesize that: (i) physiological stress increases when animals are exposed to high temperatures, and that (ii) because higher temperatures are recurring in sun-exposed microhabitats, ecological

outcomes of heat stress (such as diminished population densities) are also more severe in sun-exposed microhabitats. Thus, the limiting effects of temperature, rather than being related to latitude, seem to be tightly associated with microsite variability, reinforcing the notion that the physiological responses of intertidal organisms (and subsequent ecological consequences) are driven by the environmental conditions observed in their immediate vicinity (Helmuth et al., 2010). If these hypotheses are correct, then population densities of septentrional (cold-water) species at a given location are largely controlled by the relative abundance of hot (stressful) and cold (refugia) microhabitats. Locations with appropriate geomorphology (e.g., north-facing cliffs) or with adequate topographical complexity (e.g., large boulders with high thermal inertia) should harbor larger populations because they allow its inhabiting organisms to withstand thermally stressful periods during diurnal low tide (Gedan et al., 2011). This may explain why the "abundant-centre" distribution, with highest population densities at the centre of the distribution range and declining towards the range edges, has rarely been observed in intertidal species (Sagarin and Gaines, 2002a,b; Pironon et al., 2015), as the fraction of the local habitat that can be used as thermal refugia is not necessarily correlated with latitude. In *P. vulgata*, thermal stress in the vicinity of the hot range limits (both immediately north of the distribution gap in the Bay of Biscay and north of the absolute distribution limit in SW Iberia) is so high that although we found the same general pattern between microsites (i.e., limpets exposed to solar radiation are, on average, more stressed), even animals from shaded microsites are unable to avoid severe thermal stress. Thus, at the hot range edges, the magnitude of the amelioration provided by the shade is insufficient to provide thermal refugia, which could be the very reason why the geographical limits are there. The scarcity of thermal refugia and the extremely low population densities means that larval supply and thus recruitment are most likely compromised, which is probably made worse by a shortage of males at those latitudes (Borges et al., 2015). Fig. 3.2 suggests that the reason for the increased thermal stress at these marginal populations is not exclusively related to maximum temperatures occurring immediately prior to collection (note how both shaded and sun-exposed data points #8 and #16 are higher than expected considering only maximum temperatures). It is plausible that a second environmental stressor (or combination of stressors), such as oxygen deprivation, desiccation, salinity extremes, or pollutant contamination (which are known to increase Hsp70 production, Feder and Hofmann, 1999) are imposing additional layers of stress on these marginal populations. We speculate, however, that the cause for the increased stress is the elevated seawater temperature characteristic of these locations during summer. In fact, in that season, both the coastal waters off southern Portugal and in the southern Bay of Biscay are warmer than the surrounding regions (Valencia et al., 2004; Lima et al., 2007a). This explanation corroborates previous studies indicating that the equatorial range edge for this species is set by summer conditions (Bowman and Lewis, 1977) and is congruent with the fact that both sun-exposed and shaded microhabitats exhibited abnormally high stress levels (as both microhabitats are equally submerged during high tide). Furthermore, the proposed

mechanism is supported by recent experimental data showing that water temperatures at these locations elicit remarkably high levels of thermal stress, effectively acting as a threshold beyond which *P. vulgata* cannot exist (Seabra et al., 2015a). The same study suggests that individuals from his species living in regions such as NW Iberia and NW France, routinely exposed to cold upwelled water during summer, have opportunity to recover during high tide.

Evolutionary implications

If shaded microhabitats can be found in almost every location, why have organisms not evolved to either selectively settle in or to subsequently move to shaded microhabitats? Although that might be the case for some species (e.g., the barnacle *Perforatus perforates*, the sponge *Hymeniacidon sanguinea* or the anemone *Actinothoe sphyrodeta* which can only be found in crevices or shady rocky overhangs), it does not appear to happen with *P. vulgata*. These limpets have greater population densities in shaded microsites (Fig. 3.1b) which means that intra-generic and intra-specific competition for food and/or space is much higher in those microhabitats (Boaventura et al., 2002, 2003; Espinosa et al., 2006). In addition, sun-exposed surfaces have more light availability, and thus, within reasonable limits, have the potential to sustain higher primary productivity, which is beneficial for herbivores such as limpets (Einav et al., 1995; Harley, 2002). This hypothesis is supported by recent data suggesting that grazing pressure from limpets is much greater on south- than on north-facing substrata (Firth et al., 2015). This may, however, not be valid in extreme situations because biofilm growth is inhibited by extreme insolation during summer (Thompson et al., 2004). Thus, even though living in sun-exposed microhabitats means having to cope with higher levels of thermal stress, other factors, such as reduced competition, increased food availability or even shelter offered by canopy forming algae (Moore et al., 2007) may play important ameliorating roles, reducing the selective pressure from choosing shaded microhabitats.

Importance for climate change

The variability in thermal stress arising from local topography means that, throughout their entire distributional range, most sessile intertidal species are exposed to a mosaic of highly stressful areas interspersed with thermal refugia. This heterogeneity is likely to have profound effects on the way local populations (and therefore species as a whole) respond to either long-term increases in temperature (Lima and Wethey, 2012), or to increases in the frequency of extreme events (Wethey et al., 2011). The resilience or vulnerability of local populations to changes in climate is probably highly dependent on the abundance of thermal refugia, which may act as a thermal buffer. These refugia provide conditions that are at or below the point of collapse of the thermal performance curve (Woodin et al., 2013), overriding the long-term warming trend and allowing populations of northern species to persist, thus maintaining the overall extent of the range despite patchy extirpations in thermally stressful microhabitats. The

availability of thermal refugia may even allow the ranges of northern species to be extended equatorward to areas otherwise uninhabitable. Species with meridional affinity (warm-water species), on the other hand, benefit from hot microhabitats and thus the expansion of their ranges northwards can be assisted by the greater availability of appropriate microhabitats with global warming. In fact, contrasting patterns in the average direction of change between cold- and warm-water species (including counterintuitive equatorward range expansions of septentrional species) have already been described for a wide range of sessile intertidal organisms (e.g., Lima et al., 2007a; Hilbish et al., 2010). In the specific case of *P. vulgata*, during the last glaciation the species occurred much further south, then retreated polewards during the transition to the warmer interglacial climate, and finally re-expanded during the glacial-like conditions of Younger Dryas (see Ortea, 1986; Southward et al., 1995). Small-scale thermal refugia was most likely fundamental for the continued recruitment of *P. vulgata* towards its range edge. Since the effects of topography on site conditions have the potential to locally override the effects of global warming (Holtmeier and Broll, 2005), it is necessary to understand the link between the environmental mosaic and macro-ecological processes in order to correctly forecast the consequences of climatic change, a task which may be more complex than could be anticipated (Marshall et al., 2013). A comprehensive understanding of the abundance or scarcity of refugia (including the consideration of multiple stressors or multiple aspects of a single stressor, Seabra et al., 2015b) is thus crucial to predict where and when the effects of climate change will occur.

3.1.6 Acknowledgements

This work was funded by FEDER (FCOMP-01-0124-FEDER-010564 and FCOMP-01-0124-FEDER-020817) and FCT (PTDC/MAR/099391/2008, PTDC/MAR/117568/2010). RS and FPL were supported by FCT (IF/00043/2012 and SFRH/BD/68521/2010, respectively). DSW and TJH were supported by grants from NASA (NNX11AP77G) and NSF (OCE1129401). Authors declare no conflict of interest.

3.2 An improved noninvasive method for measuring heartbeat of intertidal animals

3.2.1 Abstract

Since its emergence two decades ago, the use of infrared technology for non-invasively measuring the heartbeat rates of invertebrates has provided valuable insight into the physiology and ecology of intertidal organisms. During that time period, the hardware needed for this method has been adapted to currently available electronic components, making the original published description obsolete. This article reviews the history of heartbeat sensing technology, and describes the design and function of a modern and simplified infrared heartbeat rate sensing system compatible with many intertidal and marine invertebrates. This technique overcomes drawbacks and obstacles encountered with previous methods of heartbeat rate measurement, and due to the sensor's small size, versatility, and noninvasive nature, it creates new possibilities for studies across a wide range of organismal types.

3.2.2 Introduction

Heartbeat rate, or cardiac activity, has been shown to serve as an effective index for whole organism physiology for a variety of intertidal invertebrates including mollusks (Helm and Trueman, 1967; Santini et al., 1999, 2000; Chelazzi et al., 2001; Marshall et al., 2011) and arthropods (De Pirro et al., 1999a; Rovero et al., 2000; Calosi et al., 2005; Bini and Chelazzi, 2006; Ungherese et al., 2008; Styrishave et al., 2010). Quantifying this parameter under a variety of natural and experimental conditions can aid in understanding the general physiological responses of these organisms to abiotic stresses in the environment (Stillman and Somero, 1996; Ungherese et al., 2008; Styrishave et al., 2010; Williams et al., 2010; Logan et al., 2012), biotic interactions (Rovero et al., 1999, 2000), and exposure to toxins (Chelazzi et al., 2004; Galloway et al., 2004; Marshall et al., 2004; Halldórsson et al., 2008). In particular, these data can improve our ability to predict the responses of species to changing environments such as increases in temperature or levels of pollution. Such predictions are particularly relevant for the intertidal zone where many species are thought to already live at or near their upper lethal limits of stress tolerance (Somero, 2002). Measuring cardiac activity of intertidal organisms has been a focus of research for many decades (Pickens, 1965; Bayne et al., 1976; Nicholson, 2002; Braby and Somero, 2006). One of the first methods, which is still used, measures the changes of circulatory structures with electrical impedance. This is an invasive technique, which requires implanting electrodes in the pericardial cavity (Helm and Trueman, 1967). Changes in the impedance between the electrodes are proportional to the change of the circulatory cavity or vessel during a heartbeat. A more recently developed alternative to the impedance method uses an infrared (IR) light emitting diode (LED), which generates an electric signal

that is electronically amplified and filtered, coupled with a phototransistor detector (hereafter IR sensor). In the late 1980s, Depledge and Andersen (1990) devised a computer-aided physiological monitoring system (CAPMON) in which the average heartbeat frequency of the target animal was automatically computed via custom-made hardware connected to a PC. This method was quickly adopted in marine and intertidal invertebrate physiology research because it was noninvasive, allowed for multiple cardiac activities to be measured simultaneously, could function in both air and water, and was capable of measuring continuously for long periods of time. Studies using the CAPMON system have been confined to a relatively small group of investigators (Santini et al., 1999; Curtis et al., 2000; Morritt et al., 2007; Styrishave et al., 2010). The CAPMON design has however been regularly upgraded to be compatible with the evolving electronics technology and modified, for example, to be connected to any data logger or oscilloscope. The original hardware described by Depledge and Andersen (1990) is difficult to assemble using parts currently available from electronics distributors. Unfortunately, upgrades to the circuit design have not been widely disseminated and therefore remain unknown to the great majority of researchers. Relatively recent studies using this technology only cite the original CAPMON design although modified versions of the apparatus are used (Chelazzi et al., 1999; De Pirro et al., 1999a,b; Santini et al., 1999; Chelazzi et al., 2001; Morritt et al., 2007; Ungherese et al., 2008; Sarà and De Pirro, 2011; Williams et al., 2010). Therefore, the aim of this paper is to disseminate widely the specific design of an IR sensor and corresponding amplification system, thus enabling a uniform method of data collection by a wide range of researchers. We also report the results of observational and experimental studies using previous versions of IR heartbeat sensors, further validating the technique as an effective way to measure heartbeat rates of intertidal invertebrates in both laboratory (Rovero et al., 2000; Calosi et al., 2005; Spooner et al., 2007; Marshall et al., 2011) and field experiments (Santini et al., 2000; Williams et al., 2005; Styrishave et al., 2010).

3.2.3 Material and Methods

The sensors typically used with the IR method of heart rate measurement combine an IR emitter and an IR detector in a small package. Fixing the sensor to the exoskeleton of an animal, above its heart, allows IR light to pass through the shell of the animal and illuminate the heart and nearby circulatory vessels. Changes in the shape or volume of the circulatory structures during a heart contraction, or heartbeat, cause a change in the amount of IR light reflected from the animal's internal anatomy back to the IR detector. These changes in reflected IR light, transduced to changes in electrical current, are then electronically amplified and filtered, and processed by the software (Fig. 3.4). The circuit board in the design presented here (Fig. 3.5) was produced on a two-layer printed circuit card (ExpressPCB Corp.). The power supply portion of the circuit (Fig. 3.5A) consists of a 6 V battery pack connected to a LM7805 fixed voltage regulator, which feeds the circuit with 5 V. Two bypass capacitors (C1

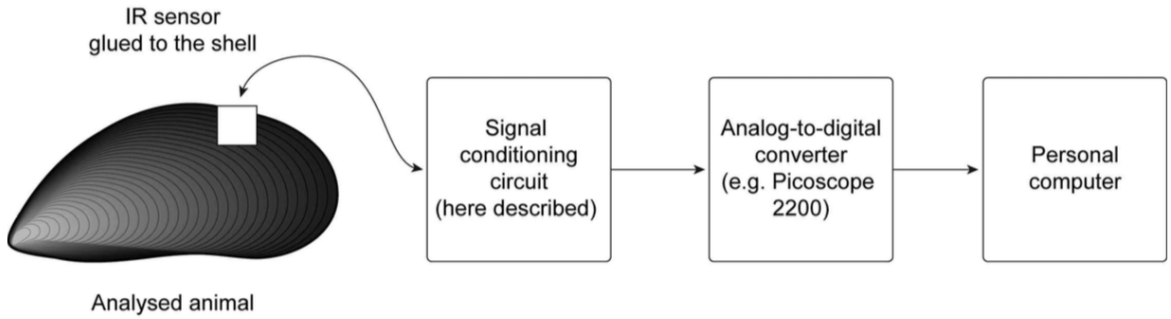

Figure 3.4: Flowchart of the heartbeat signal from the IR sensor to the data logging device.

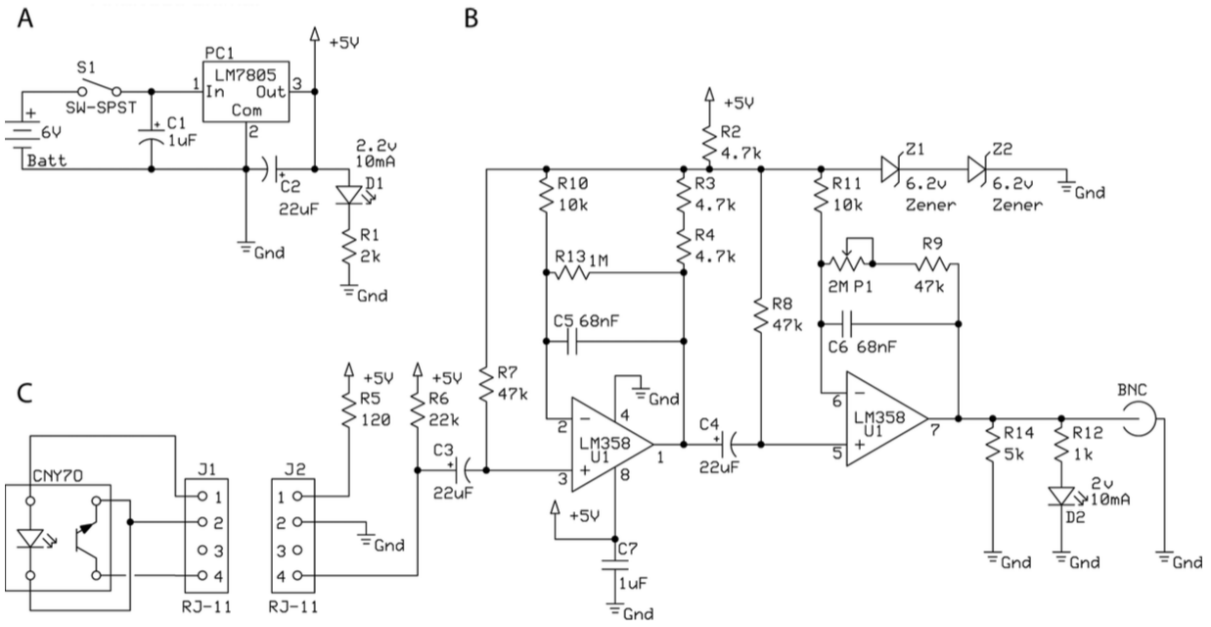

Figure 3.5: Functional schematic diagram of IR cardiac sensing amplification circuit. See Table 3.3 for the Bill of Materials. Note chip LM358 (U1) has two operational amplifiers, so each is depicted with its pin connections.

and C2, with 1 µF and 22 µF, respectively) are employed to improve supply voltage stability, and an LED (D1) indicates when the circuit is powered. This device uses a CNY70 (Vishay Intertechnologies) sensor (Fig. 3.5C), the same sensor as the original CAPMON system (1990). The sensor is connected to a thin, flexible wire (e.g., unshielded 30 AWG wirewrap wire, Digikey part K329-ND or shielded 30 AWG Pro Power 3027442, Newark part 98K8670), to minimize disturbance of the monitored animal. The other end of the wire connects to the main circuit via an RJ-11 connector (J1). The signal conditioning circuit (Fig. 3.5B) is built around a single chip (LM 358) containing two identical high-gain operational amplifiers fed by the same power supply. A 1 µF bypass capacitor (C7) at the LM 358's power input is used to further reduce power supply noise. The two noninverting amplification stages yield a maximum gain of 78 dB and are fitted with low-pass filters to reduce the amplification of unwanted high frequency electrical noise from nearby equipment or power lines. The combined cut-off frequency is 2.2

Table 3.3: Bill of Materials for the IR cardiac sensing amplification circuit. Digikey: www.digikey.com; Newark: www.newark.com.

Reference	Type	Description	Manufacturer part nr	Digikey part nr	Newark part nr
R1	Resistor	2 kΩ, 250 mW, 1%	CMF1/42001FLFTR	CMF502K0000FHEB	40M8448
R5	Resistor	120 Ω, 250 mW, 1%	MCMF0W4FF1200A50	MFP-25BRD52-120R	58K3804
R7, R8, R9	Resistor	47 kΩ, 250 mW, 1%	MCMF0W4FF4702A50	MFP-25BRD52-47K	58K3860
R6	Resistor	22 kΩ, 250 mW, 1%	MCMF0W4FF2202A50	RNMF14FTC22K0	58K3829
R10, R11	Resistor	10 kΩ, 250 mW, 1%	CMF1/41002FLFTR	MFP-25BRD52-10K	40M8391
R13	Resistor	1 MΩ, 250 mW, 1%	HVR2500001004FR500	MFR-25FRF-1M00	24R8876
R2, R3, R4	Resistor	4.7 kΩ, 250 mW, 1%	MCMF0W4FF4701A50	MFP-25BRD52-4K7	58K3858
R14	Resistor	5 kΩ, 250 mW, 1%	MCMF0W4BB5001A50	RN60D5001FB14	97M6277
R12	Resistor	1 kΩ, 250 mW, 1%	MCMF0W4FF3900A50	MFP-25BRD52-1K	58K3796
P1	Potentiometer	2 MΩ, 0.5 W	3299W-1-205LF	3299W-205LF-ND	32K7942
C5,C6	Capacitor	68 µF, 50 V, 5%, Metal Poly	BFC237022683	3012PH-ND	95C1397
C2, C3, C4	Capacitor	22 µF, 50 V, 20%, Electrolytic	ECA-1EM220	P5149-ND	58T1652
C1, C7	Capacitor	1 µF, 50 V, 20%, Radial	ECA-1HM010I	P10421TB-ND	38K1171
D1	Green LED	3 mm, 568 nm, 2.2 V, 10 mA	WP3A8GD	754-1217-ND	93K6987
D2	Red LED	5 mm, 623 nm, 2 V, 10 mA	LTL-10223W	160-1087-ND	93K6988
PC1	Voltage regulator	5 V, 1 A	LM7805CT	LM7805CT-ND	34C1092
U1	Dual op amp	700 kHz dual 8 DIP	LM358	296-9554-5-ND	41K4888
Z1, Z2	Zener diode	500 mW, 6.2 V, 5%	1N753A	—	10M6196
BNC	BNC connector	50 W	31-5431-2010	ARF1065NW-ND	—
J1	RJ-11 plug	4 conductor	30-9910	—	30-9910
J2	RJ-11 connector	4 pin	5520250-2	A31405-ND	—
CNY70	IR sensor	950 nm emitter/transducer	CNY70	751-1025-ND	95B4223

Hz (at a 3 dB level), i.e., the maximum amplification is approximately 7900x for frequencies between 0.2 Hz and 1 Hz, but at frequencies up to 3 Hz the amplification is still reasonable (gain calculated using LTspice IV software, www.linear.com). The potentiometer (P1) can be manually adjusted, reducing the overall amplification where needed. Two 22 µF capacitors (C3 and C4) at the input of each amplifier filter out the DC component in the signal. Faster capacitors (e.g., 2.2 µF) can also be used, but reduce the amplification of low frequencies and thus should not be used for animals with heart rates slower than approximately 1 Hz. The diodes Z1 and Z2 control the bias voltage (0.6 V) on the amplification stages, and the LED D2, placed at the output of the second amplifier stage, flashes as pulses are received and amplified by the circuit. The amplified signal is outputted to a BNC connector, which can be used to connect the circuit to either an external oscilloscope or PC. The complete bill of materials (BOM) is provided in Table 3.3.

A PicoScope 2200 (Pico Technology) or USB-6009 (National Instruments) is used to convert the analog signal from the signal conditioning circuit to a digital format, which is then read and plotted on a PC running PicoScope 6 software (www.picotech.com) or NI LabView Signal Express (www.ni.com/labview). Cardiac frequency is calculated using a spectral analysis procedure or manually by dividing the number of regular voltage oscillations by the amount of time recorded.

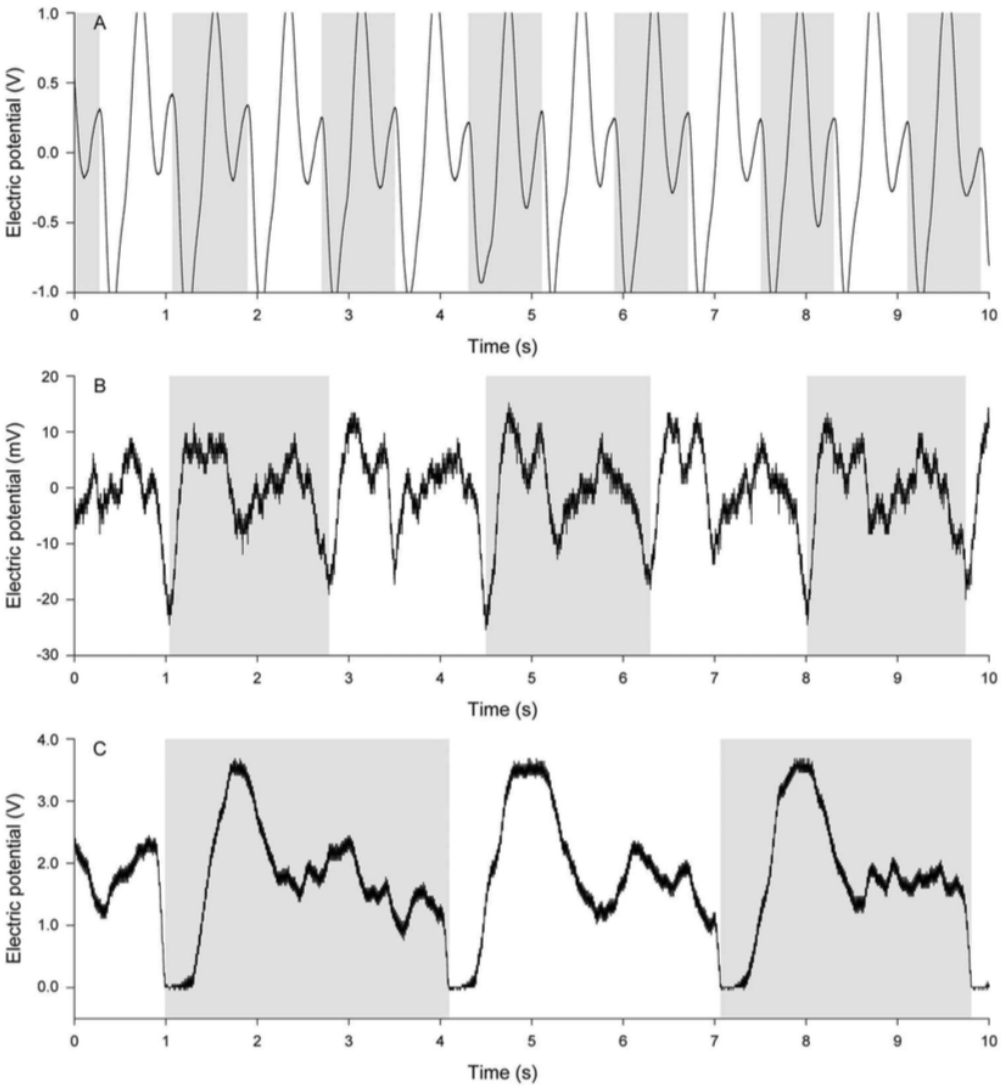

Figure 3.6: Unfiltered heartbeat signals of the limpet *Cellana grata* (A), the mussel *Septifer virgatus* (B), and the mud crab *Panopeus herbstii* (C). The scale of the y-axes varies among graphs. Note that depending on the species (and also on the sensor placement), the shape of the curve may feature multiple peaks per heartbeat. Signal noise also varies among the graphs, potentially caused by electrical noise from the oscilloscope. Therefore, automatic peak counting may not give accurate results. Shaded areas are provided to facilitate signal comparison.

3.2.4 Assessment

In contrast with the CAPMON system, the signal conditioning circuit here described does not transform the analog signals from the IR sensor into square waves for automatic calculation of cardiac frequencies (Depledge and Andersen, 1990; Depledge et al., 1996). The CAPMON system was originally intended for measuring heartbeat of decapod crustaceans, so the automatic counting feature was specific to typical decapod crustacean heartbeat patterns (Depledge and Andersen, 1990). The benefit of collecting raw, non-square heartbeat signal waves is that animals can have unique heartbeat patterns that may otherwise be misinterpreted by an automatic counting circuit (Fig. 3.6). The IR method is most easily used on arthropods

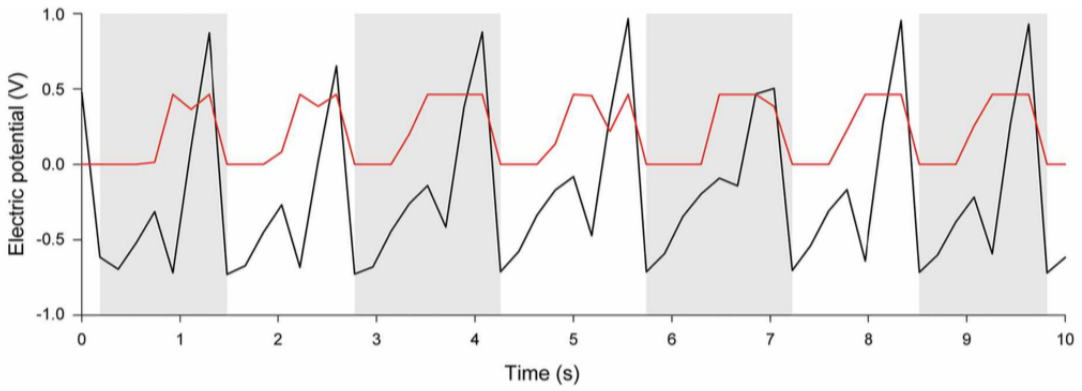

Figure 3.7: Heartbeat patterns of an Atlantic blue crab (*Callinectes sapidus*) measured simultaneously with the standard impedance method (black line) and with IR sensors (red line). Both lines show seven complete heartbeats in the 10 s interval. Shaded areas are provided to facilitate signal comparison.

and mollusks, as the exoskeletons of these animals provide the IR sensor a stable surface for attachment, enabling consistent measurements of each over time. Though this method and similar principles have been previously validated in crustaceans (Depledge and Andersen, 1990) and bivalve mollusks (Haefner et al., 1996), we compared the reliability of the updated amplifier to heartbeat recordings made with the standard impedance method (Helm and Trueman, 1967). Simultaneous heartbeat measurements were made in an adult Atlantic blue crab, *Callinectes sapidus*, using the IR method with our updated amplifier and the impedance method with the implantation of 30 gauge Teflon-coated magnet wire. Data from the two methods were collected as analog signals (impedance converted by UFI Impedance Converter, UFI) by a single data acquisition system (Sable Systems UI-2 Data Acquisition Interface, Sable Systems International) at a sampling rate of 5 Hz. Heartbeat signals from the impedance and IR methods showed the same heartbeat pattern and frequency (Fig. 3.7). The placement of the sensor has a strong effect on the quality of the heartbeat signal (see "Discussion" for details). In crabs there are markings on the carapace just dorsal to the heart, facilitating effective placement of the IR sensor. However, in a bivalve mollusk, it can be more difficult to place the sensor effectively over the heart. Using the IR method on the bivalve *Septifer virgatus* (shell length = 3 cm), we compared the quality of heartbeat signals collected at various locations around the valves of the mussel (Fig. 3.8). The heartbeat signals at an optimal position (position B) had amplitudes twice that of signals from a poorly positioned sensor, and more importantly, a regular repeating pattern. Signals with better quality for *S. virgatus* were typically found next to the mid-dorsal posterior hinge area of the valves, although each was slightly different. Shell curvature and thickness, as well as the whole animal size, certainly contribute to variations among conspecifics, so other species should be evaluated in a similar manner to find the best location for sensor placement to detect heart contractions. This evaluation can be performed by observing real-time changes in signal quality at different locations, even before bonding the sensor to the animal. Uncertainty in the placement of the sensor does not necessarily mean

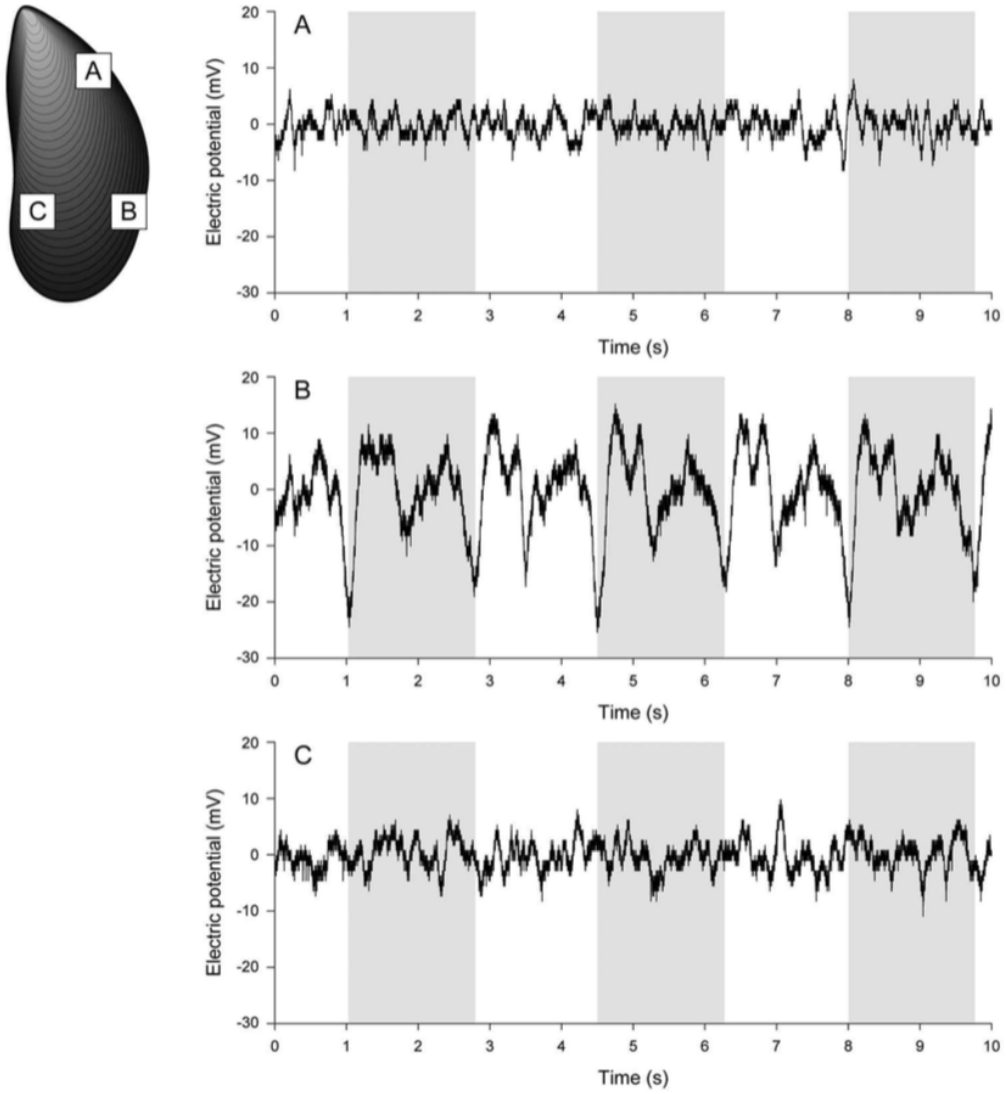

Figure 3.8: Variation in measurements of the heartbeat signal of the mussel *Septifer virgatus* with the IR sensor placed on three regions on the shell (A, B, and C). Shaded sections are provided to facilitate comparison of signals.

clear heartbeat signals are difficult to obtain. For example, limpets of the genus *Patella* are fairly resilient to handling disturbance, and it is possible to identify the most effective sensor placement by simply pressing the sensor against the limpet's shell and holding the apparatus still for the whole measurement. This method is not useful for organisms that exhibit irregular heartbeat patterns in response to handling disturbance. Conversely, with proper cleaning of the area where the sensor is to be attached and by using a strong bonding agent, a durable yet unintrusive system can be assembled, which enables longer experiments to be performed. For example, Fig. 3.9 shows a week's worth of heartbeat data obtained from a single *Patella vulgata*.

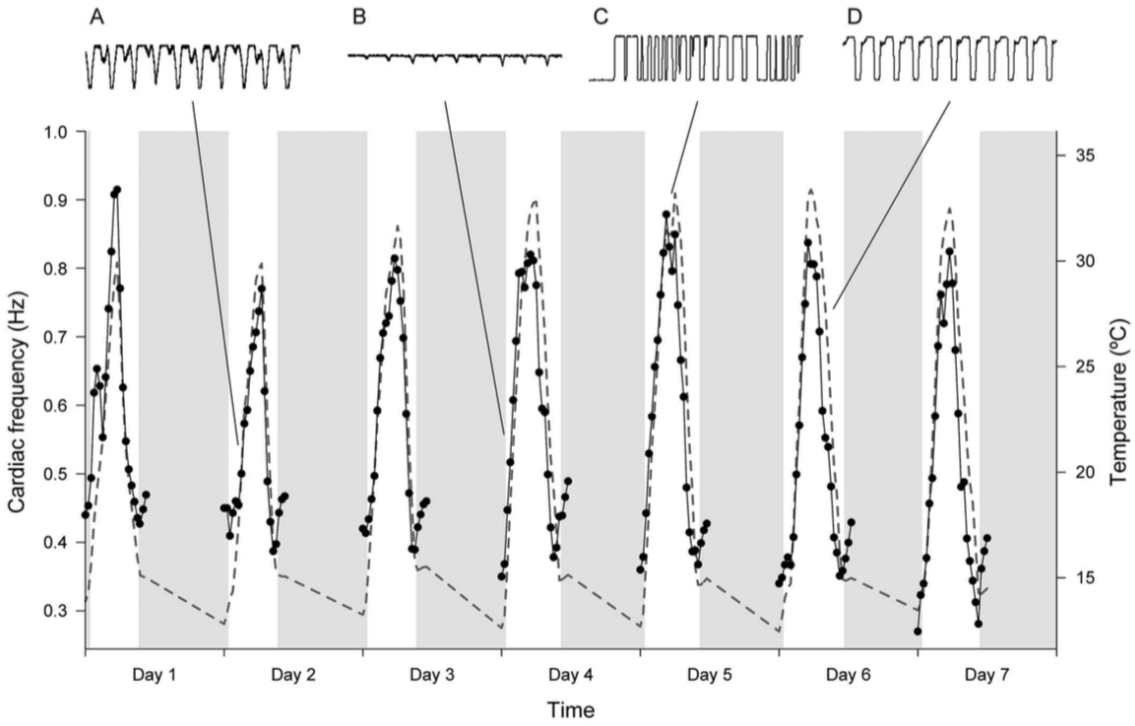

Figure 3.9: Cardiac frequency of a china limpet (*Patella vulgata*) exposed to 7 d of simulated tides under laboratory conditions. The sensor was attached to the animal during the acclimation period, and remained in place for the whole experiment. Heartbeat was measured every 30 min in the period between 1 h before the low tide and 2 h after the low tide. Closed circles show heartbeat measurements. The dashed gray line shows the thermal profile to which the animal was exposed during the experiment. The vertical shaded regions indicate periods of immersion, and the vertical unshaded regions indicate periods of emersion. Inserts A-D show the heartbeat signal recorded at the 4 different times indicated, illustrating that even with considerable variability in signal shape and amplitude, it is still possible to obtain comparable heartbeat rates. Signal amplitude was 2.5 V in A, C, and D and 1.3 V in B.

3.2.5 Discussion

In general, the IR sensor amplifier modifications described in this article are a simplification of the original CAPMON system. In lieu of an automatic triggering function that calculates average heartbeat rates, the updated amplifier preserves the raw signal after amplifying it to a specific voltage scale. Maintaining the true shape of the wave is beneficial because each organism is likely to exhibit a unique heartbeat pattern that may otherwise be misinterpreted by an automatic counting circuit, like that seen with the CAPMON system. This is particularly important for animals that have irregular heartbeat rates (Depledge et al., 1996). Noise on the IR heartbeat signal in combination with irregular or extremely slow heartbeats can create a heartbeat signal too complex for automatic analysis (e.g., FFT analysis, periodogram) and often requires heartbeat frequencies to be identified and counted manually. In this context, it is important to clarify that the IR method is primarily designed to measure heartbeat frequency and not signal amplitude. Sensor placement must therefore be optimized (see above) to obtain the best signal quality — i.e., cyclic fluctuations in voltage can be identified, the

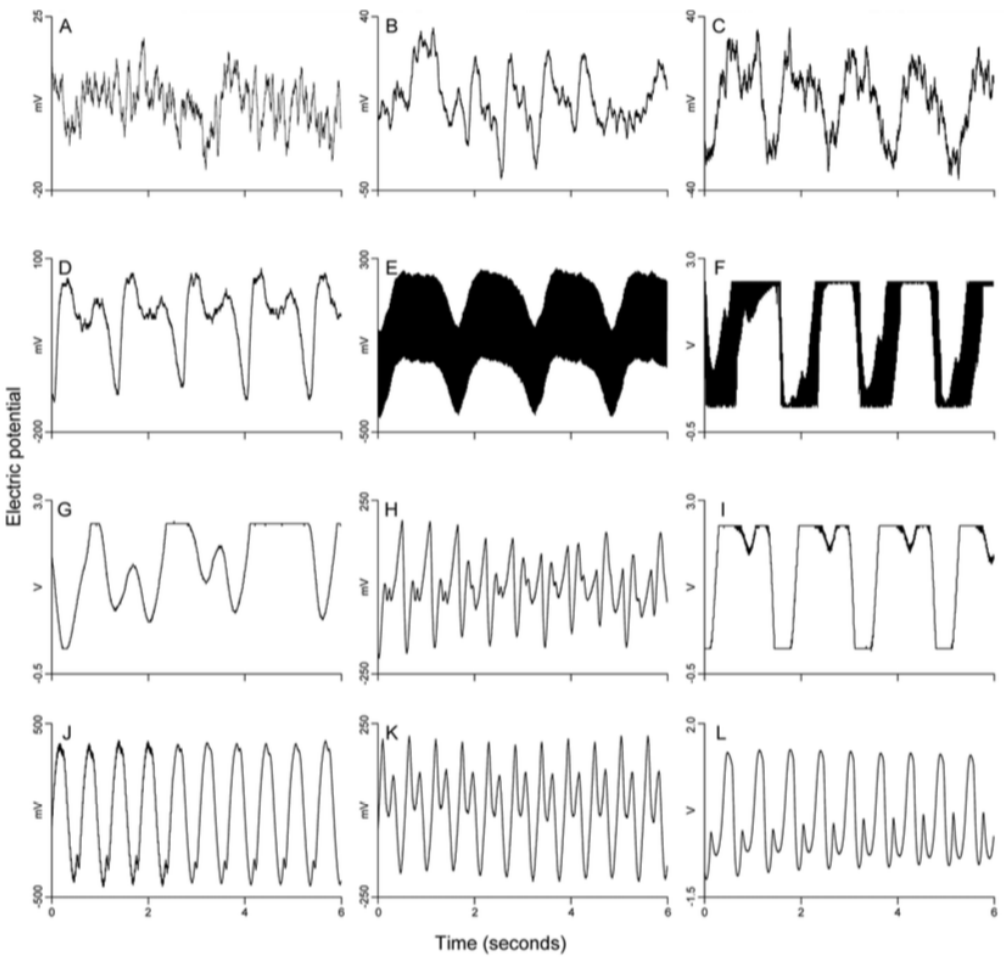

Figure 3.10: Examples of heartbeat signals of *P. vulgata* recorded under various laboratory conditions. Signal quality can be degraded by numerous factors: signal below amplification power (A, B), poor insulation of sensor wiring (C), presence of electronic noise (E, F), sub-optimal placement of the sensor (G), or movement of internal organs other than the heart (possibly H). Such conditions can render the signal useless (A) or almost useless (B), but as long as a regular repeating pattern can be found the signal has sufficient quality for heartbeat rate to be calculated (C). Signals like that in G may require additional recordings so they can be more safely interpreted. Better quality signals are usually composed of two crests per heartbeat, with crests having equal or very different amplitudes (D, H-I, K-L, but see J). Clipping occurs when the signal voltage exceeds the circuit output range (F, G, I), and results in a flat top or bottom in the signal; this situation is fairly common and does not necessarily indicate a poor signal. It can, however, be avoided by tuning the potentiometer P1 in the circuit (see Fig. 3.5).

number occurring over a continuous period can be determined, and rate can then be calculated (Fig. 3.10). Because even the continuous monitoring of one animal without repositioning the sensor can reveal changes in amplitude and shape of the signal (e.g., Fig. 3.10A-D), one cannot use the amplitude and shape of the signal to assess cardiac function. Additionally, preserving heartbeat signals in raw format may allow further analyses to be made, such as the identification of bradycardia or periods of no heartbeat (De Pirro et al., 1999b; Chelazzi et al., 2001; Marshall et al., 2004). The sensor component of the system described here has been modified to detect heartbeat of smaller invertebrates ($<$ 1 cm) by direct contact of the IR

sensor (Calosi et al., 2003) or indirectly by placing the animal within the confinement of an aluminum foil bag (Van Aardt and Vosloo, 2011). It can also be modified to measure cardiac activity of animals under simulated hyperbaric conditions (Robinson et al., 2009). Tailoring IR sensors to particular species allows the IR method to be fairly reliable, robust, flexible, and most important, noninvasive. The application of this method to other organisms has likely been limited by the availability and awareness of the method, rather than the compatibility of the sensor with the study organisms. Apart from the amplification circuitry, further simple modifications to the hardware can expand and enhance the use of the system in physiology and ecology studies. For example, finer gauge wire for the entire length between the amplifier and the IR sensor reduces movement restriction when measuring heartbeat rate in mobile or burrowing animals (shielded 30 AWG Pro Power 3027442, Newark part 98K8670), we commonly use sensor leads of 2 m without detectable signal attenuation; smaller and flatter IR sensors, e.g., reflective optical sensor TCRT1010 (Vishay Intertechnologies, Inc.), facilitate measuring heartbeat rate in smaller organisms or in burrowing organisms; multichannel analog data loggers, e.g., National Instruments USB-6009 (National Instruments Corp.), allow for multiple individuals to be monitored concurrently. The circuit described here has to be printed in a PCB board and manually assembled, using the parts listed in Table 3.3, which might be a serious obstacle to researchers unfamiliar or un-equipped to work with electronics. Alternatively, electrical contractors can easily construct the circuit boards and sensors for this system at relatively low cost (e.g., AMP-3, Newshift Lda). These professionally built systems have the additional advantage of improved voltage stability, industrial quality assemblage, and sturdy connectors. Limitations to the IR method may be encountered when recording the heartbeat of active animals. Distortions to the signal can be caused by body movements such as foot movement in small littorinid snails, radula movement in gastropods, and siphon activity in bivalves. Foot movement during locomotion or radula movement while feeding can create a signal that is momentarily greater than the signal of the true heartbeat. Detecting foot movement may be difficult to avoid in smaller active gastropods, but disturbance from the radula movement can be minimized by placing the IR sensor on an alternative location on the shell where a heartbeat signal is still detectable. To some extent this is also the case for the electrical impedance method, since the measurement of impedance variation between two points in the organism's body is also susceptible to movement artifacts. Further limitations may be encountered when using the IR method due to the penetration and detection of the IR light. Infrared light penetration of the shell depends on shell thickness and structure. Therefore, this method may not work well for animals with extremely thick shells, though the upper limit of thickness has not been established. Detecting a heartbeat signal may be difficult if changes in ambient IR light cause signal fluctuations that mask the heartbeat. This ambient IR light problem can be avoided by creating a seal around the junction of the IR sensor and the animal's shell to block out ambient IR light. The compact design and relative simplicity of the amplifier circuit and sensor described herein should facilitate more in situ

studies of marine invertebrates, particularly those in the intertidal zone. Use of a computer or oscilloscope that can be enclosed in water-proof containers or transported quickly to measure heartbeats of animals in wave-exposed parts of a shore (Santini et al., 2000; Williams et al., 2005) complements the portable design of the amplifier circuit and sensor. The noninvasive nature of the sensor promotes longer term physiological studies (Fig. 3.9) and behavioral studies (Curtis et al., 2000; Rovero et al., 2000; Santini et al., 2002) for many species that would otherwise be hindered by the disturbance from the implantation of electrodes associated with the impedance method of heartbeat measurement. Along the same lines, marine microbiological and immunological studies requiring sterile methods for measuring physiological responses (Burnett et al., 2006) can also benefit from the application of noninvasive sensing. It is the authors' hope that the integration of taxonomically diverse physiological and ecological data, as enabled by the widespread compatibility of the IR method, can provide more comprehensive surveys of ecosystem health (Galloway et al., 2004; Hagger et al., 2009) in response to environmental stressors (Chelazzi et al., 2001; Calosi et al., 2005; Williams et al., 2010) or pollution (Bloxham et al., 1999; Curtis et al., 2001; Marshall et al., 2004).

3.2.6 Acknowledgements

This work was funded by Fundação para a Ciência e a Tecnologia (FCT) through the project PTDC/MAR/099391/2008, NSF (OCE0926581, OCE1039513, OCE1129401), and NASA (NNG07AF20G, NNX11AP77). R.S. and F.P.L were supported by FCT individual grants SFRH/BD/68521/2010 and SFRH/BPD/34932/2007, respectively. N.P.B. was supported by a Magellan Scholar Grant from the University of South Carolina. L. E. Burnett provided laboratory space and impedance sensors for the *Callinectes* experiments. G. A. Williams provided laboratory space for the *Septifer* experiments.

3.3 Equatorial range limits of an intertidal ectotherm are more linked to water than air temperature

3.3.1 Abstract

As climate change is expected to impose increasing thermal stress on intertidal organisms, understanding the exact mechanisms by which body temperatures translate into major biogeographic patterns is of paramount importance. We exposed individuals of the limpet *Patella vulgata* Linnaeus, 1758, to realistic experimental treatments aimed at disentangling the contribution of water and air temperature for the build up of thermal stress. Treatments were designed based on temperature data collected at the microhabitat level, from 15 shores along the Atlantic European coast spanning nearly 20° of latitude. Cardiac activity data collected during the experiments indicate that thermal stress levels in *P. vulgata* are directly linked to elevated water temperature, while high air temperature is only stressful if water temperature is also high. In addition, the analysis of the link between population densities and thermal regimes at the studied locations suggests that the occurrence of elevated water temperature may represent a threshold *P. vulgata* is unable to tolerate. By combining projected temperatures with the temperature threshold identified, we show that climate change will likely result in the westward expansion of the historical distribution gap in the Bay of Biscay (southwest France), and northward contraction of the southern range limit in south Portugal. These findings suggest that even a minor relaxing of the upwelling off northwest Iberia could lead to a dramatic increase in thermal stress, with major consequences for the structure and functioning of the intertidal communities along Iberian rocky shores.

3.3.2 Introduction

It is widely recognized that geographic distributions of species are, to a large extent, determined by environmental factors. Of those, temperature has received much attention, being described as a major element in the establishment of range limits and phenological timings (Hutchins, 1947; Southward, 1958; Walther et al., 2002; Wethey, 2002; Parmesan and Yohe, 2003; Root et al., 2003; Hickling et al., 2006; Lima et al., 2007a; Wethey et al., 2011; Poloczanska et al., 2013). Despite the recognition of its fundamental role, much is yet to be explored in order to fully understand how exactly temperature governs the distributions of species. This is especially true for intertidal rocky shore ecosystems for three reasons. First, the intertidal thermal environment is inherently complex (Tomanek and Helmuth, 2002; Helmuth et al., 2006a; Denny et al., 2011; Seabra et al., 2011; Lathlean et al., 2014b), and can hardly be described using averages (Den Boer, 1968; Helmuth et al., 2006b, 2014; Vasseur et al., 2014; Seabra et al., 2015b), in particular because of the continuous transition between immersion and emersion resulting from tidal cycles. Secondly, animals inhabiting rocky shores are regularly

exposed to environmental extremes not only of temperature, but also of desiccation and wave impact forces (Foster, 1971; Denny et al., 1985; McMahon, 1990; Burrows et al., 2008), thus complicating the unequivocal attribution of observed responses to temperature. Thirdly, recording intertidal environmental parameters across large geographical scales is notoriously difficult (Rutz and Hays, 2009; Gandra et al., 2015, but see Seabra et al., 2011, 2015b), often leaving researchers with little option but to use remote sensed data. Such datasets, however, have spatial resolutions which are several orders of magnitude larger than the fine detail of rocky shores or the organisms therein, effectively obscuring the role microhabitat plays in determining their distribution patterns (Helmuth et al., 2006b, 2010; Denny et al., 2011; Potter et al., 2013). Nevertheless, since intertidal animals are often living close to their physiological limits (Somero, 2002; Stillman, 2003; Sunday et al., 2012), intertidal rocky shores offer a unique platform for the early detection of the effects of climate change, and its consequences for the ecology and biogeography of species. Detecting and predicting biological responses to climate change is one of the greatest challenges of today (Pereira et al., 2010). It is now recognized that climate change is a spatially and temporally complex process (Easterling et al., 2000; Lima and Wethey, 2012; IPCC, 2013; Vasseur et al., 2014), affecting, among others, the frequency and severity of extreme events heterogeneously around the globe (Easterling et al., 2000; Meehl et al., 2009), and impacting the temperature of oceans and atmosphere differently (Belkin, 2009; Hansen et al., 2010; Burrows et al., 2011). Since intertidal systems are the boundary between land and oceans, animals living there can be expected to be responding to combined effects of change in water and air temperatures (Harley et al., 2006). Furthermore, intertidal rocky shore communities in temperate zones are known to be highly structured by ecological interactions (Paine, 1974; Lubchenco and Menge, 1978; Menge and Lubchenco, 1981; Underwood, 1981), and much literature has been dedicated to describing the cascading implications of loss of certain key species (Paine, 1974; Underwood, 1980). This means complex and dramatic changes to community composition and function can occur as a consequence of climatic changes (Southward et al., 1995; Sagarin et al., 1999; Paine and Trimble, 2004; Girard et al., 2012; Jurgens et al., 2015). This study focused on the intertidal limpet *Patella vulgata* Linnaeus, 1758, and aimed at identifying the thermal conditions likely limiting its geographical distribution, disentangling the contribution of water and air temperature for the build-up of thermal stress. *P. vulgata* is an ectotherm that can be abundantly found over the majority of the Atlantic European continental coast south of Norway, but reaches its southern distribution limit in southwest Iberia and is absent from the southeast Bay of Biscay (Fischer-Piette and Gaillard, 1959; Christiaens, 1973). Several other species of algae and invertebrates exhibit the same distribution pattern (Fischer-Piette, 1955; Crisp and Fischer-Piette, 1959), hence *P. vulgata* is an appropriate model for a wider range of organisms. In addition, *P. vulgata* is a keystone species whose grazing activities control, to a large extent, local biodiversity and community structure throughout much of its range in Europe (Southward, 1964; Hawkins and Hartnoll, 1983; Raffaelli and Hawkins, 1996; Jenkins and Hartnoll, 2001; Jenkins et al., 2005;

Coleman et al., 2006). Thus, understanding the factors controlling its distribution can improve our ability to forecast responses of intertidal ecosystems to climate change.

3.3.3 Methods

Microhabitat temperature

Intertidal microhabitat temperatures were recorded at 15 exposed to moderately exposed shores along the Atlantic European coast, spanning nearly 20° of latitude, from southwest Scotland to south Portugal (Fig. 3.11a). Data were acquired using robolimpets - autonomous temperature sensing/logging devices mimicking the visual aspect and temperature trajectories of real limpets (Lima and Wethey, 2009). Loggers were deployed following Seabra et al. (2011). Temperatures were sampled from 6 distinct combinations of height above the low water mark (low, mid and high shore) and exposure to sun (shaded and sun-exposed), thus covering most of the spectrum of microhabitats occupied by intertidal species. Data were collected continuously between the summers of 2010 and 2014, at a sampling interval of 60 minutes and a resolution of 0.5 °C. For each microhabitat, logged temperatures were averaged whenever data from multiple sensors were available. Daily water temperature was extracted using the temperatures recorded by low and mid shore loggers at peak high tide (high shore loggers were not used because they may have not been submerged during neap high tides). All data manipulation was done using R 3.1.2 (R Development Core Team, 2014).

Distribution of Patella vulgata

Population densities of *P. vulgata* were measured during the summer of 2012 in all studied shores. At each field site, individuals were counted using a total of thirty 30x30 cm quadrats haphazardly placed at locations equivalent to the microhabitats where temperature loggers had been previously deployed. Reported densities correspond to average density across all quadrats, irrespective of their shore height and exposure to sun.

Exposure to thermal stress

During the population density survey we confirmed the absence of *P. vulgata* from Biarritz and Evaristo (shores H and O, respectively, Fig. 3.11a). In order to determine the role of temperature in setting those limits, in August 2012 a total of 32 individuals of *P. vulgata* (maximum shell length between 30 and 35 mm) were collected from shaded mid-shore microhabitats at Moledo, northern Portugal (shore L, Fig. 3.11a), and placed in four tanks in the lab (eight individuals in each). Animals were acclimated for one week (17 °C and 20 °C for water and air temperature, respectively) and then exposed to four thermally stressful treatments consisting of combinations of cold and hot air and cold and hot water, repeated over 30 days (Fig. 3.11b). Experiments were carried out in aquaria with tide and temperature control. Each day, tide and temperature

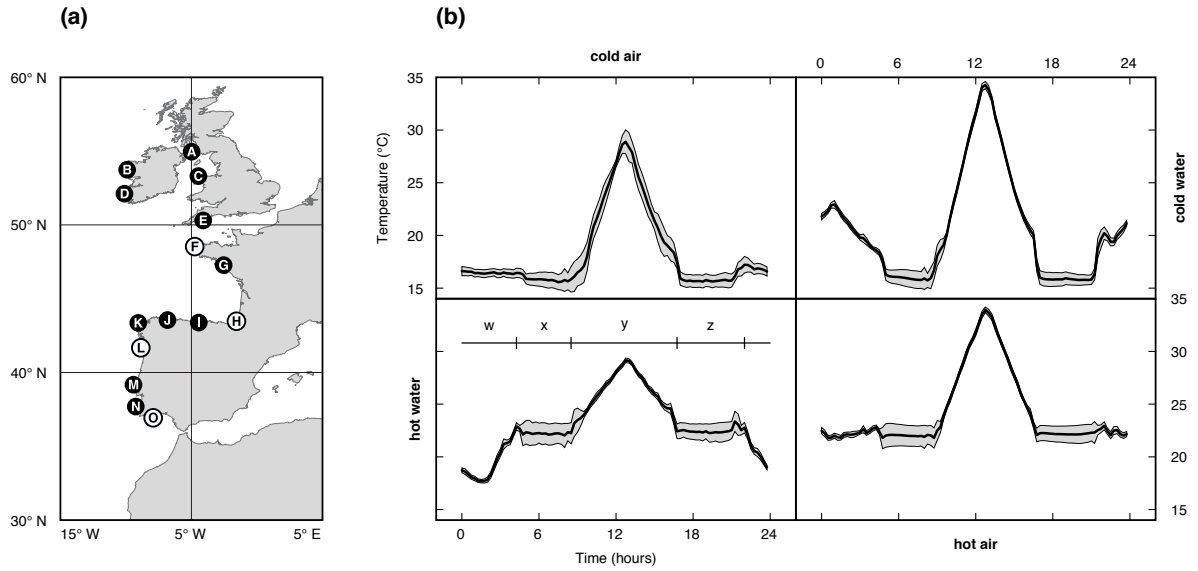

Figure 3.11: (a) Map of the study area. Letters A-O indicate the locations of the 15 shores surveyed, which cover the majority of the southern portion of *P. vulgata*'s distribution (A - South Cairn, UK; B - Emlagh, IE; C - Holyhead, UK; D - Annascaul, IE; E - Wembury, UK; F - Landunvez, FR; G - Batz-sur-Mer, FR; H - Biarritz, FR; I - Prellezo, ES; J - La Caridad, ES; K - Cabo Touriñan, ES; L - Moledo, PT; M - São Lourenço, PT; N - Alteirinhos, PT; O - Evaristo PT). (b) Average daily temperature profile (black line) ± standard deviation (grey area) effectively experienced by limpets in each of the four stressful treatments. Treatments consisted of a nocturnal low tide and high tide, and diurnal low tide and high tide (w, x, y, z, respectively) repeated over the 30 days of experiment. The temperature combinations used were "cold water, cold air", "cold water, hot air", "hot water, hot air" and "hot water, cold air" (clockwise from top left). Map created in R (R Development Core Team, 2014) using the Global Self-consistent, Hierarchical, High-resolution Geography Database (GSHHG) coastline data (Wessel and Smith, 1996).

conditions mimicked a typical semi-diurnal tidal cycle - a nocturnal low tide, followed by high tide, and then a diurnal low tide and high tide (w, x, y, z, respectively, Fig. 3.11b). Fine control of body temperature during emersion was achieved using a microprocessor to regulate the output of two 150W infrared lamps. Two robolimpets deployed inside each tank provided temperature feedback to the microprocessor. In order to keep the thermal conditions as realistic as possible, target temperatures for the diurnal and nocturnal low tides (air) and water, as well as the heating and cooling rates, were calculated using microhabitat temperatures recorded at the studied sites. Since it has been suggested the equatorial range edge for this species is set by summer conditions (Bowman and Lewis, 1977), calculations for the target temperatures were done using data from August 2011 (the hottest month during the year preceding animal collection) from (i) two "cold" shores which have cool summers and were found to harbor regionally high densities of *P. vulgata* (Landunvez and Moledo, shores F and L, respectively), and (ii) two "hot" shores, which have hot summers and where *P. vulgata* was found to be absent from (Biarritz and Evaristo, shores H and O, respectively). We computed the 75th percentile of (i) daily maximum temperature during diurnal low tide, (ii) daily maximum temperature during nocturnal low tide and (iii) average daily water temperature to obtain "day air", "night air"

and "water" temperatures for both "cold" and "hot" shores. The target temperatures obtained were 29 °C, 16 °C and 16 °C for "cold day air", "cold night air" and "cold water", and 34 °C, 22 °C and 23 °C for "hot day air", "hot night air" and "hot water", respectively. Heating and cooling rates were determined individually for each treatment's combination of air and water temperatures by computing the average heating and cooling rates occurring in the field under similar conditions. To that end, we searched the microhabitat temperature dataset for days with water and maximum air temperatures similar to each combination of target water and air temperatures ($\pm$ 1 °C). Each day's temperature data was then processed in order to determine the timing of the transitions between immersion, emersion and subsequent re-immersion during the diurnal low tide period, as well as the time at which peak air temperature was reached (which does not necessarily coincide with peak low tide). Experimental heating and cooling rates were obtained by averaging all heating (water to maximum air temperature) and cooling (maximum air to water temperature) rates for each combination of target temperatures (e.g., for the "cold water, hot air" combination we used all days in the microhabitat temperature dataset with water temperature between 15 and 17 °C and maximum air temperature between 33 and 35 °C). The resulting profiles can be found in Fig. 3.11b and will be hereafter referred as "cold water, cold air", "cold water, hot air", "hot water, hot air" and "hot water, cold air". As a consequence of using this method for the establishment of realistic experimental thermal profiles, heating/cooling rates and emersion time varied between treatments, reflecting what indeed happens in the field when such temperatures occur.

Cardiac activity: Experimental design and execution

Throughout the experiment (acclimation and thermal stress), limpets' overall physiological response was evaluated from their cardiac activity. Cardiac data was obtained non-invasively using the method described by Burnett et al. (2013). Infrared sensors were glued to the shells during the first two days of acclimation and the cardiac activity of each animal was recorded during periods of one minute every 15 minutes. Every day, before the diurnal low tide, detached or malfunctioning sensors were replaced, and limpets which were not adherent to the substratum were declared "ecologically dead" (Wolcott, 1973).

Cardiac activity: Data manipulation

In total, over 100,000 recordings of cardiac activity were obtained throughout the experiment. As discussed by Burnett et al. (2013), data obtained with this method can vary in quality, hence every recording was visually inspected to determine if a heartbeat signal was clearly detectable. All recordings with fragmented or undetectable heartbeats were discarded. Furthermore, fragmented data were also discarded. After all filtering, we were able to retain data from a total of four, seven, five and five individuals for the "cold water, cold air", "cold water, hot air", "hot water, hot air" and "hot water, cold air" treatments, respectively. Since the basal

heartbeat frequency of limpets can vary greatly, we calculated normalized heartbeat frequencies using the average heartbeat frequency during the last day of acclimation and used this as the basal value. Therefore, cardiac activity was expressed as the ratio of each limpet's heartbeat frequency in relation to its own basal heartbeat frequency (if a limpet had an average basal heartbeat frequency of 0.8 Hz, a normalized heartbeat frequency of 2 would be equivalent to a frequency of 1.6 Hz, i.e., a two-fold increase in the heart rate).

Cardiac activity: Assessment of induced thermal stress

Levels of induced thermal stress were first analyzed by fitting linear regression models of cardiac activity as a function of temperature for each treatment and examining their slopes and adjusted means by Analysis of Covariance (ANCOVA). Since the "cold water, cold air" treatment was the least thermally stressful of the four treatments tested, we used its linear regression model as a descriptor of the basal relationship between cardiac activity and temperature. In other terms, the linear regression model for the "cold water, cold air" treatment reveals the expected heartbeat frequency for any given temperature when *P. vulgata* is not thermally stressed. Therefore, stress levels in the remaining treatments were evaluated by comparing their linear regression models against the basal model. We tested the null hypothesis that slopes and adjusted means were statistically identical for all treatments - i.e., that the thermal regimes imposed in each treatment did not affect the relationship between heartbeat frequency and temperature. During a preliminary analysis we found that the temporal autocorrelation of the heartbeat frequency data approached zero for lags greater than 6 hours. Therefore, to avoid temporal autocorrelations, we randomly selected subsamples of cardiac activity (one heartbeat frequency measurement per limpet, per 1 °C bin, per treatment, totaling 112 measurements), and used them to calculate 200 bootstrapped ANCOVAs. This procedure resulted in a highly conservative minimum time difference between measurements in all subsamples of ~19 hours. ANCOVA models included heartbeat frequency as the dependent variable, temperature as the covariate and treatment as the independent variable. We compared the observed heartbeat frequencies in the stressful treatments with the heartbeat frequencies that would be expected if the basal relationship between cardiac activity and temperature was maintained in all treatments. To that end, a dataset of predicted cardiac activity was built for each treatment. Predicted cardiac activity was computed by applying the baseline linear regression model to the temperatures experienced by limpets in each treatment, throughout the entire length of the experiment. This predicted cardiac activity reveals what should be the cardiac response of limpets exposed to a stressful treatment if they were to exhibit the same cardiac activity vs. temperature relationship as the limpets in the "cold water, cold air" treatment. Density curves of the residuals obtained from subtracting the predicted heartbeat frequencies from their observed counterparts reveal the collective shift of individual heartbeat frequency measurements - a positive shift means heart rates were faster than expected.

Past and future environmental conditions

Upon identifying the relationship between water and air temperatures in the build-up of thermal stress, we were interested in evaluating its importance for the distribution range of *P. vulgata*. To that end, we investigated past and future patterns of co-occurrence of high water and air temperatures along the studied sites. Average water temperature and average daily maximum temperature for shaded microhabitats extracted from our biomimetic temperature dataset were used to obtain a highly detailed view of extreme heat events across the studied shores. The analysis of extreme heat events was extended using model output from the ENSEMBLES project (Hewitt and Griggs, 2004). This project used a combination of global circulation models (GCM) and regional circulation models (RCM) to generate predictions of daily sea surface temperature (SST) on a 25 km grid, for the period 1951-2099, under the A1B climate change scenario. We used model outputs from 9 GCM/RCM combinations available in the ENSEMBLES data archive (http://ensemblesrt3.dmi.dk, accessed 2015-08-01) (Appendix A) to run 9 separate forecasts of years with at least 30 days with SST equal or exceeding 23 °C. This threshold corresponds to the "hot water" treatments, which resulted in a marked increase of thermal stress levels in *P. vulgata*. Computations were performed individually for each model, and for each coastal pixel along the Atlantic European shores, from south Portugal to northwest France. The final output of the analysis depicts the number of models that agree that the threshold was, or will be crossed, per year.

3.3.4 Results

Cardiac activity

A total of ~41,000 valid heartbeat frequency readings were obtained over the 37 days of acclimation and thermal stress treatments. Heartbeat frequency data show that cardiac activity doubled for each 24 °C of temperature increase for all treatments (regression slopes homogenous in 96% of 200 bootstraps, see also Fig. 3.12a). The positive link between temperature and cardiac activity encompassed the entire temperature range in all treatments [note the absence of a breaking point similar to the one described by Stillman and Somero (1996), Fig. 3.12a]. In addition, no mortality was observed during the experiment, confirming that animals never went beyond their thermal tolerance limit. This likely resulted from the relatively short time during which limpets were exposed to each treatments' highest air temperature - approximately 15 minutes compared to hours in other studies (Dong and Williams, 2011; Fitzgerald-Dehoog et al., 2012; Zhang et al., 2014). Importantly, while slopes remained unchanged among treatments, adjusted means (elevations) of some lines differed (Fig. 3.12a,c). Heartbeat frequencies vs. temperature recorded in the "cold water, hot air" treatment were collinear with the trajectories of the baseline treatment ("cold water, cold air"), indicating that the few higher heartbeat rates recorded in the "cold water, hot air" treatment resulted solely from the higher temperatures

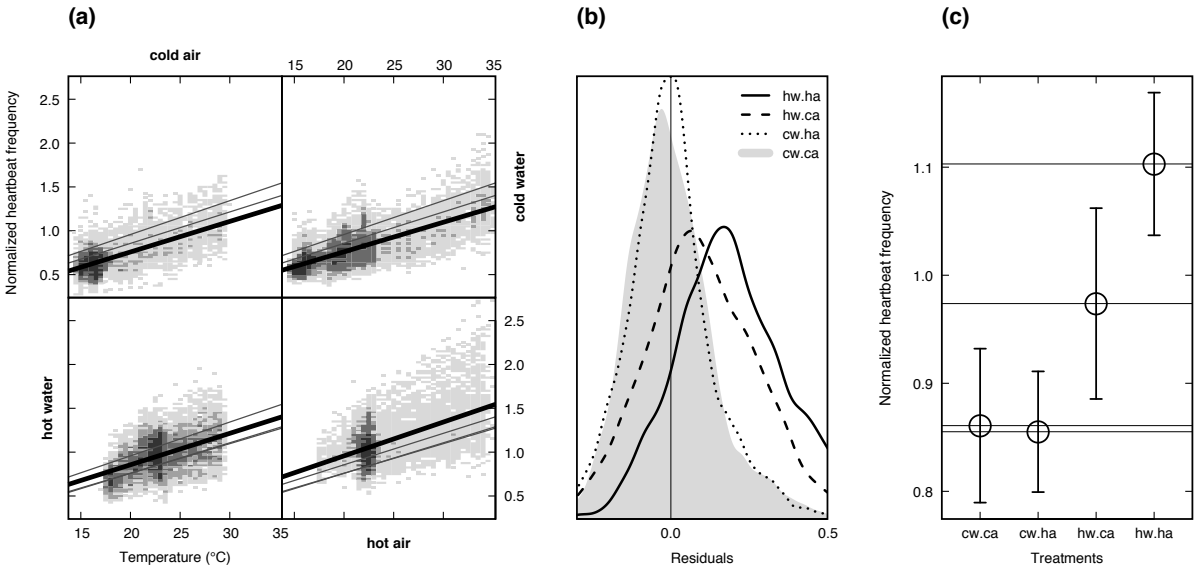

Figure 3.12: Cardiac activity of *P. vulgata*. (a) Scatterplots of normalized heartbeat frequencies as a function of temperature, for all four treatments. Darker pixels indicate values that occurred more often. Thick lines show the linear regression for each treatment, while thin lines show the linear regressions for all other treatments, for comparison. (b) Density curves of the differences between observed and predicted normalized heartbeat frequency. The shaded are represents the baseline treatment ("cold water, cold air"). A positive shift means higher heartbeat frequencies than would be expected for a given temperature. (c) Adjusted means of the normalized heartbeat frequencies recorded in each of the four treatments ± standard deviation (calculated using 200 bootstraps).

experienced. This similarity was further evidenced by the virtually identical density curves of the residuals (Fig. 3.12b) and the adjusted means (Fig. 3.12c). On the other hand, on average, limpets in the "hot water, cold air" treatment exhibited heartbeat frequencies 10% higher than "cold water, cold air treatment", while limpets in the most extreme treatment ("hot water, hot air") had on average 21% faster heart rates than controls (Fig. 3.12b). Furthermore, density curves also showed that limpets in the "hot water, cold air" and "hot water, hot air" treatments only had heartbeat frequencies at or below the baseline "cold water, cold air" frequencies during 29% and 10% of the time, respectively. This was also reflected in the increased adjusted means (Fig. 3.12c). In particular, the adjusted mean from the "hot water, hot air" treatment was significantly higher than the adjusted means of any of the cold water treatments (Tukey's Post Hoc test significant in over 85% of 200 bootstraps).

Distribution of *P. vulgata*

Population densities were highest in the British Isles - over 150 individuals per square meter - and steadily decreased southwards (grey bars, Fig. 3.13). Outside the British Isles, Landunvez and Moledo, shores F and L, respectively, exhibited the highest densities. Following extensive search, *P. vulgata* was confirmed absent from two shores, Biarritz and Evaristo (shores H and O, respectively). In São Lourenço (shore M) individuals were only found in shaded microhabitats.

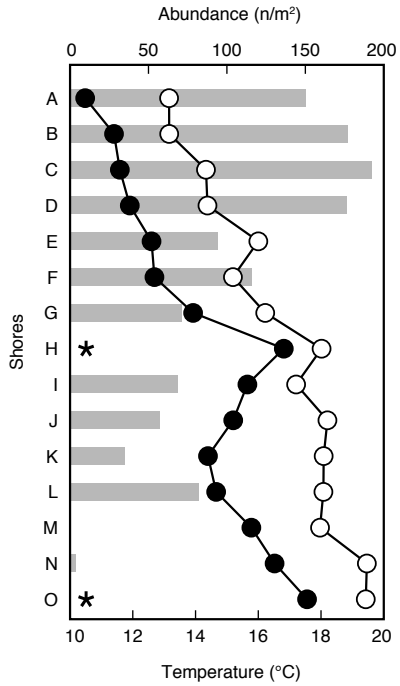

Figure 3.13: Relationship between abundance of *P. vulgata* and temperature recorded by robolimpets. Grey bars show average abundance in each shore across all microhabitats. Stars in shores H and O indicate absence of individuals. Closed circles show average water temperature and open circles show average air temperature in shaded microhabitats.

Thermal limits

Microhabitat environmental conditions at the 15 locations surveyed, over the past five years, were summarized using the average daily maximum air temperature in shade and average daily water temperature (Fig. 3.13). The correlation between population densities and the sum of average air and water temperatures for each shore was remarkably high (correlation coefficient of -0.93, $p < 0.05$). However, even though most locations in the Iberian Peninsula (shores I-O) exhibited high air temperature averages, the only two shores where *P. vulgata* was not found - Biarritz and Evaristo - were those with highest average water temperature (shores H and O, Fig. 3.13) and where water temperatures greater than or equal to 23 °C occurred frequently (23 and 28 days per year, respectively, Fig. 3.14). This appears to suggest that the water temperature is the key factor controlling the distribution pattern of *P. vulgata*. Furthermore, by analyzing the pattern of co-occurrence of high water and air temperatures, we show that moderately high air temperatures occurred at shaded habitats of almost all shores, but the degree of association between water and air temperature varied markedly. For example, the highest correlations between water and air temperatures were found in shores within the Bay of Biscay (shores G-I, correlation coefficients of 0.9, 0.95 and 0.9, respectively, $p < 0.05$), while the lowest occurred in shores along northwest Iberia (shores K and L, correlation coefficients of 0.43 and 0.5, respectively, $p < 0.05$). During summer, northwest Iberia typically experiences an oscillation between periods of upwelling intensification - high air temperature and low water temperature - and relaxation - low air temperature and high water temperature (Moncoiffe et al., 2000; Relvas et al., 2007). In northwest Iberia, the highest air temperatures never coincided with the highest water temperatures (Fig. 3.14). On a wider time scale, analysis of

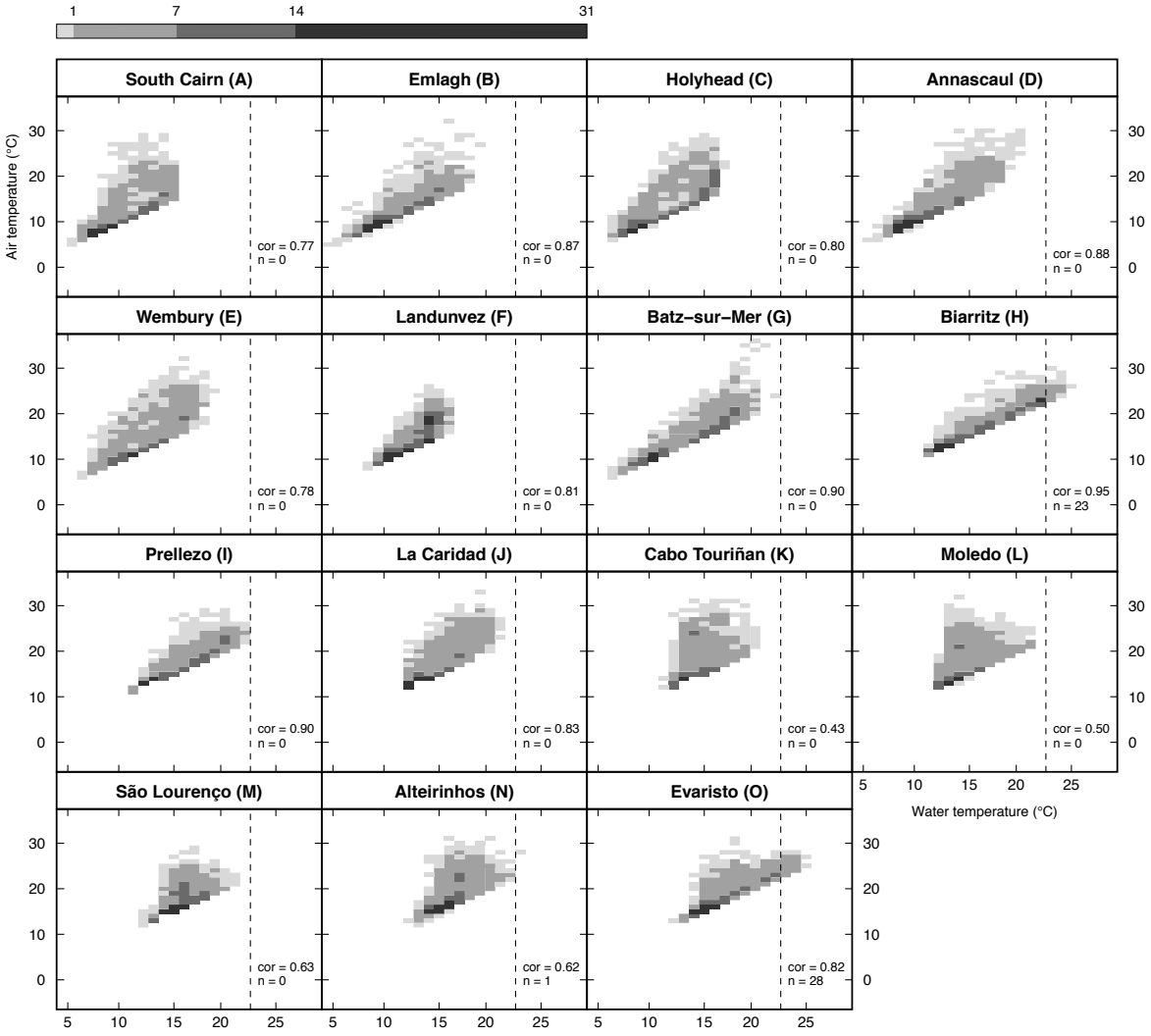

Figure 3.14: Pattern of co-occurrence of water and air temperatures at all studied shores, based on temperatures recorded by the robolimpets. Dashed line marks the 23 °C SST threshold. Note that Moledo exhibits many days with high air temperatures and low water temperatures, a pattern typical from locations within regions with coastal upwelling. The correlation between water and air temperatures, and the number of days with water temperature at or above 23 °C are also depicted.

ENSEMBLES model data revealed a major trend of deteriorating conditions in the coming years, from the perspective of *P. vulgata* (Fig. 3.15). Importantly, the general trend is clear despite known variability between model outputs (Brands et al., 2011; Ramos et al., 2011; Kharin et al., 2013). The change is particularly remarkable along the southwest coast of Portugal (Fig. 3.15, between shores M and N), with most models agreeing that conditions will become unsurvivable by the end of the century. Conditions in the southeast Bay of Biscay (around shore H) are also forecasted to worsen, as indicated by the increasing number of models predicting that the 23 °C SST threshold will be crossed in the future. In other regions like northwest France and northwest Iberia (Fig. 3.15, northwards of shore G and between shores K and I), however, most models agree that the threshold will not be crossed, suggesting that these regions will remain habitable for *P. vulgata*.

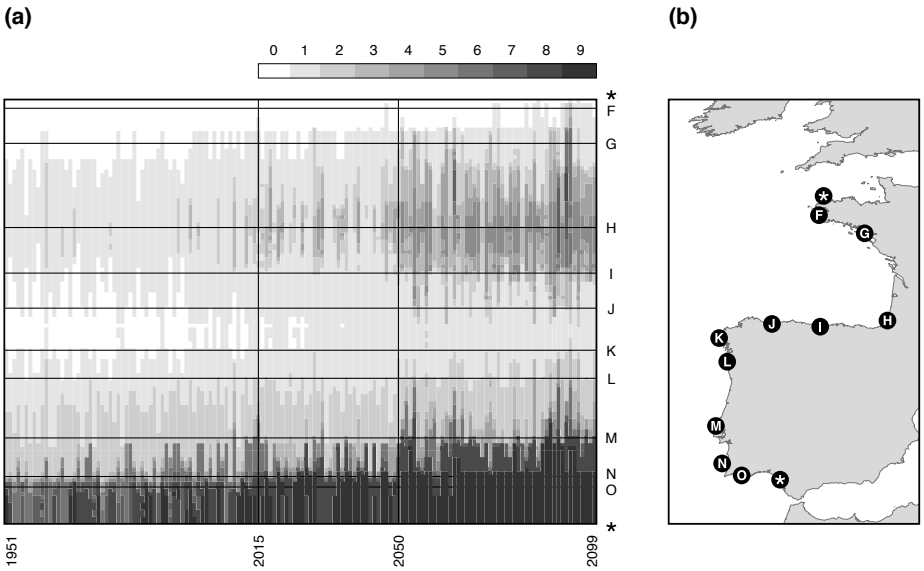

Figure 3.15: (a) Long-term analysis of the occurrence of extreme water temperature for the period 1951-2099 along coastal areas from south Portugal to northwest France, a region encompassing the southern limit and a gap in the present distribution of *P. vulgata*. Each pixel in the graph indicates number of ENSEMBLES models used that predicts 30 or more days with water temperature at or above 23 °C, per year, for each coastal pixel. Darker colors indicate higher agreement between models. A marked increase in the prevalence of such extreme events towards the end of the century can clearly be seen along most of the coast. Horizontal lines identify the locations of the shores surveyed (b) and asterisks mark the edges of the coastline analyzed. Map created in R (R Development Core Team, 2014) using Global Self-consistent, Hierarchical, High-resolution Geography Database (GSHHG) coastline data (Wessel and Smith, 1996).

3.3.5 Discussion

Since heart rate and metabolism are positively linked in ectotherms (Frederich and Pörtner, 2000), elevated heartbeat frequencies are indicative of additional metabolic costs, which, if recurrent, reduce fitness and limit scope for growth (Somero, 2002, 2010; Woodin et al., 2013). Thus, our results suggest that the intertidal ectotherm *P. vulgata* is especially susceptible to increases in water temperature, and that air temperature plays a secondary role, being relevant only when water temperature is also high. We speculate that this pattern may be linked to the rhythmic behavior exhibited by this species. *P. vulgata* is most active during immersion but remains mostly inactive, tightly clamping down to its home scar while exposed to low-tide high temperatures (Branch, 1981). Therefore, it appears that the immersion period sets the basal metabolic level and controls the ability to recover from stressful periods, while the emersion period only influences the severity of the stress itself. Several studies on other marine invertebrates support this suggestion (Bayne et al., 1976; Branch, 1981; Tomanek and Somero, 2000; Mota et al., 2015). Under this mechanism, if water is cold, proper recovery can be achieved even after a stressful event and metabolic levels remain largely unaltered. However, when water is hot, the basal metabolic level is immediately elevated, and if air is also hot, recovery from its deleterious effect may become severely impaired, thus resulting in a further

increase of the metabolic level. The ecological significance of these findings is supported by our temperature dataset, which corroborates the hypothesis that SST is as a major driver of *P. vulgata*'s distribution (Fig. 3.13). In particular, regarding the identification of thermal regimes conducive to the exclusion of *P. vulgata*, there is convincing support for the existence of an upper threshold to water temperature above which even moderately high air temperatures result in unsustainable stress levels. Considering the results presented in this study, we suggest that this threshold is crossed when water temperature is equal or exceeds 23 °C. The existence of this threshold is in agreement with recent findings which revealed that *P. vulgata* is unable to acclimate to the conditions present at thermally stressful microhabitats (Chapperon et al., 2015, submitted), and that the levels of thermal stress in *P. vulgata* are particularly high on shores close to its limit of distribution, even in shaded microhabitats (Lima et al., 2015), since SST on these shores regularly approach the 23 °C threshold (shores G, I and N, Fig. 3.14). The present findings also highlight the central role played by regional oceanographic features in shaping the environmental mosaic. In particular, coastal upwelling, which is a dominant feature along northwest Iberia during summer (Lemos and Pires, 2004), can be seen severely disrupting the link between water and air temperature, ensuring that either water temperature is high, or air temperature is high, but never both (e.g., Moledo, shore L; Fig. 3.14). This means that in northwest Iberia limpets are either enduring very stressful low tides but subsequently recover during low tide, or their basal metabolic level is elevated but low tides are relatively forgiving. Conversely, in the southeast Bay of Biscay and south Portugal, limpets would have to withstand more than 20 days per year of highly stressful low tides from which recovery during high tide would not be possible, due to extremely high water temperature (Fig. 3.14). When examining longer timespans, model data revealed a dramatic change in the thermal landscape along the Atlantic European coast over the period 1950-2100 (Fig. 3.15). Most models agree that conditions were largely favorable during the 1950s, and that the 23 °C SST threshold was consistently crossed only southwards of shore N. This pattern is inline with the distribution of *P. vulgata* reported at that time (Crisp and Fischer-Piette, 1959), especially regarding the southernmost range limit, which was described to be at Odeceixe, southwest Portugal, a shore less than 10 km south of shore N. In addition, uncertainty concerning the conditions in southeast Bay of Biscay (few models agreed conditions were severe during the 1950s; Fig. 3.15, around shore H) is also matched in the reports on the distribution of *P. vulgata* (Crisp and Fischer-Piette, 1959), which highlight its absence from wave-exposed locations around Biarritz (shore H), but presence in wave-sheltered areas of Saint-Jean-de-Luz (less than 15 km south of shore H). Towards the end of the 21st century, however, all models agree that conditions will severely deteriorate off southwest Portugal (i.e., almost all years after 2050 were predicted to have at least 30 days with SST at or above 23 °C; Fig. 3.15, between shores M and O), and most models agree that conditions will also worsen along the coast of the Bay of Biscay and off northwest Portugal (Fig. 3.15, between shores G and I, and L and M, respectively). By the end of the 21st century, only the northwest of France and northwest of Iberia are projected to

still have thermal conditions that are permissive to *P. vulgata*. Assuming that all populations of *P. vulgata* respond identically to temperature extremes and will not be able to evolve (but see Austin, 2002; Hoffmann and Sgrò, 2011), the increase in extreme high temperatures can potentially lead to the northward retreat of the equatorial limit of *P. vulgata* in south Portugal and the westward widening of the gap in the Bay of Biscay. The impending retreat of range limits identified here represents an important risk, well beyond the mere exclusion from a single stretch of coast. On the one hand, the westward widening of the gap in the Bay of Biscay would extend even further a natural gap present northward from Biarritz, where, with few exceptions, the coast is mostly sandy (i.e., not suitable for rocky shore organisms such as *P. vulgata*). This means connectivity between populations from northeast Iberia and northwest France could become reduced, or even compromised. On the other hand, the northward shift of the southern limit would increasingly compress the Iberian populations into the northwest of the peninsula. Populations of *P. vulgata* in this region seem to be sustained by cool water temperatures during summer, brought about by regional coastal upwelling, which allow limpets to withstand the locally high air temperatures (shores J, K and L; Figs. 3.13, 3.14). Since there are indications that the Iberian upwelling regime could be becoming more relaxed (Lemos and Pires, 2004; Lemos and Sansó, 2006; Pardo et al., 2011), contrary to global intensification trends (Varela et al., 2015; Wang et al., 2015), there is a risk that rising SST could render the whole west Iberia too hot for many intertidal species. In addition, the reported and predicted geographical heterogeneity of climate change, as well as the different rates at which oceans and the atmosphere are warming (Lima and Wethey, 2012), further enhance the uncertainty of these scenarios. The present study emphasizes the role of thermal stress in shaping the distribution of organisms and provides tools for the establishment of highly detailed mechanistic models for the forecast of species' distributions via the characterization of a temperature threshold. It also illustrates how coupling information on the physiological limits of species with highly detailed microhabitat environmental data is crucial for the correct interpretation of complex biogeographic responses to climatic changes, as has been previously suggested (Wethey et al., 2011; Seabra et al., 2015b). These findings reinforce the notion that intertidal species are especially vulnerable to climate change, and that regional climatic and oceanographic features such as coastal upwelling may be acting as linchpins, and their removal could trigger abrupt cascading changes throughout entire intertidal communities.

3.3.6 Acknowledgements

This work was funded by FEDER (FCOMP-01-0124-FEDER-010564, FCOMP-01-0124-FEDER-020817), FCT (PTDC/MAR/099391/2008, PTDC/MAR/117568/2010, SFRH/BD/68521/2010 and IF/00043/2012), NASA (NNX11AP77G) and NSF (OCE1129401). Past and future model SST data were obtained from the ENSEMBLES project, funded by the European Commission's 6th Framework Programme through contract GOCE-CT-2003-505539.

The comments of Nuno Queiroz and Nick Burnett contributed significantly to the quality of this study. The authors declare no conflict of interest.

3.3.7 Appendix A

Global Circulation Model/Regional Circulation Model combinations used in ensemble predictions of future biogeographic change. C4I - Community Climate Change Consortium for Ireland, CNRM - Météo France, DMI - Danish Meteorological Institute, ETHZ - Swiss Institute of Technology, ICTP - International Centre for Theoretical Physics (Italy), KNMI - Royal Netherlands Meteorological Institute, MPI - Max Planck Institute (Germany), SMHI - Swedish Meteorological and Hydrological Institute.

Modeling group	**Global circulation model**	**Regional circulation model**
C4I	ECHAM5	RCA3
CNRM	ARPEGE	Aladin
DMI	ARPEGE	HIRHAM5
DMI	ECHAM5-r3	HIRHAM5
ETHZ	HadCM3Q0	CLM
ICTP	ECHAM5-r3	RegCM
KNMI	ECHAM5-r3	RACMO2
MPI	ECHAM5-r3	REMO
SMHI	ECHAM5-r3	RCA

4. Biogeographic patterns

4.1 Understanding complex biogeographic responses to climate change

4.1.1 Abstract

Predicting the extent and direction of species' range shifts is a major priority for scientists and resource managers. Seminal studies have fostered the notion that biological systems responding to climate change-impacted variables (e.g., temperature, precipitation) should exhibit poleward range shifts but shifts contrary to that expectation have been frequently reported. Understanding whether those shifts are indeed contrary to climate change predictions involves understanding the most basic mechanisms determining the distribution of species. We assessed the patterns of ecologically relevant temperature metrics (e.g., daily range, min, max) along the European Atlantic coast. Temperature metrics have contrasting geographical patterns and latitude or the grand mean are poor predictors for many of them. Our data suggest that unless the appropriate metrics are analyzed, the impact of climate change in even a single metric of a single stressor may lead to range shifts in directions that would otherwise be classified as "contrary to prediction".

4.1.2 Main text

Changes in the distributional ranges of species are among the expected outcomes of climate change (IPCC, 2014). Several comprehensive studies report a broad prevalence of range shifts at poleward or upper range boundaries consistent with climate change predictions (Walther et al., 2002; Parmesan and Yohe, 2003; Root et al., 2003; Hickling et al., 2006; Lima et al., 2007a; Poloczanska et al., 2013). Still, shifts contrary to that expectation have been frequently reported (Moritz et al., 2008; Hilbish et al., 2010; Chen et al., 2011; Goatley and Bellwood, 2014). Range shifts contrary to predictions may occur because organisms are responding to a different variable (related or unrelated to climate change), or because the predicted direction was wrongly established to begin with. In fact, by identifying appropriate controlling stressors, and refining how the predicted direction of change is established, recent analyses have shown that species may be tracking climate change even when distribution ranges are shifting in otherwise unexpected directions (Burrows et al., 2011; Crimmins et al., 2011; VanDerWal et al., 2013). Making sense of shifts contrary to predictions is important as it may impact the confidence level of climate change attribution, and therefore influence public opinion and policy. It is well recognized that the mean is a metric that oversimplifies much of the complexity of

stressors (Den Boer, 1968; Helmuth et al., 2006b, 2014; Vasseur et al., 2014), and specific aspects of some stressors (e.g., minimum water temperature during winter) have been identified as playing key roles in determining biogeographic patterns (Helmuth et al., 2010; Wethey et al., 2011). However, since environmental data at the appropriate temporal and spatial scales are often lacking, the patterns of many aspects of stressors remain largely uncharacterized with appropriate detail. To fill this void, general perception seems to hold that whatever spatial gradient is detected in the mean must be reflected to a large extent by all other metrics, especially for cases where the mean neatly fits preconceived assumptions. There is, however, no statistical ground supporting that view, and we argue that this misunderstanding may lead to improper estimation of what exactly is the predicted direction of range shifts of a particular species as a response to changes in the patterns of a single stressor. This effect should be especially noticeable for systems following Liebig's law of the minimum to some extent, which emphasizes the role of the scarcest resource (or, in this case, the least favorable bioclimatic variable) in determining habitat suitability at a given location and time. Using temperature extremes as an example, the present study aims at characterizing the contrasting patterns encapsulated within a single stressor, as well as showing that climate change-induced alterations of aspects of that stressor can potentially lead to otherwise non-intuitive range shifts.

4.1.3 Material and Methods

Microhabitat temperature

Intertidal microhabitat temperatures were recorded at 15 exposed to moderately exposed shores along the European Atlantic coast, spanning nearly 20° of latitude, from Southwest Scotland to South Portugal (Fig. 4.1a, A – South Cairn, B – Emlagh, C – Holyhead, D – Annascaul, E – Wembury, F – Landunvez, G – Batz-sur-Mer, H – Royan, I – Biarritz, J – Prellezo, K – La Caridad, L – Cabo Touriñan, M – Moledo, N – São Lourenço, O – Evaristo). Data were acquired using robolimpets (autonomous temperature sensing/logging devices mimicking the visual aspect and temperature trajectories of real limpets, see Lima and Wethey, 2009, for details). Loggers were deployed following Seabra et al. (2011). Temperatures were sampled from 6 distinct combinations of height above the low water mark (low, mid and high shore) and exposure to sun (shaded and sun-exposed), thus covering most of the spectrum of microhabitats occupied by intertidal species. Data were collected continuously between the summers of 2010 and 2014, at a sampling rate of 60 minutes and a resolution of 0.5 °C. For each microhabitat, logged temperatures were averaged whenever data from multiple sensors were available. All data manipulation and analyses were done using R 3.1.2 (R Development Core Team, 2014).

Data analysis

A total of 17 ecologically relevant temperature metrics were computed for each shore. Metrics were computed per year and then averaged over the four years of data available. Metrics

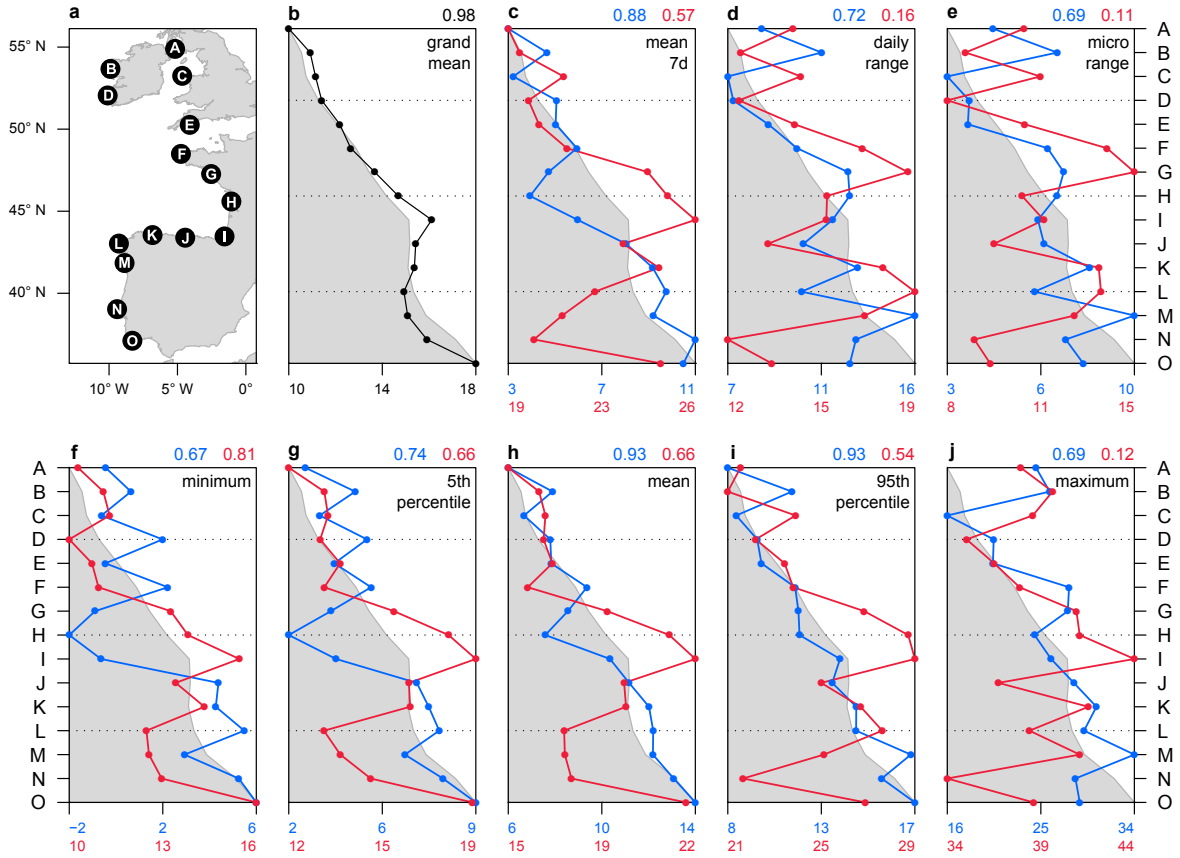

Figure 4.1: Patterns of temperature metrics across the European Atlantic intertidal ecosystem. **a**, Locations surveyed. Geographic pattern of metrics: **b**, grand mean, **c**, 7 day mean, **d**, daily range, **e**, microhabitat range, **f**, minimum, **g**, 5th percentile, **h**, mean, **i**, 95th percentile, **j**, maximum. Black line (**b**) is grand mean, calculated using all data from each shore. Red and blue lines (**c**-**j**) calculated using the warmest and coldest 30 days of each year (7 days for **c**), per shore. The shaded area is the pattern expected if each metric was perfectly correlated with latitude. Points in shaded area are "cooler than expected given latitude", and points outside shaded area are "hotter than expected". Correlation coefficients between each metric and latitude are depicted in the top right corner of each panel (blue for cold and red for warm periods).

computed include the mean using all available data for each shore (grand mean), the mean temperature during the hottest/coldest seven days of each year ('mean 7d'), and the mean daily range of temperatures ('daily range'), mean daily range of all microhabitats' maximum temperatures (i.e., microhabitat range, or 'micro range'), minimum, 5th percentile, mean, 95th percentile and maximum during the hottest/coldest 30 days of each year. For easier terminology, metrics computed during the hottest periods were prefixed "summer", and metrics computed during the coldest periods were prefixed "winter" (e.g., 'summer minimum', 'winter mean 7d', etc.). The correlation coefficient between each metric and latitude was also calculated.

Direction of range shifts

An example is presented to illustrate how range shifts driven by climate change can occur both towards the poles or the equator. We modeled the relative abundance (from 0 – absent, to 1 –

highest abundance) of a theoretical species under two climate change scenarios. We modeled an equatorial species which is intolerant of cold stress and tolerant of heat stress. Abundance was determined as the lowest value of either 'winter minimum' or 'summer 5th percentile' at each shore (following Liebig's law of the minimum). To allow the comparison of both metrics (which are not equivalent in absolute terms) we normalized each metric to vary from 0 to 1, reflecting the range observed within the study region. Zero abundance occurred at shores where at least one of the metrics had a value of zero, meaning that either 'winter minimum' or 'summer 5th percentile', or both, prevented the species from existing. Both metrics were used without any change for the initial conditions. The first climate change scenario considers climate change as a monotonic increase of both aspects of temperature, and the abundance pattern was computed using "hot" versions of both 'winter minimum' and 'summer 5th percentile' (resulting in increased habitat suitability). The second scenario considers climate change as an increase of variability in which some metrics may actually become colder. In this case the abundance pattern was computed using the "cold" version of 'winter minimum' and the "hot" version 'summer 5th percentile'. The initial range limit was identified as the most poleward shore with abundance greater than zero. The location of the range limit was re-evaluated for both climate change scenarios to determine the direction of change (poleward or equatorward).

4.1.4 Results and Discussion

We used a dataset comprised of 90 individual 4-year-long temperature time series (six microhabitats on 15 shores from 37 °N to 55 °N latitude, Fig. 4.1a) to evaluate to what extent the patterns of ecologically relevant metrics of a stressor are indeed captured by that stressor's mean. Extreme temperature is a major stressor in most ecosystems, and especially in the rocky intertidal (Helmuth et al., 2006b), where animals and plants a few centimeters apart can be experiencing dramatic differences in body temperature (Helmuth et al., 2006a; Seabra et al., 2011). The overall mean temperature, which is often used as a reference for estimating species distributions (Helmuth et al., 2014), was shown to match latitude surprisingly well ($R = 0.98$, Fig. 4.1b), thus reinforcing the idea of a relatively smooth, continuous gradient from warmer to colder temperatures with increasing latitudes along the European Atlantic coastline. However, with the exception of 'winter mean' and 'winter 95th percentile' (Fig. 4.1h, i, blue lines), all other metrics ('summer mean', 'summer 95th percentile', and winter and summer '7 day mean', 'daily range', 'microhabitat range', 'minimum', '5th percentile' and 'maximum') exhibited patterns deviating substantially from that of the grand mean. These differences highlight the key role played by climatic, geomorphologic and oceanographic factors at the local level, and more importantly, show that such factors can change skewness or kurtosis of the distribution of temperatures (or even causing multimodality) without affecting the mean. For example, seasonality, which is strongest within the Bay of Biscay - shores H and I - appears not to drive the grand mean for these shores too far away from the expected value given their

latitude, but results in remarkably high summer temperatures (in fact the highest recorded in the study area; Fig. 4.1i, j, red lines) and equally remarkably low temperatures during winter (again, the lowest within the study area; Fig. 4.1f, g, blue lines). In another example, upwelling, which is typically stronger around shores F and L during summer (Lemos and Pires, 2004), can be seen driving 'summer daily range' and 'summer microhabitat range' (Fig. 4.1d, e, red lines), likely due to the co-occurrence of low water temperatures and high air temperatures. Again, this effect does not result in any important deviation of the grand mean from the latitudinal pattern for these shores, and would be largely missed if data at the appropriate spatial scale had not been collected. Additionally, the combination of regional factors and local context can result in surprising temperature distributions, such as seen at shore N. At this shore, all metrics were found to be lower or equal to the expected value based on latitude. However, the grand mean does not reflect the magnitude of this difference, especially considering that shore N is the coldest in the study area for some of the metrics calculated. The many patterns encapsulated within the distribution of values of a single stressor clearly indicates that the grand mean may largely misrepresent many other ecologically relevant aspects of that stressor. This is in accordance with previous studies (Helmuth et al., 2006a; Lathlean et al., 2014b) and reinforces the notion that *a priori* knowledge of the physiological requirements of a species and a detailed characterization of the thermal extremes at the study area are fundamental to ascertain the real stress landscape imposed on organisms. Furthermore, using to a theoretical example we show that complex biogeographic responses to climate change can be interpreted by using the appropriate metrics (Fig. 4.2). We assume that the distribution of a theoretical species is determined by a group of relevant metrics (in this case the thermal extremes measured as 'winter minimum' and 'summer 5^{th} percentile') and follows Liebig's law of the minimum (i.e., at each location density is dependent on the least favorable relevant metric). In the simplest form, the distribution pattern (Fig. 4.2a) will be determined by the least favorable of a number of relevant metrics (Fig. 4.2a, light orange area). If climate change results in a favorable monotonic change of all metrics (Fig. 4.2b), the extent of suitable locations increases and a range expansion can be expected – the "general perception" poleward scenario. However, studies have highlighted that climate change not only can result in increased mean, minimum and maximum temperatures but also in increased variability – and that the exact signature of climate change varies regionally (Easterling et al., 2000; Lima and Wethey, 2012; IPCC, 2013; Vasseur et al., 2014). In this case, if at least one metric becomes less favorable due to the increased variability, the whole distribution can be adversely affected, and an equatorward range contraction may occur (Fig. 4.2c). Using the metrics computed in this study it is possible to further expand the example. If the distribution of a species was found to be dependent on the interplay between extremes like 'winter minimum' and 'summer 5^{th} percentile' (Fig. 4.2d), the initial distribution pattern should include a gap at shore H, and a polar range limit at shore B (Fig. 4.2d). If both 'winter minimum' and 'summer 5^{th} percentile' become warmer, a poleward range expansion can be expected (Fig. 4.2e), but if 'summer 5^{th} percentile' becomes

warmer while 'winter minimum' becomes colder, the harshness of winter conditions prevail over the favorable summers and a equatorward range contraction should occur (Fig. 4.2f). Interestingly, in a few locations suitability would actually increase because the limiting factor was 'summer 5^{th} percentile' and not 'winter minimum' (shores L and N, Fig. 4.2h), highlighting the consequences of different mechanisms limiting species' densities across different locations (Woodin et al., 2013). The crucial point is that if field surveys were to reveal an equatorward range contraction for this species, this range shift would not be contrary to predictions, as general perception would suggest. Instead, it would be consistent with the predicted direction of change for this biological system's response to climate change, thus representing positive evidence towards the establishment of a link to climate change. In addition, it is conceivable that some organisms' physiological requirements may include more complex interactions of aspects of a stressor than those depicted here (Fu et al., 2015; Magozzi and Calosi, 2015). For example, a mobile organism will be able to explore the various microhabitats available within a site for thermoregulation. If that organisms' physiology is found to be negatively impacted by 'summer maximum', it is likely that the appropriate metric to study will instead be the difference between 'summer maximum' and 'summer microhabitat range', as very high temperatures can be avoided if cooler microhabitats are available. These complex interactions between aspects of a stressor can generate new stress landscape patterns that do not match that of the grand mean, 'summer maximum' or 'summer microhabitat range', further increasing the likelihood of erroneous expectations about the extent and direction of range shifts in face of climate change if the stress landscape is not properly characterized. The findings presented in this study reinforce the notion that using the appropriate metrics of a stressor and identifying the appropriate stressor (VanDerWal et al., 2013) can provide decisive insights towards the detection, interpretation and prediction of complex distribution patterns, spatial and temporal variations of mechanisms controlling species distributions and the direction of range shifts. In addition, the conceptual framework here outlined emphasizes the paramount importance of coupling the collection of environmental data at the appropriate scales with a detailed characterization of species' physiological requirements (see Ashcroft et al., 2014; Greenberg et al., 2015, for analogous approaches using modeled data). Although focused on the thermal regimes of the European Atlantic intertidal ecosystem, the concepts here outlined can be extended to other geographical regions, ecosystems, and stressors. Taken with necessary caution (see, for example, the cautionary advice by Austin, 2002) regarding assumptions of linear response to temperature), these results suggest that some of the cases where species have been shown to be shifting in directions contrary to expectations, the predicted direction of change may have been wrongly established.

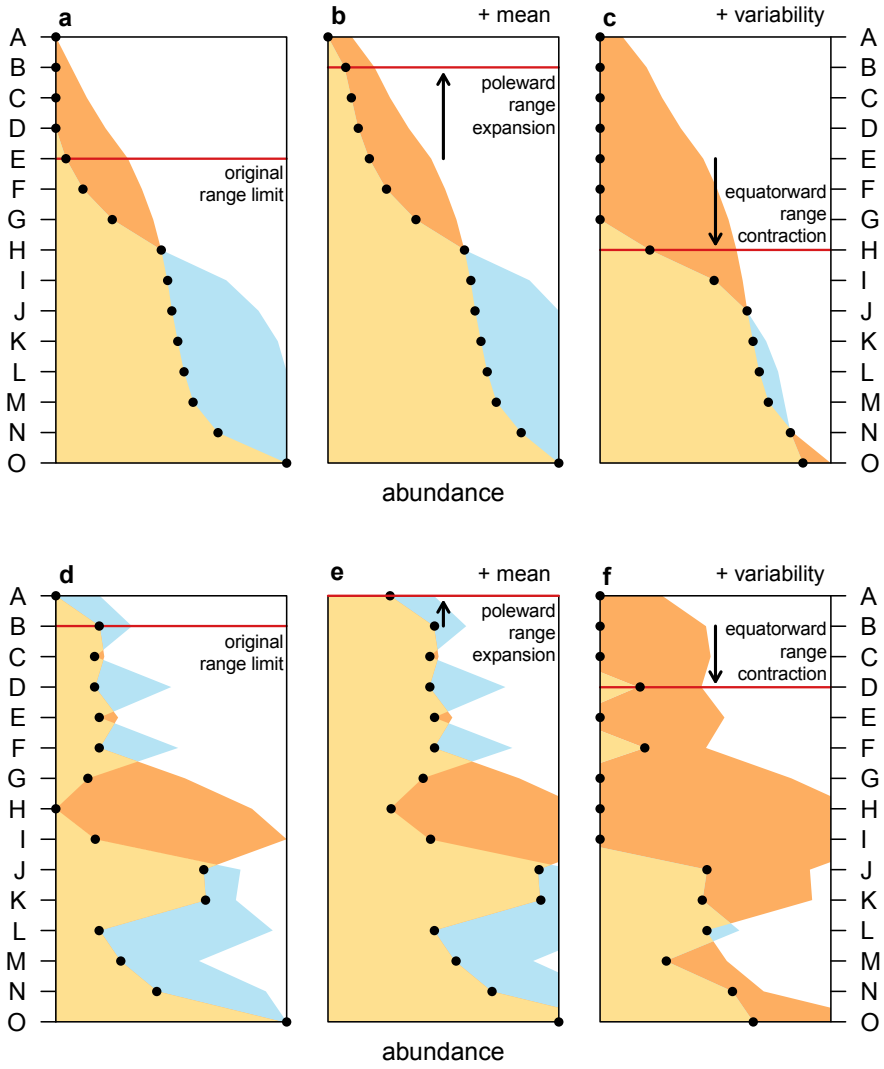

Figure 4.2: Climate change can generate complex biogeographic responses. Conceptual framework (**a**-**c**) and example built using real temperature data (**d**-**f**) illustrating the mechanism through which climate change may induce complex biogeographic responses. Black dots show the abundance of a hypothetical species in each location (A-O, see Fig. 4.1a), which results from the interplay of 'winter minimum' (blue areas) and 'summer 5th percentile' (dark orange areas). Light orange results from the overlap between blue and orange areas and shows the outcome of the Liebig's law of the minimum. **a** and **d** show the initial conditions, **b** and **e** result from the monotonic increase of both winter minimum and summer 5th percentile (scenario of increased mean), and **c** and **f** from increase of one aspect of temperature and decrease of the other (scenario of increased variability but stable mean).

4.1.5 Acknowledgements

This work was funded by FEDER (FCOMP-01-0124-FEDER-010564), FCT (PTDC/MAR/117568/2010, SFRH/BD/68521/2010 and IF/00043/2012), NASA (NNX11AP77G) and NSF (OCE1129401). The comments of Sarah A. Woodin contributed significantly to the quality of this study. This is contribution 82 in Ecological Forecasting from the University of South Carolina.

5. General discussion

The link between species' distribution patterns and the environment is a central issue to biogeography. In the past, correlative approaches have dominated research efforts in this field, but their power is limited. Mechanistic models, however, hold great promise as predictive tools, but are hard to implement because they require environmental data at the scale of organisms, and deep knowledge on how it translates into physiological responses. This thesis aimed at filling this gap, improving general knowledge about the micro-environment experienced by intertidal organisms, the physiological consequences of existing under such conditions, and the mechanisms by which micro-environment variability impacts continental-scale patterns of distributions.

Using state-of-the-art biomimetic sensors (robolimpets), the present work advances the characterization of the intertidal environment, providing a detailed perspective of the thermal environment experienced by a key intertidal species – the limpet *Patella vulgata*. More than one year of data from contrasting microhabitats at multiple sites along the Iberian Peninsula have shown that within-site variability of thermal environments is a general feature that results from the effect of micro-topography on the amount of incident solar radiation, and that it exceeds thermal variability brought about by latitude, season and shore-level. In a broader context, similarities between the dataset produced during this work and datasets originated by networks of biomimetic temperature sensors deployed in North America (Helmuth and Hofmann, 2001; Helmuth et al., 2009), South Africa (Zardi et al., 2010) and Australia (Lathlean et al., 2011, 2014a) suggest that intertidal thermal profiles from temperate regions share the same basic characteristics. During the course of this work, the network of sensors was expanded, and now includes shores from south Portugal to Scotland. Interestingly, data collected thus far show that the contrasts between microhabitats observed in the Iberian study remain qualitatively the same. For example, organisms in sun-exposed mid-intertidal microhabitats in Scotland are regularly exposed to daily maximum temperatures well above those experienced by individuals in shaded mid-intertidal microhabitats not only in Scotland, but also in the south of Portugal (Fig. 5.1). In addition, making use of a recently released high-resolution digital elevation model, it was shown that the effect of topographical shading remains an important factor determining habitat complexity and the distribution of refugia at the regional and continental levels. These results appear to indicate that, with respect to the emersion period, intertidal organisms have a wide range of thermal environments to explore, both at the individual and population levels, confirming the detachment between climatic variables and organismal climatology (Helmuth et al., 2010). If the temperature during the emersion period is a determinant factor for the build-up of thermal stress, as can be inferred from many studies (e.g., Helmuth et al., 2006a;

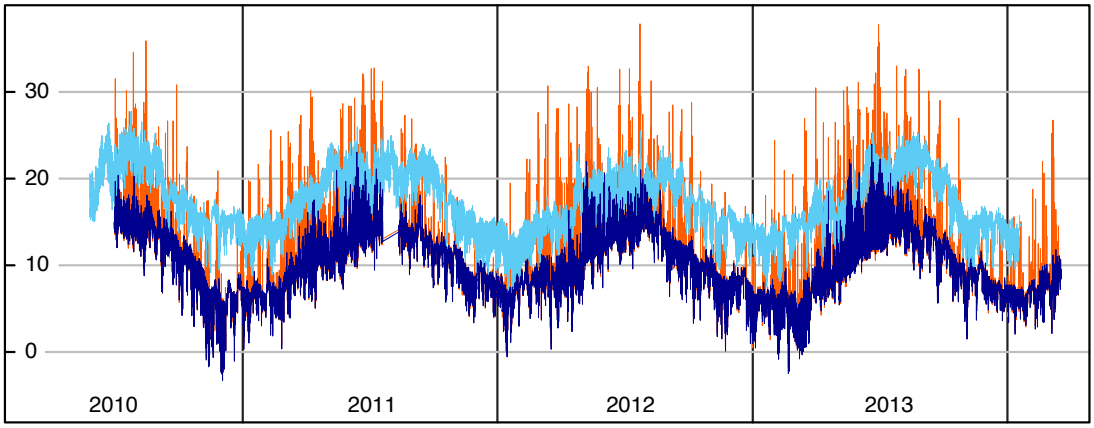

Figure 5.1: Four years of robolimpet data from mid-intertidal microhabitats. Dark blue, shaded microhabitats in South Cairn, Scotland; light blue, shaded microhabitats in Evaristo, south Portugal; orange, sun-exposed microhabitats in South Cairn.

Dong and Williams, 2011; Mislan et al., 2014; Zhang et al., 2014), this would suggest that effective refugia should be available wherever shade is present. Indeed, by quantifying the levels of thermal stress-related proteins (heat-shock proteins, Hsp70) of animals collected from shaded and unshaded microhabitats along the European Atlantic coast it was shown that animals living in the shade have consistently lower levels of thermal stress than those collected from sun-exposed surfaces. However, an interesting pattern emerged: at shores closer to the limits of distribution of *P. vulgata* the ameliorating effect of shaded microhabitats was significantly diminished even though marked differences in the temperature profiles recorded at these contrasting microhabitats were still evident. In order to address this issue, a series of laboratorial experiments were executed to evaluate the relative contribution of water and air temperature during emersion for the levels of thermal stress of *P. vulgata*. Using cardiac activity as a proxy for stress level, it was shown that elevated water temperature always results in increased thermal stress, while elevated air temperature only appears to matter when water temperature is also high. Importantly, of all the locations surveyed in this work, the two where *P. vulgata* is not present are the ones with highest water temperature during summer, indicating that thermal stress resulting from high water temperatures may be too high for individuals of this species to endure.

Throughout the work presented in this thesis, several complex tasks were planned for which appropriate methodologies or technologies were inexistent at the time. In particular, the experiments necessary for the assessment of the relative contribution of water and air temperatures for the build-up of thermal stress presented a significant methodological challenge. A standard methodology used in similar studies involves subjecting individuals to thermal regimes under controlled laboratorial conditions (Fig. 5.2a). However, due to the lack of proper environmental datasets, target temperatures and rates of heating/cooling are typically taken from empirical knowledge or datasets at scales very different from the scale of the organisms being tested. As a result, many studies involve unrealistic testing conditions (e.g.,

Denny et al., 2006; Dong et al., 2008; Bjelde and Todgham, 2013), generally exposing animals to excessive temperatures and heating rates, and therefore likely overestimating thermal sensitivity. In order to avoid that outcome, we used data from the network of biomimetic sensors described in section 2.1 to identify appropriate target temperatures and heating/cooling rates (Fig. 5.2b). Furthermore, temperature within the experiment tanks was probed using the same type of sensors that are being deployed in the field, therefore ensuring that potential biases originated by this type of sensor are maintained, resulting in highly realistic experimental conditions. Importantly, mortality of individuals of *P. vulgata* subjected to thermal stress using this methodology was extremely low, even when animals were subjected to daily peak temperatures of 40 °C, hence better reflecting the lack of mass mortality events of limpets in the European Atlantic coast during heatwaves. A second concern was to minimize the impact of the laboratorial experiments on the demographics of natural populations of *P. vulgata*. For that reason, it was important to use the lowest possible number of animals collected from the field. Thus, a reliable yet non-invasive way to estimate stress levels was required, so that animals wouldn't have to be sacrificed to produce data points (as is the case with the quantification of Hsp70 levels). Given its direct link to metabolism, attempts were initially made to use oxygen consumption, but the system proved impractical to use. Cardiac activity, which is also linked to the physiological state of invertebrates (Frederich and Pörtner, 2000), was then selected. However, the equipment described in the literature at the time had significant flaws, and it was extremely difficult to obtain reliable data. After various iterations of prototyping, a new highly improved version of hardware and software was designed and assembled (section 3.2), allowing the collection of real-time, non-invasive recordings of cardiac activity that can later be used to estimate stress levels (Fig. 5.2c). Finally, due to the temporal extent of the experiments (months), it was important that the conditions were maintained with minimal user supervision, and that a range of parameters were logged for posterior quality control. Since commercial, ready-to-use products didn't provide the level of flexibility required, a micro-controller board was designed, assembled and programmed to autonomously control and log air temperature during emersion, tidal and light cycles inside the purposely-built experiment tanks (Fig. 5.2d). This new equipment allowed tight control over experimental parameters, substantially reducing user-related errors, and one experiment was autonomously run for a period longer than one year. Despite the aforementioned advances, two major bottlenecks remain. First, the processing of heartbeat data is extremely computer and labor intensive, requiring visual inspection of the data collected (over 100,000 files for the experiment presented in section 3.3), delaying the communication of results. Secondly, the highly realistic conditions make it extremely difficult to establish proper experimental controls, greatly limiting generalizations of the conclusions drawn from the experiments.

Regarding the mechanisms controlling the distribution limits of *P. vulgata* in southwest Europe, and how they are scaled up from organisms to populations, the evidence collected during this work is not definitive. Nevertheless, combining the findings here presented with

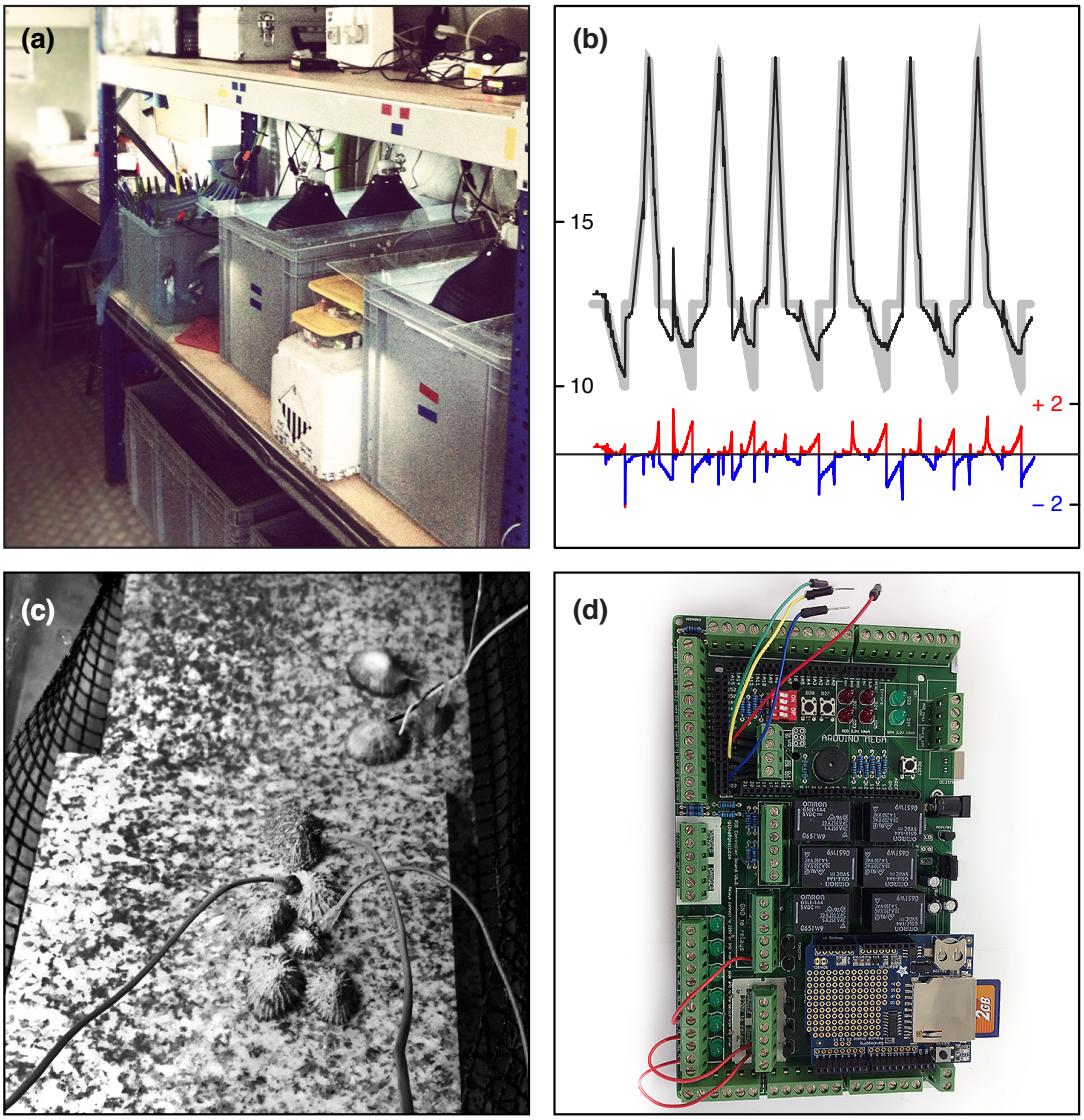

Figure 5.2: (a) Aquaria facility where physiological experiments were performed. (b) Target and effective temperature during one experiment at the aquaria facility. Thick grey line, target temperature; black line, effective treatment temperature, as recorded by one biomimetic sensor deployed inside the tank; red and blue lines show the error between effective and target temperature. The thermal profiles used were based in real collected by biomimetic sensors deployed in the field, and the use of similar sensors as input for the temperature controllers meant that the profiles were replicated with high accuracy. (c) Individuals of *P. vulgata* fitted with non-invasive infrared heartbeat sensors. (d) The programmable controller boards designed allow great experimental flexibility and require minimal user supervision for extended periods of time.

additional observations one plausible hypothesis emerged. We suggest that individuals of this species are fairly resilient to elevated air temperature during emersion, clamping down in their home scar during low tide and minimizing activity. This is supported by the fact that animals exposed to realistic temperature profiles exhibited remarkably low mortality (even during month-long experiments), indicating that *P. vulgata* can survive at the upper margin of the range of air temperatures experienced in the field during low tide. In addition, a similar strategy has been described for Fucus vesiculosus (Mota et al., 2015). Individuals of this alga that are attached to exposed rock outcrops dry faster upon exposure to solar radiation, and the resulting metabolic stasis appears to spare them from additional cellular damage. On the other hand, we propose that high water temperatures, by imposing an elevated metabolic rate, severely limit the scope-for-growth (Woodin et al., 2013), and that limpets die or fail to timely reproduce due to the inability to consume enough food. An interesting observation provides further support to this last assertion. Royan, a site along the north shore of the Gironde estuary (France, Fig. 5.3a, b), is one of the hottest shores analyzed during this work (Fig. 4.1). During fieldwork at this shore, it was noted that rocky outcrops a few km apart had strikingly different densities of *P. vulgata*, despite their temperature profiles being virtually identical (145 individuals per square meter in the location with highest abundance, compared to 6 in the location with lowest abundance; Figs. 5.3b, c). However, limpets at the shore with the highest population density were smaller in size, and biofilm mats were remarkably thick, with rasping marks surrounding each limpet (Fig. 5.3d, e). Hence, we hypothesize that, at this unique shore, the abnormally high amount of available food allows limpets to maintain positive scope-for-growth despite the otherwise excessive maintenance rate due to the high summer water temperature. Since this amount of food is not found along the remaining shores studied, it is possible that at the other locations where water temperature is similarly high - and from which *P. vulgata* is absent, limpets cannot feed at the necessary rate, thus not having sufficient scope-for-growth (Fly and Hilbish, 2012).

By combining the results outlined in this thesis with the mechanism described above it is possible to formulate a summary explanation for the observed pattern of distribution of *P. vulgata*. First, *P. vulgata* can be present in high densities in shores with low water temperature, regardless of the presence of high air temperature during low tide(Fig. 5.3a, green segments). Conversely, *P. vulgata* will be absent from shores where water temperature during summer exceeds a threshold, estimated in this work to be around 23 °C (Fig. 5.3a, red segments). Lastly, in shores with high water temperature that does not cross the threshold, *P. vulgata* can exists in intermediate densities (Fig. 5.3a, yellow segments), which will be higher if topographical shading provides sufficient amelioration of low tide temperatures (Fig. 5.3a, yellow segment *).

The concepts addressed in this thesis, coupled with the outlining of an hypothesis about the mechanism setting the southern limits of distribution of *P. vulgata*, provide a solid foundation for the development of future research projects. Some of the future lines of research stemming from this thesis include performing new experiments testing the effect of varying levels of food

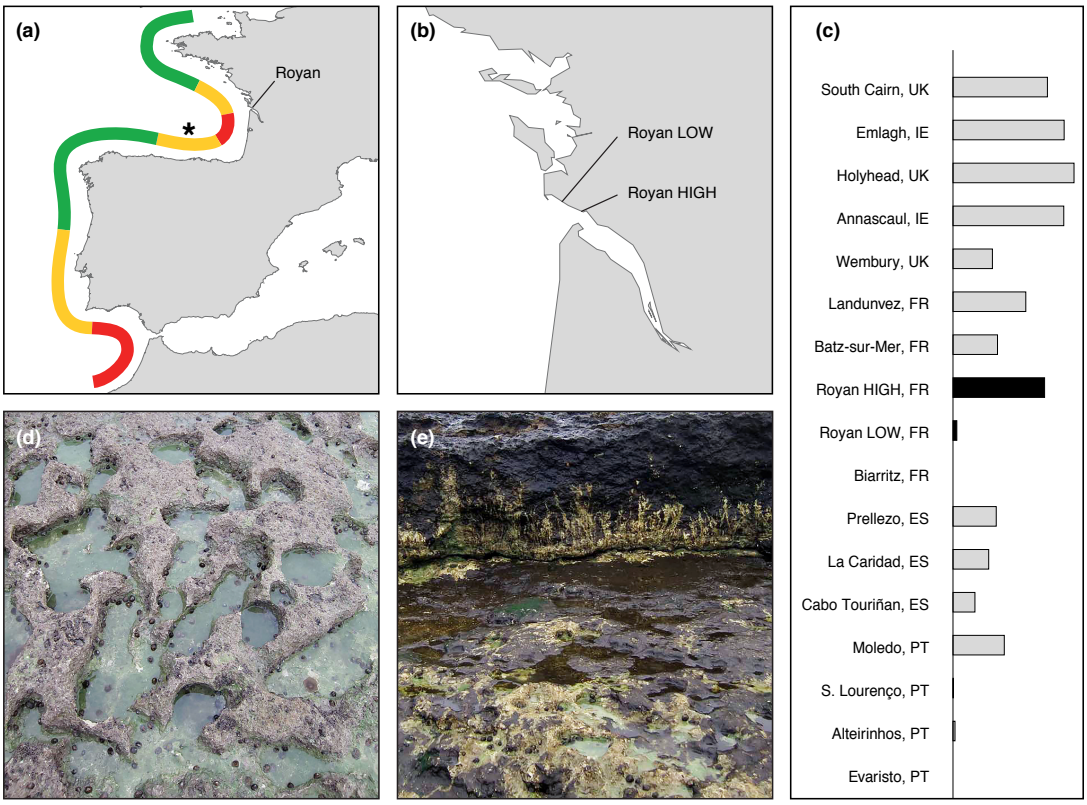

Figure 5.3: (a) The southern edge of the distribution of *P. vulgata*. Animals collected from the locations marked with green had low concentrations of Hsp70, while concentrations were higher in animals collected from locations in the yellow areas. *P. vulgata* is absent from the red areas. While water temperature is similar along the yellow segment, the concentration of Hsp70 was comparatively lower in animals collected from locations along the segment *, suggesting that topographical shading may be reducing thermal stress. (b) Detail of the coastline around Royan. (c) Abundance of *P. vulgata* along the studied shores. Contrasting with the low density of *P. vulgata* found at the western end of the estuary, a shore a few km to the east exhibited both some of the highest densities of *P. vulgata* of all the studied shores (d) and thick biofilm mats (e).

availability and thermal stress, examining differential responses at different stages of life or using other key intertidal species (e.g., mussels, barnacles, macroalgae), and characterizing the intertidal environment at increasingly high detail (continental-wide 3D scanning of rocky shores, measuring of other relevant variables, such as wave force and desiccation).

Bibliography

Abramoff, M. D., Magalhães, P. J., and Ram, S. J. (2004). *Image processing with ImageJ*, volume 11. Laurin Publishing.

Allen, J. A., Krauss, K. W., and Hauff, R. D. (2003). Factors limiting the intertidal distribution of the mangrove species *Xylocarpus granatum*. *Oecologia*, 135(1):110–121.

Allouche, O., Kalyuzhny, M., Moreno-Rueda, G., Pizarro, M., and Kadmon, R. (2012). Area-heterogeneity tradeoff and the diversity of ecological communities. *Proceedings of the National Academy of Sciences of the United States of America*, 109(43):17495–17500.

Ardré, F. (1970). Contribution à l'étude des algues marines du Portugal I. La flore. *Portugaliae Acta Biologica*, 10:1–423.

Ashcroft, M. B., Cavanagh, M., Eldridge, M. D. B., and Gollan, J. R. (2014). Testing the ability of topoclimatic grids of extreme temperatures to explain the distribution of the endangered brush-tailed rock-wallaby (*Petrogale penicillata*). *Journal of Biogeography*, 41(7):1402–1413.

Austin, M. P. (2002). Spatial prediction of species distribution: an interface between ecological theory and statistical modelling. *Ecological Modelling*, 157(2-3):101–118.

Bakun, A. (1990). Global climate change and intensification of coastal ocean upwelling. *Science*, 247(4939):198–201.

Baumann, H. and Doherty, O. (2013). Decadal changes in the World's coastal latitudinal temperature gradients. *PLOS ONE*, 8(6):e67596.

Bayne, B. L., Bayne, C. J., Carefoot, T. C., and Thompson, R. J. (1976). The physiological ecology of *Mytilus californianus* Conrad. *Oecologia*, 22(3):211–228.

Belanger, C. L., Jablonski, D., Roy, K., Berke, S. K., Krug, A. Z., and Valentine, J. W. (2012). Global environmental predictors of benthic marine biogeographic structure. *Proceedings of the National Academy of Sciences of the United States of America*, 109(35):14046–14051.

Belkin, I. M. (2009). Rapid warming of Large Marine Ecosystems. *Progress in Oceanography*, 81(1-4):207–213.

Bennie, J., Huntley, B., Wiltshire, A., Hill, M. O., and Baxter, R. (2008). Slope, aspect and climate: Spatially explicit and implicit models of topographic microclimate in chalk grassland. *Ecological Modelling*, 216(1):47–59.

Berke, S. K., Mahon, A. R., Lima, F. P., Halanych, K. M., Wethey, D. S., and Woodin, S. A. (2010). Range shifts and species diversity in marine ecosystem engineers: patterns and predictions for European sedimentary habitats. *Global Ecology and Biogeography*, 19(2):223–232.

Bertness, M. D., Leonard, G. H., Levine, J. M., and Bruno, J. F. (1999). Climate-driven interactions among rocky intertidal organisms caught between a rock and a hot place. *Oecologia*, 120(3):446–450.

Bini, G. and Chelazzi, G. (2006). Acclimatable cardiac and ventilatory responses to copper in the freshwater crayfish *Procambarus clarkii*. *Comparative Biochemistry and Physiology C*, 144(3):235–241.

Bischof, K., Gómez, I., Molis, M., Hanelt, D., Karsten, U., Lüder, U., Roleda, M. Y., Zacher, K., and Wiencke, C. (2006). Ultraviolet radiation shapes seaweed communities. *Reviews in Environmental Science and Biotechnology*, 5(2-3):141–166.

Bjelde, B. E. and Todgham, A. E. (2013). Thermal physiology of the fingered limpet *Lottia digitalis* under emersion and immersion. *Journal of Experimental Biology*, 216(Pt 15):2858–2869.

Blockley, D. J. (2007). Effect of wharves on intertidal assemblages on seawalls in Sydney Harbour, Australia. *Marine Environmental Research*, 63(4):409–427.

Bloxham, M. J., Worsfold, P. J., and Depledge, M. H. (1999). Integrated biological and chemical monitoring: *in situ* physiological responses of freshwater crayfish to fluctuations in environmental ammonia concentrations. *Ecotoxicology*, 8(3):225–237.

Boaventura, D., Fonseca, L. C., and Hawkins, S. J. (2002). Analysis of competitive interactions between the limpets *Patella depressa* Pennant and *Patella vulgata* L. on the northern coast of Portugal. *Journal of Experimental Marine Biology and Ecology*, 271(2):171–188.

Boaventura, D., Fonseca, L. C., and Hawkins, S. J. (2003). Size matters: competition within populations of the limpet *Patella depressa*. *Journal of Animal Ecology*, 72(3):435–446.

Bode, A., Alvarez-Ossorio, M. T., Cabanas, J. M., Miranda, A., and Varela, M. (2009). Recent trends in plankton and upwelling intensity off Galicia (NW Spain). *Progress in Oceanography*, 83(1-4):342–350.

Bordewijk, J. A., Slaper, H., Reinen, H. A. J. M., and Schlamann, E. (1995). Total solar radiation and the influence of clouds and aerosols on the biologically effective UV. *Geophysical Research Letters*, 22(16):2151–2154.

Borges, C. D. G., Doncaster, C. P., Maclean, M. A., and Hawkins, S. J. (2015). Broad-scale patterns of sex ratios in *Patella* spp.: a comparison of range edge and central range populations in the British Isles and Portugal. *Journal of the Marine Biological Association of the United Kingdom*, 95(06):1141–1153.

Borja, A., Fontán, A., Sáenz, J., and Valencia, V. (2008). Climate, oceanography, and recruitment: the case of the Bay of Biscay anchovy (*Engraulis encrasicolus*). *Fisheries Oceanography*, 17(6):477–493.

Borja, A., Uriarte, A., Valencia, V., Motos, L., and Uriarte, A. (1996). Relationships between anchovy (*Engraulis encrasicolus* L.) recruitment and the environment in the Bay of Biscay. *Scientia Marina*, 60:179–192.

Bowman, R. S. and Lewis, J. R. (1977). Annual fluctuations in the recruitment of *Patella vulgata* L. *Journal of the Marine Biological Association of the United Kingdom*, 57(03):793–815.

Braby, C. E. and Somero, G. N. (2006). Following the heart: temperature and salinity effects on heart rate in native and invasive species of blue mussels (genus *Mytilus*). *Journal of Experimental Biology*, 209(Pt 13):2554–2566.

Branch, G. M. (1981). The biology of limpets: Physical factors, energy flow, and ecological interactions. In Barnes, H., Ansell, A. D., and Gibson, R. N., editors, *Oceanography and Marine Biology: An Annual Review*, pages 235–380. University College London Press.

Brands, S., Herrera, S., San-Martín, D., and Gutiérrez, J. M. (2011). Validation of the ENSEMBLES global climate models over southwestern Europe using probability density functions, from a downscaling perspective. *Climate Research*, 48(2):145–161.

Bristow, K. L. and Campbell, G. S. (1984). On the relationship between incoming solar radiation and daily maximum and minimum temperature. *Agricultural and Forest Meteorology*, 31(2):159–166.

Brock, T. D. (1981). Calculating solar radiation for ecological studies. *Ecological Modelling*, 14(1-2):1–19.

Buckley, B. A., Owen, M., and Hofmann, G. E. (2001). Adjusting the thermostat: the threshold induction temperature for the heat-shock response in intertidal mussels (genus *Mytilus*) changes as a function of thermal history. *Journal of Experimental Biology*, 204(20):3571–3579.

Burnett, L. E., Holman, J. D., Jorgensen, D. D., Ikerd, J. L., and Burnett, K. G. (2006). Immune defense reduces respiratory fitness in *Callinectes sapidus*, the Atlantic Blue crab. *Biological Bulletin*, 211(1):50.

Burnett, N. P., Seabra, R., De Pirro, M., Wethey, D. S., Woodin, S. A., Helmuth, B., Zippay, M., Sarà, G., Monaco, C. J., and Lima, F. P. (2013). An improved noninvasive method for measuring heartbeat of intertidal animals. *Limnology and Oceanography: Methods*, 11:91–100.

Burrows, M. T., Harvey, R., and Robb, L. (2008). Wave exposure indices from digital coastlines and the prediction of rocky shore community structure. *Marine Ecology-Progress Series*, 353:1–12.

Burrows, M. T., Schoeman, D. S., Buckley, L. B., Moore, P. J., Poloczanska, E. S., Brander, K., Brown, C. J., Bruno, J. F., Duarte, C. M., Halpern, B. S., Holding, J., Kappel, C. V., Kiessling, W., O'Connor, M. I., Pandolfi, J. M., Parmesan, C., Schwing, F., Sydeman, W. J., and Richardson, A. J. (2011). The pace of shifting climate in marine and terrestrial ecosystems. *Science*, 334(6056):652–655.

Cade, B. S. and Noon, B. R. (2013). A gentle introduction to quantile regression for ecologists. *Frontiers in Ecology and the Environment*, 1(8):412–420.

Cade, B. S., Terrell, J. W., and Schroeder, R. L. (1999). Estimating effects of limiting factors with regression quantiles. *Ecology*, 80(1):311–323.

Calosi, P., Chelazzi, G., and Ugolini, A. (2003). Optocardiographic recording of heart rate in *Talitrus saltator* (Amphipoda: Talitridae). *Physiological Entomology*, 28(4):344–348.

Calosi, P., Ugolini, A., and Morritt, D. (2005). Physiological responses to hyposmotic stress in the supralittoral amphipod *Talitrus saltator* (Crustacea: Amphipoda). *Comparative Biochemistry and Physiology A*, 142(3):267–275.

Chapperon, C. and Seuront, L. (2011). Behavioral thermoregulation in a tropical gastropod: links to climate change scenarios. *Global Change Biology*, 17(4):1740–1749.

Chapperon, C., Volkenborn, N., Clavier, J., Séité, S., Seabra, R., and Lima, F. P. (2015). Thermal sensitivity and tolerance limits of an intertidal ectotherm under heat stress: not all vulnerable to climate warming. *Submitted*.

Chelazzi, G., De Pirro, M., and Williams, G. A. (2001). Cardiac responses to abiotic factors in two tropical limpets, occurring at different levels of the shore. *Marine Biology*, 139(6):1079–1085.

Chelazzi, G., De Pirro, M., and Williams, G. A. (2004). Different cardiac response to copper in limpets from metal polluted and clean shores of Hong Kong. *Marine Environmental Research*, 58(1):83–93.

Chelazzi, G., Williams, G. A., and Gray, D. R. (1999). Field and laboratory measurement of heart rate in a tropical limpet, *Cellana grata*. *Journal of the Marine Biological Association of the United Kingdom*, 79(4):749–751.

Chen, I. C., Hill, J. K., Ohlemüller, R., Roy, D. B., and Thomas, C. D. (2011). Rapid range shifts of species associated with high levels of climate warming. *Science*, 333(6045):1024–1026.

Christiaens, J. (1973). Révision du genre *Patella* (Mollusca, Gastropoda). *Bulletin du Muséum National d'Histoire Naturelle*, 182:1–88.

Coleman, R. A., Underwood, A. J., Benedetti-Cecchi, L., Åberg, P., Arenas, F., Arrontes, J., Castro, J., Hartnoll, R. G., Jenkins, S. R., Paula, J., Santina, P. D., and Hawkins, S. J. (2006). A continental scale evaluation of the role of limpet grazing on rocky shores. *Oecologia*, 147(3):556–564.

Connell, J. H. (1972). Community interactions on marine rocky intertidal shores. *Annual Review of Ecology and Systematics*, 3:169–192.

Corripio, J. G. (2003). Vectorial algebra algorithms for calculating terrain parameters from DEMs and solar radiation modelling in mountainous terrain. *International Journal of Geographical Information Science*, 17(1):1–23.

Crimmins, S. M., Dobrowski, S. Z., Greenberg, J. A., Abatzoglou, J. T., and Mynsberge, A. R. (2011). Changes in climatic water balance drive downhill shifts in plant species' optimum elevations. *Science*, 331(6015):324–327.

Crisp, D. J. and Fischer-Piette, E. (1959). Répartition des principales espèces intercotidales de la côte Atlantique Française en 1954-1955. *Annales de l'Institut Océanographique (Monaco)*, 36:275–388.

Curtis, T., Williamson, R., and Depledge, M. H. (2000). Simultaneous, long-term monitoring of valve and cardiac activity in the blue mussel *Mytilus edulis* exposed to copper. *Marine Biology*, 136(5):837–846.

Curtis, T., Williamson, R., and Depledge, M. H. (2001). The initial mode of action of copper on the cardiac physiology of the blue mussel, *Mytilus edulis*. *Aquatic Toxicology*, 52(1):29–38.

Dahlhoff, E. P., Buckley, B. A., and Menge, B. A. (2001). Physiology of the rocky intertidal predator *Nucella ostrina* along an environmental stress gradient. *Ecology*, 82(10):2816–2829.

Dalvi, R. S., Pal, A. K., Tiwari, L. R., and Baruah, K. (2011). Influence of acclimation temperature on the induction of heat-shock protein 70 in the catfish *Horabagrus brachysoma* (Günther). *Fish Physiology and Biochemistry*, 38(4):919–927.

Darwin, C. R. (1859). *The origin of species*. By means of natural selection, or the preservation of favoured races in the struggle for life. John Murray, London.

De Pirro, M., Cannicci, S., and Santini, G. (1999a). A multi-factorial experiment on heart rate variations in the intertidal crab *Pachygrapsus marmoratus*. *Marine Biology*, 135(2):341–345.

De Pirro, M., Santini, G., and Chelazzi, G. (1999b). Cardiac responses to salinity variations in two differently zoned Mediterranean limpets. *Journal of Comparative Physiology B*, 169(7):501–506.

Den Boer, P. J. (1968). Spreading of risk and stabilization of animal numbers. *Acta Biotheoretica*, 18(1-4):165–194.

Denny, M. W., Daniel, T. L., and Koehl, M. A. R. (1985). Mechanical limits to size in wave-swept organisms. *Ecological Monographs*, 55(1):69–102.

Denny, M. W., Dowd, W. W., Bilir, L., and Mach, K. (2011). Spreading the risk: small-scale body temperature variation among intertidal organisms and its implications for species persistence. *Journal of Experimental Marine Biology and Ecology*, 400(1-2):175–190.

Denny, M. W. and Harley, C. D. G. (2006). Hot limpets: predicting body temperature in a conductance-mediated thermal system. *Journal of Experimental Biology*, 209(13):2409–2419.

Denny, M. W., Miller, L. P., and Harley, C. D. G. (2006). Thermal stress on intertidal limpets: long-term hindcasts and lethal limits. *Journal of Experimental Biology*, 209(Pt 13):2420–2431.

Denny, M. W. and Wethey, D. S. (2000). Physical processes that generate patterns in marine communities. In Bertness, M. D., Gaines, S., and Hay, M. E., editors, *Marine Community Ecology*, pages 3–37. Sinauer Associates, Sunderland, Massachusetts.

Depledge, M. H. and Andersen, B. B. (1990). A computer-aided physiological monitoring system for continuous, long-term recording of cardiac activity in selected invertebrates. *Comparative Biochemistry and Physiology A*, 96(4):473–477.

Depledge, M. H., Lundebye, A. K., Curtis, T., Aagaard, A., and Andersen, B. B. (1996). Automated interpulse-duration assessment (AIDA): a new technique for detecting disturbances in cardiac activity in selected macroinvertebrates. *Marine Biology*, 126(2):313–319.

Dong, Y. and Dong, S. (2008). Induced thermotolerance and expression of heat shock protein 70 in sea cucumber *Apostichopus japonicus*. *Fisheries Science*, 74(3):573–578.

Dong, Y., Miller, L. P., Sanders, J. G., and Somero, G. N. (2008). Heat-shock protein 70 (Hsp70) expression in four limpets of the genus *Lottia*: interspecific variation in constitutive and inducible synthesis correlates with in situ exposure to heat stress. *Biological Bulletin*, 215(2):173–181.

Dong, Y. and Williams, G. A. (2011). Variations in cardiac performance and heat shock protein expression to thermal stress in two differently zoned limpets on a tropical rocky shore. *Marine Biology*, 158(6):1223–1231.

Easterling, D. R., Meehl, G. A., Parmesan, C., Changnon, S. A., Karl, T. R., and Mearns, L. O. (2000). Climate extremes: Observations, modeling, and impacts. *Science*, 289(5487):2068–2074.

Einav, R., Breckle, S., and Beer, S. (1995). Ecophysiological adaptation strategies of some intertidal marine macroalgae of the Israeli Mediterranean coast. *Marine Ecology-Progress Series*, 125:219–228.

Espinosa, F., Guerra-García, J. M., Fa, D., and García-Gómez, J. C. (2006). Effects of competition on an endangered limpet *Patella ferruginea* (Gastropoda: Patellidae): Implications for conservation. *Journal of Experimental Marine Biology and Ecology*, 330(2):482–492.

Evans, R. G. (1948). The lethal temperatures of some common British littoral molluscs. *Journal of Animal Ecology*, 17(2):165–173.

Farman, J. C., Gardiner, B. G., and Shanklin, J. D. (1985). Large losses of total ozone in Antarctica reveal seasonal ClOx/NOx interaction. *Nature*, 315(6016):207–210.

Farnsworth, E. J. and Ellison, A. M. (1996). Sun-shade adaptability of the red mangrove, *Rhizophora mangle* (Rhizophoraceae): changes through ontogeny at several levels of biological organization. *American Journal of Botany*, 83(9):1131.

Farr, T. G., Rosen, P. A., Caro, E., Crippen, R., Duren, R., Hensley, S., Kobrick, M., Paller, M., Rodriguez, E., Roth, L., Seal, D., Shaffer, S., Shimada, J., Umland, J., Werner, M., Oskin, M., Burbank, D., and Alsdorf, D. (2007). The Shuttle Radar Topography Mission. *Reviews of Geophysics*, 45(2):RG2004.

Feder, M. E. and Hofmann, G. E. (1999). Heat-shock proteins, molecular chaperones, and the stress response: Evolutionary and ecological physiology. *Annual Review of Physiology*, 61(1):243–282.

Firth, L. B., Knights, A. M., and Bell, S. S. (2011). Air temperature and winter mortality: implications for the persistence of the invasive mussel, *Perna viridis* in the intertidal zone of the south-eastern United States. *Journal of Experimental Marine Biology and Ecology*, 400(1-2):250–256.

Firth, L. B., White, F. J., Schofield, M., Hanley, M. E., Burrows, M. T., Thompson, R. C., Skov, M. W., Evans, A. J., Moore, P. J., and Hawkins, S. J. (2015). Facing the future: the importance of substratum features for ecological engineering of artificial habitats in the rocky intertidal. *Australian Journal of Marine and Freshwater Research*.

Fischer-Piette, E. (1935). Systematique et biogeographie – les Patelles d'Europe et d'Afrique du nord. *Journal de Conchyliologie*, 79:5–66.

Fischer-Piette, E. (1953). Répartition de quelques mollusques intercotidaux communs le long des côtes septentrionales de l'Espagne. *Journal de Conchyliologie*, 93:39–73.

Fischer-Piette, E. (1955). Répartition, le long des côtes septentrionales de l'Espagne, des principales espèces peuplant les rochers intercotidaux. *Annales de l'Institut Océanographique (Monaco)*, 31:37–124.

Fischer-Piette, E. (1959). Contribution à l'écologie intercotidale du Détroit de Gibraltar. *Bulletin de l'Institut Oceanographique (Monaco)*, 1145.

Fischer-Piette, E. (1963). La distribuition des principaux organismes intercotidaux Nord-Ibériques en 1954-1955. *Annales de l'Institut Océanographique (Monaco)*, XL:165–312.

Fischer-Piette, E. and Gaillard, J. M. (1959). Les Patelles, au long des côtes Atlantiques Ibériques et Nord-Marocaines. *Journal de Conchyliologie*, 99:135–200.

Fitzgerald-Dehoog, L., Browning, J., and Allen, B. J. (2012). Food and heat stress in the California Mussel: Evidence for an energetic trade-off between survival and growth. *Biological Bulletin*, 223(2):205–216.

Fitzhenry, T., Halpin, P., and Helmuth, B. (2004). Testing the effects of wave exposure, site, and behavior on intertidal mussel body temperatures: applications and limits of temperature logger design. *Marine Biology*, 145(2):339–349.

Fjeldså, J., Bowie, R. C. K., and Rahbek, C. (2012). The role of mountain ranges in the diversification of birds. *Annual Review of Ecology Evolution and Systematics*, 43(1):249–265.

Fly, E. K. and Hilbish, T. J. (2012). Physiological energetics and biogeographic range limits of three congeneric mussel species. *Oecologia*, 172(1):35–46.

Foster, B. A. (1971). Desiccation as a factor in the intertidal zonation of barnacles. *Marine Biology*, 8(1):12–29.

Franklin, L. A. and Forster, R. M. (1997). The changing irradiance environment: consequences for marine macrophyte physiology, productivity and ecology. *European Journal of Phycology*, 32(03):207–232.

Frederich, M. and Pörtner, H.-O. (2000). Oxygen limitation of thermal tolerance defined by cardiac and ventilatory performance in spider crab, *Maja squinado*. *American Journal of Physiology - Regulatory, Integrative and Comparative Physiology*, 279(5):R1531–R1538.

Frederick, J. E. and Snell, H. E. (1990). Tropospheric influence on solar ultraviolet radiation: the role of clouds. *Journal of Climate*, 3(3):373–381.

Fu, Y. H., Piao, S., Vitasse, Y., Zhao, H., De Boeck, H. J., Liu, Q., Yang, H., Weber, U., Hänninen, H., and Janssens, I. A. (2015). Increased heat requirement for leaf flushing in temperate woody species over 1980-2012: effects of chilling, precipitation and insolation. *Global Change Biology*, 21:2687–2697.

Fuller, A., Dawson, T., Helmuth, B., Hetem, R. S., Mitchell, D., and Maloney, S. K. (2010). Physiological mechanisms in coping with climate change. *Physiological and Biochemical Zoology*, 83(5):713–720.

Galloway, T. S., Brown, R. J., Browne, M., Dissanayake, A., Lowe, D., Jones, M. B., and Depledge, M. H. (2004). A multibiomarker approach to environmental assessment. *Environmental Science and Technology*, 38:1723–1731.

Gandra, M., Seabra, R., and Lima, F. P. (2015). A low-cost, versatile data logging system for ecological applications. *Limnology and Oceanography: Methods*, 13(3):115–126.

Gedan, K. B., Bernhardt, J., Bertness, M. D., and Leslie, H. M. (2011). Substrate size mediates thermal stress in the rocky intertidal. *Ecology*, 92(3):576–582.

Gilman, S. E., Wethey, D. S., and Helmuth, B. (2006). Variation in the sensitivity of organismal body temperature to climate change over local and geographic scales. *Proceedings of the National Academy of Sciences of the United States of America*, 103(25):9560–9565.

Girard, D., Clemente, S., Toledo-Guedes, K., Brito, A., and Hernández, J. C. (2012). A mass mortality of subtropical intertidal populations of the sea urchin *Paracentrotus lividus*: analysis of potential links with environmental conditions. *Marine Ecology*, 33(3):377–385.

Goatley, C. H. R. and Bellwood, D. R. (2014). Moving towards the equator: reverse range shifts in two subtropical reef fish species, *Chromis nitida* (Pomacentridae) and *Pseudolabrus guentheri* (Labridae). *Marine Biodiversity Records*, 7:e12.

Gray, D. R. and Naylor, E. (1996). Foraging and homing behaviour of the limpet, *Patella vulgata*: a geographical comparison. *Journal of Molluscan Studies*, 62(1):121–124.

Greenberg, J. A., Santos, M. J., Dobrowski, S. Z., Vanderbilt, V. C., and Ustin, S. L. (2015). Quantifying environmental limiting factors on tree cover using geospatial data. *PLOS ONE*, 10(2):e0114648.

Haefner, P. A., Sheppard, B., Barto, J., Mcneil, E., and Cappellino, V. (1996). Application of ultrasound technology to molluscan physiology: Noninvasive monitoring of cardiac rate in the blue mussel, *Mytilus edulis* Linnaeus, 1758 . *Journal of Shellfish Research*, 15:685–687.

Hagger, J. A., Galloway, T. S., Langston, W. J., and Jones, M. B. (2009). Application of biomarkers to assess the condition of European Marine Sites. *Environmental Pollution*, 157(7):2003–2010.

Halldórsson, H. P., De Pirro, M., Romano, C., Svavarsson, J., and Sarà, G. (2008). Immediate biomarker responses to benzo[a]pyrene in polluted and unpolluted populations of the blue mussel (*Mytilus edulis* L.) at high-latitudes. *Environment International*, 34(4):483–489.

Halpin, P., Sorte, C. J., Hofmann, G. E., and Menge, B. A. (2002). Patterns of variation in levels of Hsp70 in natural rocky shore populations from microscales to mesoscales. *Integrative and Comparative Biology*, 42(4):815–824.

Hannah, L., Flint, L., Syphard, A. D., Moritz, M. A., Buckley, L. B., and McCullough, I. M. (2014). Fine-grain modeling of species' response to climate change: holdouts, stepping-stones, and microrefugia. *Trends in Ecology & Evolution*, 29(7):390–397.

Hansen, J., Ruedy, R., Sato, M., and Lo, K. (2010). Global surface temperature change. *Reviews of Geophysics*, 48(4):RG4004.

Harley, C. D. G. (2002). Light availability indirectly limits herbivore growth and abundance in a high rocky intertidal community during the winter. *Limnology and Oceanography*, 47(4):1217–1222.

Harley, C. D. G. (2008). Tidal dynamics, topographic orientation, and temperature-mediated mass mortalities on rocky shores. *Marine Ecology-Progress Series*, 371:37–46.

Harley, C. D. G., Hughes, A. R., Hultgren, K., Miner, B. G., Sorte, C. J., Thornber, C. S., Rodriguez, L. F., Tomanek, L., and Williams, S. L. (2006). The impacts of climate change in coastal marine systems. *Ecology Letters*, 9(2):228–241.

Hartnoll, R. G. and Wright, J. R. (1977). Foraging movements and homing in the limpet *Patella vulgata* L. *Animal Behaviour*, 25:806–810.

Hawkins, S. J. and Hartnoll, R. G. (1982). The influence of barnacle cover on the growth and behaviour of *Patella vulgata* on a vertical pier. *Journal of Experimental Marine Biology and Ecology*, 62(4):855–867.

Hawkins, S. J. and Hartnoll, R. G. (1983). Grazing of intertidal algae by marine invertebrates . In Barnes, H., Ansell, A. D., and Gibson, R. N., editors, *Oceanography and Marine Biology: An Annual Review*, pages 195–282. University College London Press.

Hawkins, S. J., Moore, P. J., Burrows, M. T., Poloczanska, E. S., Mieszkowska, N., Herbert, R. J. H., Jenkins, S. R., Thompson, R. C., Genner, M. J., and Southward, A. J. (2008). Complex interactions in a rapidly changing world: responses of rocky shore communities to recent climate change. *Climate Research*, 37(2-3):123–133.

Hawkins, S. J., Sugden, H. E., Mieszkowska, N., Moore, P. J., Poloczanska, E., Leaper, R., Herbert, R., Genner, M. J., Moschella, P. S., Thompson, R. C., Jenkins, S. R., Southward, A. J., and Burrows, M. T. (2009). Consequences of climate-driven biodiversity changes for ecosystem functioning of North European rocky shores. *Marine Ecology-Progress Series*, 396:245–259.

Helm, M. M. and Trueman, E. R. (1967). The effect of exposure on the heart rate of the mussel, *Mytilus edulis* L. *Comparative Biochemistry and Physiology*, 21(1):171–177.

Helmuth, B. (1998). Intertidal mussel microclimates: predicting the body temperature of a sessile invertebrate. *Ecological Monographs*, 68(1):51–74.

Helmuth, B. (1999). Thermal biology of rocky intertidal mussels: quantifying body temperatures using climatological data. *Ecology*, 80(1):15–34.

Helmuth, B. (2002). How do we measure the environment? Linking intertidal thermal physiology and ecology through biophysics. *Integrative and Comparative Biology*, 42(4):837–845.

Helmuth, B., Broitman, B. R., Blanchette, C. A., Gilman, S. E., Halpin, P., Harley, C. D. G., O'Donnell, M. J., Hofmann, G. E., Menge, B. A., and Strickland, D. (2006a). Mosaic patterns of thermal stress in the rocky intertidal zone: implications for climate change. *Ecological Monographs*, 76(4):461–479.

Helmuth, B., Broitman, B. R., Szathmary, P. L., Mislan, K. A. S., and Blanchette, C. A. (2009). Predator-prey interactions under climate change: the importance of habitat vs body temperature. *Oikos*, 118(2):219–224.

Helmuth, B., Broitman, B. R., Yamane, L., Gilman, S. E., Mach, K., Mislan, K. A. S., and Denny, M. W. (2010). Organismal climatology: analyzing environmental variability at scales relevant to physiological stress. *Journal of Experimental Biology*, 213(6):995–1003.

Helmuth, B. and Hofmann, G. E. (2001). Microhabitats, thermal heterogeneity, and patterns of physiological stress in the rocky intertidal zone. *Biological Bulletin*, 201(3):374–384.

Helmuth, B., Kingsolver, J., and Carrington, E. (2005). Biophysics, physiological ecology, and climate change: does mechanism matter? *Annual Review of Physiology*, 67(1):177–201.

Helmuth, B., Mieszkowska, N., Moore, P. J., and Hawkins, S. J. (2006b). Living on the edge of two changing worlds: forecasting the responses of rocky intertidal ecosystems to climate change. *Annual Review of Ecology Evolution and Systematics*, 37:373–404.

Helmuth, B., Russell, B. D., Connell, S. D., Dong, Y., Harley, C. D. G., Lima, F. P., Sarà, G., Williams, G. A., and Mieszkowska, N. (2014). Beyond long-term averages: making biological sense of a rapidly changing world. *Climate Change Responses*, 1(1):6.

Helmuth, B., Yamane, L., Lalwani, S., Matzelle, A., Tockstein, A., and Gao, N. (2011). Hidden signals of climate change in intertidal ecosystems: What (not) to expect when you are expecting. *Journal of Experimental Marine Biology and Ecology*, 400(1-2):191–199.

Hemer, M. A., Fan, Y., Mori, N., Semedo, A., and Wang, X. L. (2013). Projected changes in wave climate from a multi-model ensemble. *Nature Climate Change*, 3(5):471–476.

Hewitt, C. D. and Griggs, D. J. (2004). Ensembles-based predictions of climate changes and their impacts. *Eos, Transactions American Geophysical Union*, 85(52):566–567.

Hickling, R., Roy, D. B., Hill, J. K., Fox, R., and Thomas, C. D. (2006). The distributions of a wide range of taxonomic groups are expanding polewards. *Global Change Biology*, 12(3):450–455.

Hilbish, T. J., Brannock, P. M., Jones, K. R., Smith, A. B., Bullock, B. N., and Wethey, D. S. (2010). Historical changes in the distributions of invasive and endemic marine invertebrates are contrary to global warming predictions: the effects of decadal climate oscillations. *Journal of Biogeography*, 37(3):423–431.

Hoffmann, A. and Sgrò, C. M. (2011). Climate change and evolutionary adaptation. *Nature*, 470(7335):479–485.

Hofmann, G. E. (2005). Patterns of Hsp gene expression in ectothermic marine organisms on small to large biogeographic scales. *Integrative and Comparative Biology*, 45(2):247–255.

Hofmann, G. E., Buckley, B. A., Place, S. P., and Zippay, M. (2002). Molecular chaperones in ectothermic marine animals: biochemical function and gene expression. *Integrative and Comparative Biology*, 42(4):808–814.

Hofmann, G. E. and Somero, G. N. (1995). Evidence for protein damage at environmental temperatures: seasonal changes in levels of ubiquitin conjugates and hsp70 in the intertidal mussel *Mytilus trossulus*. *Journal of Experimental Biology*, 198:1509–1518.

Hofmann, G. E. and Todgham, A. E. (2010). Living in the now: physiological mechanisms to tolerate a rapidly changing environment. *Annual Review of Physiology*, 72:127–145.

Holtmeier, F. K. and Broll, G. (2005). Sensitivity and response of northern hemisphere altitudinal and polar treelines to environmental change at landscape and local scales. *Global Ecology and Biogeography*, 14(5):395–410.

Huey, R. B. (1991). Physiological consequences of habitat selection. *The American Naturalist*, 137(s1):S91.

Huey, R. B., Peterson, C. R., Arnold, S. J., and Porter, W. P. (1989). Hot rocks and not-so-hot rocks: retreat-site selection by Garter snakes and its thermal consequences. *Ecology*, 70(4):931–944.

Hutchins, L. W. (1947). The bases for temperature zonation in geographical distribution. *Ecological Monographs*, 17(3):325–335.

IPCC (2013). *Climate Change 2013: The Physical Science Basis. Contribution of Working Group I to the Fifth Assessment Report of the Intergovernmental Panel on Climate Change*. Cambridge University Press, Cambridge, United Kingdom and New York, NY, USA.

IPCC (2014). *Climate Change 2014: Impacts, Adaptation, and Vulnerability. Part A: Global and Sectoral Aspects. Contribution of Working Group II to the Fifth Assessment Report of the Intergovernmental Panel of Climate Change*. Cambridge University Press, Cambridge, United Kingdom and New York, NY, USA.

Jenkins, S. R., Coleman, R. A., Della Santina, P., Hawkins, S. J., Burrows, M. T., and Hartnoll, R. G. (2005). Regional scale differences in the determinism of grazing effects in the rocky intertidal. *Marine Ecology*.

Jenkins, S. R. and Hartnoll, R. G. (2001). Food supply, grazing activity and growth rate in the limpet *Patella vulgata* L.: a comparison between exposed and sheltered shores. *Journal of Experimental Marine Biology and Ecology*, 258(1):123–139.

Jenkins, S. R., Moore, P. J., Burrows, M. T., Garbary, D. J., Hawkins, S. J., Ingólfsson, A., Sebens, K. P., Snelgrove, P. V. R., Wethey, D. S., and Woodin, S. A. (2008). Comparative ecology of North Atlantic shores: do differences in players matter for process? *Ecology*, 89(sp11):S3–S23.

Jones, S. J., Lima, F. P., and Wethey, D. S. (2010). Rising environmental temperatures and biogeography: poleward range contraction of the blue mussel, *Mytilus edulis* L., in the western Atlantic. *Journal of Biogeography*, 37(12):2243–2259.

Jurgens, L. J., Rogers-Bennett, L., Raimondi, P. T., Schiebelhut, L. M., Dawson, M. N., Grosberg, R. K., and Gaylord, B. (2015). Patterns of mass mortality among rocky shore invertebrates across 100 km of Northeastern Pacific coastline. *PLOS ONE*, 10(6):e0126280.

Karl, T. R., Arguez, A., Huang, B., Lawrimore, J. H., McMahon, J. R., Menne, M. J., Peterson, T. C., Vose, R. S., and Zhang, H. (2015). Possible artifacts of data biases in the recent global surface warming hiatus. *Science*, 348(6242):1469–1472.

Kasten, F. and Young, A. T. (1989). Revised optical air mass tables and approximation formula. *Applied Optics*, 28(22):4735–4738.

Kearney, M. and Porter, W. P. (2009). Mechanistic niche modelling: combining physiological and spatial data to predict species' ranges. *Ecology Letters*, 12(4):334–350.

Kharin, V. V., Zwiers, F. W., Zhang, X., and Wehner, M. (2013). Changes in temperature and precipitation extremes in the CMIP5 ensemble. *Climatic Change*, 119(2):345–357.

King, R. J. and Schramm, W. (1976). Photosynthetic rates of benthic marine algae in relation to light intensity and seasonal variations. *Marine Biology*, 37(3):215–222.

Lathlean, J. A., Ayre, D. J., Coleman, R. A., and Minchinton, T. E. (2014a). Using biomimetic loggers to measure interspecific and microhabitat variation in body temperatures of rocky intertidal invertebrates. 66(1):86–94.

Lathlean, J. A., Ayre, D. J., and Minchinton, T. E. (2011). Rocky intertidal temperature variability along the southeast coast of Australia: comparing data from in situ loggers, satellite-derived SST and terrestrial weather stations. *Marine Ecology-Progress Series*, 439:83–95.

Lathlean, J. A., Ayre, D. J., and Minchinton, T. E. (2014b). Estimating latitudinal variability in extreme heat stress on rocky intertidal shores. *Journal of Biogeography*, 41(8):1478–1491.

Lemon, J. (2006). Plotrix: a package in the red light district of R. *R-News*, 6:8–12.

Lemos, R. T. and Pires, H. O. (2004). The upwelling regime off the west Portuguese coast, 1941-2000. *International Journal of Climatology*, 24(4):511–524.

Lemos, R. T. and Sansó, B. (2006). Spatio-temporal variability of ocean temperature in the Portugal Current System. *Journal of Geophysical Research*, 111(C4):C04010.

Lima, F. P., Burnett, N. P., Helmuth, B., and Kish, N. (2010). Monitoring the intertidal environment with biomimetic devices. *Biomimetic Based Applications*.

Lima, F. P., Gomes, F., Seabra, R., Wethey, D. S., Seabra, M. I., Cruz, T., Santos, A. M., and Hilbish, T. J. (2015). Loss of thermal refugia near equatorial range limits. *Global Change Biology*.

Lima, F. P., Queiroz, N., Ribeiro, P. A., Hawkins, S. J., and Santos, A. M. (2006). Recent changes in the distribution of a marine gastropod, *Patella rustica* Linnaeus, 1758, and their relationship to unusual climatic events. *Journal of Biogeography*, 33(5):812–822.

Lima, F. P., Queiroz, N., Ribeiro, P. A., Xavier, R., Hawkins, S. J., and Santos, A. M. (2009). First record of *Halidrys siliquosa* on the Portuguese coast: counter-intuitive range expansion? *Marine Biodiversity Records*, 2(e1):1–4.

Lima, F. P., Ribeiro, P. A., Queiroz, N., Hawkins, S. J., and Santos, A. M. (2007a). Do distributional shifts of northern and southern species of algae match the warming pattern? *Global Change Biology*, 13(12):2592–2604.

Lima, F. P., Ribeiro, P. A., Queiroz, N., Xavier, R., Tarroso, P., Hawkins, S. J., and Santos, A. M. (2007b). Modelling past and present geographical distribution of the marine gastropod P*atella rustica* as a tool for exploring responses to environmental change. *Global Change Biology*, 13(10):2065–2077.

Lima, F. P. and Wethey, D. S. (2009). Robolimpets: measuring intertidal body temperatures using biomimetic loggers. *Limnology and Oceanography: Methods*, 7:347–353.

Lima, F. P. and Wethey, D. S. (2012). Three decades of high-resolution coastal sea surface temperatures reveal more than warming. *Nature Communications*, 3(704).

Lockwood, B. L. and Somero, G. N. (2011). Invasive and native blue mussels (genus *Mytilus*) on the California coast: the role of physiology in a biological invasion. *Journal of Experimental Marine Biology and Ecology*, 400:167–174.

Logan, C. A., Kost, L. E., and Somero, G. N. (2012). Latitudinal differences in *Mytilus californianus* thermal physiology. *Marine Ecology-Progress Series*, 450:93–105.

Lubchenco, J. and Menge, B. A. (1978). Community development and persistence in a low rocky intertidal zone. *Ecological Monographs*, 48(1):67–94.

Lubin, D., Jensen, E. H., and Gies, H. P. (1998). Global surface ultraviolet radiation climatology from TOMS and ERBE data. *Journal of Geophysical Research*, 103(D20):26061–26091.

Maclean, I. M. D., Hopkins, J. J., Bennie, J., Lawson, C. R., and Wilson, R. J. (2015). Microclimates buffer the responses of plant communities to climate change. *Global Ecology and Biogeography*, 24(11):1340–1350.

Magozzi, S. and Calosi, P. (2015). Integrating metabolic performance, thermal tolerance, and plasticity enables for more accurate predictions on species vulnerability to acute and chronic effects of global warming. *Global Change Biology*, 21(1):181–194.

Mahlstein, I., Daniel, J. S., and Solomon, S. (2013). Pace of shifts in climate regions increases with global temperature. *Nature Climate Change*, 3(8):739–743.

Marshall, D. J., Baharuddin, N., and McQuaid, C. D. (2013). Behaviour moderates climate warming vulnerability in high-rocky-shore snails: interactions of habitat use, energy consumption and environmental temperature. *Marine Biology*, pages 1–6.

Marshall, D. J., Dong, Y., McQuaid, C. D., and Williams, G. A. (2011). Thermal adaptation in the intertidal snail *Echinolittorina malaccana* contradicts current theory by revealing the crucial roles of resting metabolism. *Journal of Experimental Biology*, 214(Pt 21):3649–3657.

Marshall, D. J., Peter, R., and Chown, S. L. (2004). Regulated bradycardia in the pulmonate limpet *Siphonaria* (Gastropoda: Mollusca) during pollutant exposure: implication for biomarker studies. *Comparative Biochemistry and Physiology A*, 139(3):309–316.

McMahon, R. F. (1990). Thermal tolerance, evaporative water loss, air-water oxygen consumption and zonation of intertidal prosobranchs: a new synthesis. *Hydrobiologia*, 193(1):241–260.

Meager, J. J. and Schlacher, T. A. (2013). New metric of microhabitat complexity predicts species richness on a rocky shore. *Marine Ecology*, 34(4):484–491.

Meehl, G. A., Tebaldi, C., Walton, G., Easterling, D., and McDaniel, L. (2009). Relative increase of record high maximum temperatures compared to record low minimum temperatures in the U.S. *Geophysical Research Letters*, 36(23):L23701.

Meinel, A. B. and Meinel, M. P. (1976). *Applied Solar Energy*. Addison Wesley Publishing Co., New York.

Meng, X., Ji, T., Dong, Y., Wang, Q., and Dong, S. (2009). Thermal resistance in sea cucumbers (*Apostichopus japonicus*) with differing thermal history: The role of Hsp70. *Aquaculture*, 294(3-4):314–318.

Menge, B. A. and Lubchenco, J. (1981). Community organization in temperate and tropical rocky intertidal habitats: Prey refuges in relation to consumer pressure gradients. *Ecological Monographs*, 51(4):429–450.

Miller, L. P., Harley, C. D. G., and Denny, M. W. (2009). The role of temperature and desiccation stress in limiting the local-scale distribution of the owl limpet, *Lottia gigantea*. *Functional Ecology*, 23(4):756–767.

Mislan, K. A. S., Helmuth, B., and Wethey, D. S. (2014). Geographical variation in climatic sensitivity of intertidal mussel zonation. *Global Ecology and Biogeography*, 23(7):744–756.

Mislan, K. A. S., Wethey, D. S., and Helmuth, B. (2009). When to worry about the weather: role of tidal cycle in determining patterns of risk in intertidal ecosystems. *Global Change Biology*, 15(12):3056–3065.

Moncoiffe, G., Alvarez-Salgado, X. A., Figueiras, F. G., and Savidge, C. (2000). Seasonal and short-time-scale dynamics of microplankton community production and respiration in an inshore upwelling system. *Marine Ecology-Progress Series*, 196:111–126.

Moore, P. J., Hawkins, S. J., and Thompson, R. C. (2007). Role of biological habitat amelioration in altering the relative responses of congeneric species to climate change. *Marine Ecology-Progress Series*, 334:11–19.

Moritz, C., Patton, J. L., Conroy, C. J., Parra, J. L., White, G. C., and Beissinger, S. R. (2008). Impact of a century of climate change on small-mammal communities in Yosemite National Park, USA. *Science*, 322(5899):261–264.

Morritt, D., Leung, K. M. Y., De Pirro, M., Yau, C., Wai, T., and Williams, G. A. (2007). Responses of the limpet, *Cellana grata* (Gould 1859), to hypo-osmotic stress during simulated tropical, monsoon rains. *Journal of Experimental Marine Biology and Ecology*, 352(1):78–88.

Mota, C., Engelen, A. H., Serrão, E. A., and Pearson, G. A. (2015). Some don't like it hot: microhabitat-dependent thermal and water stresses in a trailing edge population. *Functional Ecology*, 29:640–649.

Nicastro, K. R., Zardi, G. I., Teixeira, S., Neiva, J., Serrão, E. A., and Pearson, G. A. (2013). Shift happens: trailing edge contraction associated with recent warming trends threatens a distinct genetic lineage in the marine macroalga *Fucus vesiculosus*. *BMC Biology*, 11(1):6.

Nicholson, S. (2002). Ecophysiological aspects of cardiac activity in the subtropical mussel *Perna viridis* (L.) (Bivalvia: Mytilidae). *Journal of Experimental Marine Biology and Ecology*, 267(2):207–222.

Ortea, J. (1986). The malacology of La Riera cave. *Arizona State University Anthropological Research Papers*, (36):289–298.

Orton, J. H. (1929). On the occurrence of *Echinus esculentus* on the foreshore in the British Isles. *Journal of the Marine Biological Association of the United Kingdom*, 16(01):289–296.

Paine, R. T. (1974). Intertidal community structure: experimental studies on the relationship between a dominant competitor and its principal predator. *Oecologia*, 15(2):93–120.

Paine, R. T. and Trimble, A. C. (2004). Abrupt community change on a rocky shore - biological mechanisms contributing to the potential formation of an alternative state. *Ecology Letters*, 7(6):441–445.

Pardo, P. C., Padín, X. A., Gilcoto, M., Farina-Busto, L., and Pérez, F. F. (2011). Evolution of upwelling systems coupled to the long-term variability in sea surface temperature and Ekman transport. *Climate Research*, 48(2):231–246.

Parmesan, C. and Yohe, G. (2003). A globally coherent fingerprint of climate change impacts across natural systems. *Nature*, 421:37–42.

Pearson, G. A., Lago-Leston, A., and Mota, C. (2009). Frayed at the edges: selective pressure and adaptive response to abiotic stressors are mismatched in low diversity edge populations. *Journal of Ecology*, 97(3):450–462.

Peliz, Á., Rosa, T. L., Santos, A. M., and Pissarra, J. L. (2002). Fronts, jets, and counter-flows in the Western Iberian upwelling system. *Journal of Marine Systems*, 35(1-2):61–77.

Pereira, H. M., Leadley, P. W., Proença, V., Alkemade, R., Scharlemann, J. P. W., Fernandez-Manjarrés, J. F., Araújo, M. B., Balvanera, P., Biggs, R., Cheung, W. W. L., Chini, L., Cooper, H. D., Gilman, E. L., Guénette, S., Hurtt, G. C., Huntington, H. P., Mace, G. M., Oberdorff, T., Revenga, C., Rodrigues, P., Scholes, R. J., Sumaila, U. S., and Walpole, M. (2010). Scenarios for global biodiversity in the 21st century. *Science*, 330(6010):1496–1501.

Pereira, S. G., Lima, F. P., Queiroz, N., Ribeiro, P. A., and Santos, A. M. (2006). Biogeographic patterns of intertidal macroinvertebrates and their association with macroalgae distribution along the Portuguese coast. *Hydrobiologia*, 555(1):185–192.

Pickens, P. E. (1965). Heart rate of mussels as a function of latitude, intertidal height, and acclimation temperature. *Physiological Zoology*, 38(4):390–405.

Pincebourde, S., Sanford, E., and Helmuth, B. (2008). Body temperature during low tide alters the feeding performance of a top intertidal predator. *Limnology and Oceanography*, 53(4):1562–1573.

Pinckney, J. and Zingmark, R. G. (1991). Effects of tidal stage and sun angles on intertidal benthic microalgal productivity. *Marine Ecology-Progress Series*, 76:81–89.

Pironon, S., Villellas, J., Morris, W. F., Doak, D. F., and García, M. B. (2015). Do geographic, climatic or historical ranges differentiate the performance of central versus peripheral populations? *Global Ecology and Biogeography*, 24(6):611–620.

Poloczanska, E. S., Brown, C. J., Sydeman, W. J., Kiessling, W., Schoeman, D. S., Moore, P. J., Brander, K., Bruno, J. F., Buckley, L. B., Burrows, M. T., Duarte, C. M., Halpern, B. S., Holding, J., Kappel, C. V., O'Connor, M. I., Pandolfi, J. M., Parmesan, C., Schwing, F., Thompson, S. A., and Richardson, A. J. (2013). Global imprint of climate change on marine life. *Nature Climate Change*, 3:919–925.

Poloczanska, E. S., Hawkins, S. J., Southward, A. J., and Burrows, M. T. (2008). Modeling the response of populations of competing species to climate change. *Ecology*, 89(11):3138–3149.

Porter, W. P. and Gates, D. M. (1969). Thermodynamic equilibria of animals with environment. *Ecological Monographs*, 39(3):227–244.

Potter, K. A., Woods, H. A., and Pincebourde, S. (2013). Microclimatic challenges in global change biology. *Global Change Biology*, 19(10):2932–2939.

R Development Core Team (2010). R: A language and environment for statistical computing. *http://www.R-project.org*.

R Development Core Team (2014). R: A language and environment for statistical computing. *http://www.R-project.org*.

R Development Core Team (2015). R: A language and environment for statistical computing. *http://www.R-project.org*.

Raffaelli, D. G. and Hawkins, S. J. (1996). *Intertidal Ecology*. Chapman and Hall, London.

Ramos, A. M., Trigo, R. M., and Santo, F. E. (2011). Evolution of extreme temperatures over Portugal: recent changes and future scenarios. *Climate Research*, 48(2-3):177–192.

Relvas, P., Barton, E. D., Dubert, J., Oliveira, P. B., Peliz, Á., da Silva, J. C. B., and Santos, A. M. (2007). Physical oceanography of the western Iberia ecosystem: latest views and challenges. *Progress in Oceanography*, 74(2-3):149–173.

Robinson, N. J., Thatje, S., and Osseforth, C. (2009). Heartbeat sensors under pressure: a new method for assessing hyperbaric physiology. *High Pressure Research*, 29(3):422–430.

Root, T. L., Price, J. T., Hall, K. R., Schneider, S. H., Rosenzweig, C., and Pounds, J. A. (2003). Fingerprints of global warming on wild animals and plants. *Nature*, 421(6918):57–60.

Rovero, F., Hughes, R. N., and Chelazzi, G. (1999). Cardiac and behavioural responses of mussels to risk of predation by dogwhelks. *Animal Behaviour*, 58(4):707–714.

Rovero, F., Hughes, R. N., Whiteley, N. M., and Chelazzi, G. (2000). Estimating the energetic cost of fighting in shore crabs by noninvasive monitoring of heartbeat rate. *Animal Behaviour*, 59(4):705–713.

Rutz, C. and Hays, G. C. (2009). New frontiers in biologging science. *Biology Letters*, 5(3):289–292.

Sagarin, R. D., Barry, J. P., Gilman, S. E., and Baxter, C. H. (1999). Climate-related change in an intertidal community over short and long time scales. *Ecological Monographs*, 69(4):465–490.

Sagarin, R. D. and Gaines, S. (2002a). Geographical abundance distributions of coastal invertebrates: using one-dimensional ranges to test biogeographic hypotheses. *Journal of Biogeography*, 29:985–997.

Sagarin, R. D. and Gaines, S. (2002b). The 'abundant centre' distribution: to what extent is it a biogeographical rule? *Global Change Biology*, 5(1):137–147.

Sagarin, R. D. and Somero, G. N. (2006). Complex patterns of expression of heat-shock protein 70 across the southern biogeographical ranges of the intertidal mussel *Mytilus californianus* and snail *Nucella ostrina*. *Journal of Biogeography*, 33(4):622–630.

Santini, G., Bianchi, T., and Chelazzi, G. (2002). Metabolic responses to food deprivation in two limpets with different foraging regimes, revealed by recording of cardiac activity. *Journal of Zoology*, 256(1):11–15.

Santini, G., De Pirro, M., and Chelazzi, G. (1999). In situ and laboratory assessment of heart rate in a Mediterranean limpet using a noninvasive technique. *Physiological and Biochemical Zoology*, 72(2):198–204.

Santini, G., Thompson, R. C., Tendi, C., Hawkins, S. J., Hartnoll, R. G., and Chelazzi, G. (2004). Intra-specific variability in the temporal organisation of foraging activity in the limpet *Patella vulgata*. *Marine Biology*, 144(6):1165–1172.

Santini, G., Williams, G. A., and Chelazzi, G. (2000). Assessment of factors affecting heart rate of the limpet *Patella vulgata* on the natural shore. *Marine Biology*, 137(2):291–296.

Sarà, G. and De Pirro, M. (2011). Heart beat rate adaptations to varying salinity of two intertidal Mediterranean bivalves: The invasive *Brachidontes pharaonis* and the native *Mytilaster minimus*. *Italian Journal of Zoology*, 78(2):193–197.

Scheffers, B. R., Edwards, D. P., Diesmos, A., Williams, S. E., and Evans, T. A. (2014). Microhabitats reduce animal's exposure to climate extremes. *Global Change Biology*, 20(2):495–503.

Schill, R. O., Gayle, P. M. H., and Köhler, H. R. (2002). Daily stress protein (hsp70) cycle in chitons (*Acanthopleura granulata* Gmelin, 1791) which inhabit the rocky intertidal shoreline in a tropical ecosystem. *Comparative Biochemistry and Physiology C*, 131(3):253–258.

Schneider, K. R., van Thiel, L. E., and Helmuth, B. (2010). Interactive effects of food availability and aerial body temperature on the survival of two intertidal *Mytilus* species. *Journal of Thermal Biology*, 35(4):161–166.

Seabra, R., Wethey, D. S., Santos, A. M., Gomes, F., and Lima, F. P. (2015a). Equatorial range limits of an intertidal ectotherm are more linked to water than air temperature. *Submitted*.

Seabra, R., Wethey, D. S., Santos, A. M., and Lima, F. P. (2011). Side matters: microhabitat influence on intertidal heat stress over a large geographical scale. *Journal of Experimental Marine Biology and Ecology*, 400(1-2):200–208.

Seabra, R., Wethey, D. S., Santos, A. M., and Lima, F. P. (2015b). Understanding complex biogeographic responses to climate change. *Scientific Reports*, 5:12930.

Smith, F. G. W. (1935). The development of *Patella vulgata*. *Philosophical Transactions of the Royal Society of London. Series B*, 225(520):95–125.

Snyder, M. J. and Rossi, S. (2004). Stress protein (HSP70 family) expression in intertidal benthic organisms: the example of *Anthopleura elegantissima* (Cnidaria: Anthozoa). *Scientia Marina*, 68:155–162.

Somero, G. N. (2002). Thermal physiology and vertical zonation of intertidal animals: optima, limits, and costs of living. *Integrative and Comparative Biology*, 42(4):780–789.

Somero, G. N. (2005). Linking biogeography to physiology: Evolutionary and acclimatory adjustments of thermal limits. *Frontiers in zoology*, 2(1):1.

Somero, G. N. (2010). The physiology of climate change: how potentials for acclimatization and genetic adaptation will determine "winners" and "losers". *Journal of Experimental Biology*, 213(6):912–920.

Sorte, C. J. and Hofmann, G. E. (2004). Thermotolerance and heat-shock protein expression in Northeastern Pacific *Nucella* species with different biogeographical ranges. *Marine Biology*, 146(5):985–993.

Sorte, C. J., Jones, S. J., and Miller, L. P. (2011). Geographic variation in temperature tolerance as an indicator of potential population responses to climate change. *Journal of Experimental Marine Biology and Ecology*, 400(1-2):209–217.

Southward, A. J. (1958). Note on the temperature tolerances of some intertidal marine animals in relation to environmental temperatures and geographic distribution. *Journal of the Marine Biological Association of the United Kingdom*, 37:49–66.

Southward, A. J. (1964). Limpet grazing and the control of vegetation on rocky shores. In Crisp, D. J., editor, *Grazing in Terrestrial and Marine Environments*, pages 265–273. Oxford.

Southward, A. J. and Crisp, D. J. (1952). Changes in the distribution of the intertidal barnacles in relation to the environment. *Nature*, 170:416–417.

Southward, A. J. and Crisp, D. J. (1954). Recent changes in the distribution of intertidal barnacles *Chthamalus stellatus* (Poli) and *Balanus balanoides* (L.) in the British Isles. *Journal of Animal Ecology*, 23(1):163–177.

Southward, A. J., Hawkins, S. J., and Burrows, M. T. (1995). Seventy years' observations of changes in distribution and abundance of zooplankton and intertidal organisms in the western English Channel in relation to rising sea temperature. *Journal of Thermal Biology*, 20(1-2):127–155.

Spooner, E. H., Coleman, R. A., and Attrill, M. J. (2007). Sex differences in body morphology and multitrophic interactions involving the foraging behaviour of the crab *Carcinus maenas*. *Marine Ecology*, 28(3):394–403.

Spotila, J. R., Lommen, P. W., Bakken, G. S., and Gates, D. M. (1973). A mathematical model for body temperatures of large reptiles: implications for dinossaur ecology. *The American Naturalist*, 107(955):391–404.

Stillman, J. H. (2003). Acclimation capacity underlies susceptibility to climate change. *Science*, 301(5629):65–65.

Stillman, J. H. and Somero, G. N. (1996). Adaptation to temperature stress and aerial exposure in congeneric species of intertidal porcelain crabs (genus *Petrolisthes*): correlation of physiology, biochemistry and morphology with vertical distribution. *Journal of Experimental Biology*, 199(8):1845–1855.

Styrishave, B., Andersen, O., and Depledge, M. H. (2010). In situ monitoring of heart rates in shore crabs *Carcinus maenas* in two tidal estuaries: Effects of physico-chemical parameters on tidal and diel rhythms. *Marine and Freshwater Behaviour and Physiology*, 36(3):161–175.

Sunday, J. M., Bates, A. E., and Dulvy, N. K. (2012). Thermal tolerance and the global redistribution of animals. *Nature Climate Change*, 2:686–690.

Szathmary, P. L., Helmuth, B., and Wethey, D. S. (2009). Climate change in the rocky intertidal zone: predicting and measuring the body temperature of a keystone predator. *Marine Ecology-Progress Series*, 374:43–56.

Taylor, K. E. (2001). Summarizing multiple aspects of model performance in a single diagram. *Journal of Geophysical Research*, 106(D7):7183–7192.

Taylor, S. C., Berkelman, T., Yadav, G., and Hammond, M. (2013). A defined methodology for reliable quantification of western blot data. *Molecular Biotechnology*, 55(3):217–226.

Thompson, R. C., Norton, T. A., and Hawkins, S. J. (2004). Physical stress and biological control regulate the producer–consumer balance in intertidal biofilms. *Ecology*, 85(5):1372–1382.

Tittensor, D. P., Mora, C., Jetz, W., Lotze, H. K., Ricard, D., Berghe, E. V., and Worm, B. (2010). Global patterns and predictors of marine biodiversity across taxa. *Nature*, 466(7310):1098–1101.

Tomanek, L. and Helmuth, B. (2002). Physiological ecology of rocky intertidal organisms: a synergy of concepts. *Integrative and Comparative Biology*, 42(4):771–775.

Tomanek, L. and Sanford, E. (2003). Heat-shock protein 70 (Hsp70) as a biochemical stress indicator: an experimental field test in two congeneric intertidal gastropods (Genus: *Tegula*). *Biological Bulletin*, 205(3):276–284.

Tomanek, L. and Somero, G. N. (2000). Time course and magnitude of synthesis of heat-shock proteins in congeneric marine snails (Genus *Tegula*) from different tidal heights. *Physiological and Biochemical Zoology*, 73(2):249–256.

Tuller, S. E. (1976). The relationship between diffuse, total and extra terrestrial solar radiation. *Solar Energy*, 18(3):259–263.

Underwood, A. J. (1980). The effects of grazing gastropods and physical factors on the upper limits of distribution of intertidal macroalgae. *Oecologia*, 46(2):201–213.

Underwood, A. J. (1981). Structure of a rocky intertidal community in New South Wales: patterns of vertical distribution and seasonal changes. *Journal of Experimental Marine Biology and Ecology*, 51(1):57–85.

Ungherese, G., Boddi, V., and Ugolini, A. (2008). Eco-physiology of *Palaemonetes antennarius* (Crustacea, Decapoda): the influence of temperature and salinity on cardiac frequency. *Physiological Entomology*, 33(2):155–161.

Valencia, V., Franco, J., Borja, A., and Fontán, A. (2004). Hydrography of the southeastern Bay of Biscay. In *Oceanography and Marine Environment of the Basque Country*, pages 159–194. Elsevier.

Van Aardt, W. J. and Vosloo, A. (2011). Modifications to an optocardiographic method for measurement of heart rate in a range of invertebrate species. *South African Journal of Marine Science*, 31:97–100.

VanDerWal, J., Murphy, H. T., Kutt, A. S., Perkins, G. C., Bateman, B. L., Perry, J. J., and Reside, A. E. (2013). Focus on poleward shifts in species' distribution underestimates the fingerprint of climate change. *Nature Climate Change*, 3:239–243.

Varai, A., Homonnai, V., Janosi, I. M., and Müller, R. (2015). Early signatures of ozone trend reversal over the Antarctic. *Earth's Future*, 3(3):95–109.

Varela, R., Álvarez, I., Santos, F., deCastro, M., and Gómez-Gesteira, M. (2015). Has upwelling strengthened along worldwide coasts over 1982-2010? *Scientific Reports*, 5:10016.

Vasseur, D. A., DeLong, J. P., Gilbert, B., Greig, H. S., Harley, C. D. G., McCann, K. S., Savage, V., Tunney, T. D., and O'Connor, M. I. (2014). Increased temperature variation poses a greater risk to species than climate warming. *Proceedings of the Royal Society B*, 281(1779):20132612.

Vincent, W. F. and Neale, P. J. (2000). Mechanisms of UV damage to aquatic organisms. In de Mora, S., Demers, S., and Vernet, M., editors, *The effects of UV radiation in the marine environment*, pages 149–176. Cambridge University Press, Cambridge.

Walther, G. E., Post, E., Convey, P., Menzel, A., Parmesan, C., Beebee, T. J., Fromentin, J. M., Hoegh-Guldberg, O., and Bairlein, F. (2002). Ecological responses to recent climate change. *Nature*, 416:389–395.

Wang, D., Gouhier, T. C., Menge, B. A., and Ganguly, A. R. (2015). Intensification and spatial homogenization of coastal upwelling under climate change. *Nature*, 518(7539):390–394.

Wessel, P. and Smith, W. H. F. (1996). A global, self-consistent, hierarchical, high-resolution shoreline database. *Journal of Geophysical Research*, 101(B4):8741–8743.

Wethey, D. S. (1984). Sun and shade mediate competition in the barnacles *Chthamalus* and *Semibalanus*: a field experiment. *Biological Bulletin*, 167(1):176–185.

Wethey, D. S. (2002). Biogeography, competition, and microclimate: the barnacle *Chthamalus fragilis* in New England. *Integrative and Comparative Biology*, 42(4):872–880.

Wethey, D. S., Lima, F. P., Woodin, S. A., Hilbish, T. J., Jones, S. J., and Brannock, P. M. (2011). Response of intertidal populations to climate: effects of extreme events versus long term change. *Journal of Experimental Marine Biology and Ecology*, 400(1-2):132–144.

Wethey, D. S. and Woodin, S. A. (2008). Ecological hindcasting of biogeographic responses to climate change in the European intertidal zone. *Hydrobiologia*, 606(1):139–151.

Williams, G. A., De Pirro, M., Cartwright, S. R., Khangura, K., Ng, W. C., Leung, P. T., and Morritt, D. (2010). Come rain or shine: the combined effects of physical stresses on physiological and protein-level responses of an intertidal limpet in the monsoonal tropics. *Functional Ecology*, 25(1):101–110.

Williams, G. A., De Pirro, M., Leung, K. M. Y., and Morritt, D. (2005). Physiological responses to heat stress on a tropical shore: the benefits of mushrooming behaviour in the limpet *Cellana grata*. *Marine Ecology-Progress Series*, 292:213–224.

Wing, S. R., Leichter, J. J., Perrin, C., Rutger, S. M., Bowman, M. H., and Cornelisen, C. D. (2007). Topographic shading and wave exposure influence morphology and ecophysiology of *Ecklonia radiata* (C. Agardh 1817) in Fiordland, New Zealand. *Limnology and Oceanography*, 52(5):1853–1864.

Wolcott, T. G. (1973). Physiological ecology and intertidal zonation in limpets (*Acmaea*): a critical look at "limiting factors". *Biological Bulletin*, 145(2):389–422.

Woodin, S. A., Hilbish, T. J., Helmuth, B., Jones, S. J., and Wethey, D. S. (2013). Climate change, species distribution models, and physiological performance metrics: predicting when biogeographic models are likely to fail. *Ecology and Evolution*, 3(10):3334–3346.

Yamane, L. and Gilman, S. E. (2009). Opposite responses by an intertidal predator to increasing aquatic and aerial temperatures. *Marine Ecology-Progress Series*, 393:27–36.

Zardi, G. I., Nicastro, K. R., McQuaid, C. D., Hancke, L., and Helmuth, B. (2010). The combination of selection and dispersal helps explain genetic structure in intertidal mussels. *Oecologia*, 165(4):947–958.

Zhang, S., Han, G., and Dong, Y. (2014). Temporal patterns of cardiac performance and genes encoding heat shock proteins and metabolic sensors of an intertidal limpet *Cellana toreuma* during sublethal heat stress. *Journal of Thermal Biology*, 41:31–37.